THE SPECTRAL DOMAIN DECOMPOSITION METHOD GENEO AS A ROBUST PRECONDITIONER FOR SINGLE-PHASE FLOW IN FRACTURED POROUS MEDIA

Pierre JOLIVET[1], Michel KERN[2,3], Frédéric NATAF[2,4], Géraldine PICHOT[2,3], Raphaël ZANELLA[2], Daniel ZEGARRA VASQUEZ[2,3]

[1] LIP6, CNRS UMR 7606, Sorbonne Université.
[2] Inria Paris.
[3] CERMICS, École Nationale des Ponts et Chaussées.
[4] LJLL, CNRS UMR 7598, Sorbonne Université.

SMAI – CANUM – June 2026 – Saint-Jacut-de-la-Mer (22)
Mini-symposium « The underground : water, gas, fractures … and math ! »

Introduction

Introduction

Fractured media geophysical context

Introduction

Fractured media geophysical context

Fractures : discontinuities in the subsurface medium in the form of thin structures.

Fractured media geophysical context

Fractures : discontinuities in the subsurface medium in the form of thin structures.

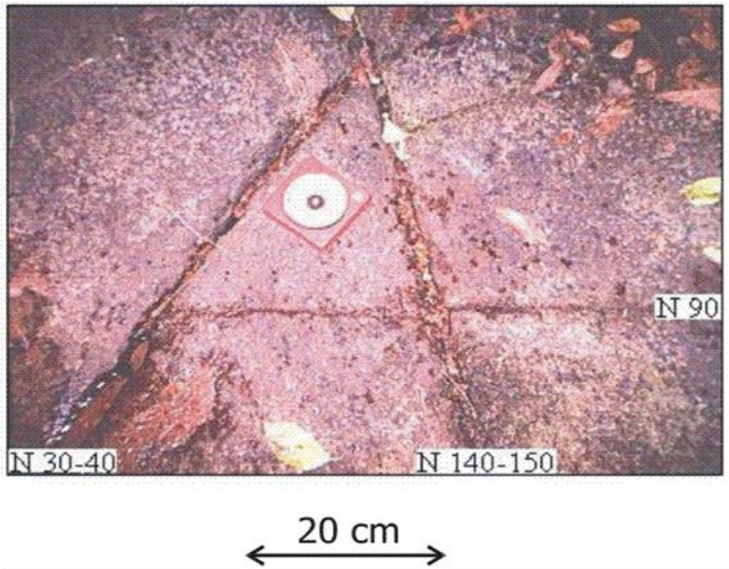

Some fracture examples. Copyright: Géosciences Rennes.

Fractured media geophysical context

Fractures : discontinuities in the subsurface medium in the form of thin structures.

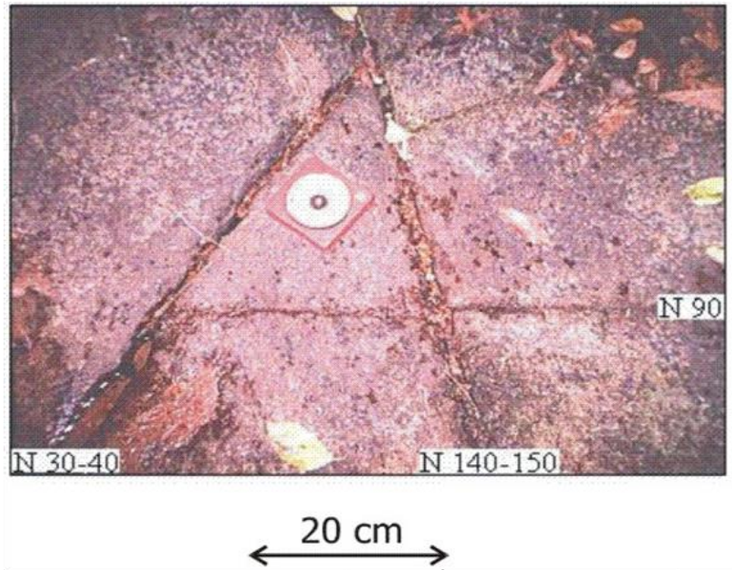

Some fracture examples. Copyright: Géosciences Rennes.

Present at different scales, from µm to km. In this work: from 10 cm to 100 m.

Fractured media geophysical context

Fractures : discontinuities in the subsurface medium in the form of thin structures.

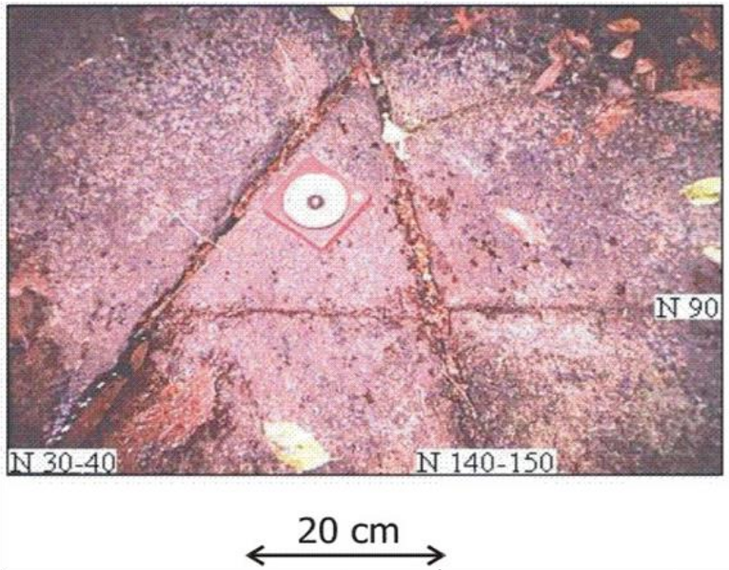

Some fracture examples. Copyright: Géosciences Rennes.

Present at different scales, from µm to km. In this work: from 10 cm to 100 m.

May be conductive pathways for the flow or barriers. In this work: conductive.

Fractured media geophysical context

Fractures : discontinuities in the subsurface medium in the form of thin structures.

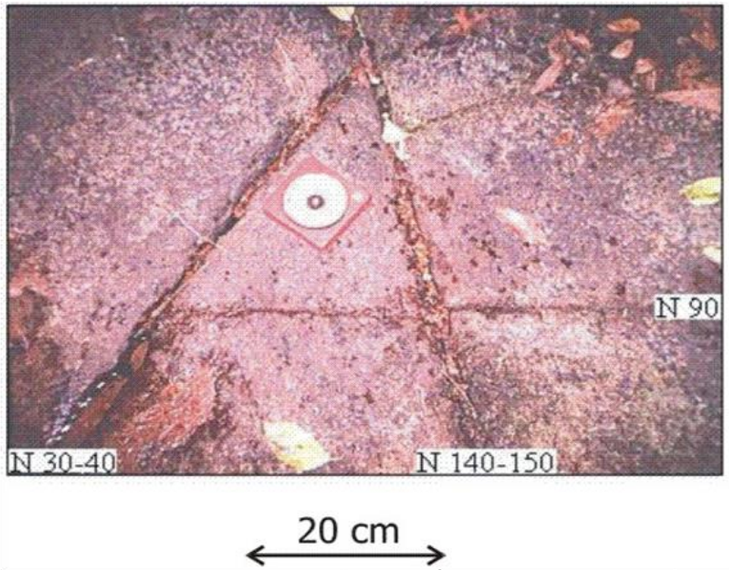

Some fracture examples. Copyright: Géosciences Rennes.

Present at different scales, from µm to km. In this work: from 10 cm to 100 m.

May be conductive pathways for the flow or barriers. In this work: conductive.

Key role in industrial applications : oil and gas extraction, CO_2 sequestration in the subsurface, geothermal energy production, underground nuclear waste storage, water extraction, etc.

Introduction

Modeling underground fractured media

Introduction

Modeling underground fractured media

Fractures = two-dimensional flat surfaces (e.g. polygons or disks) immersed in a three-dimensional space.

LabCom *fractory*:
- ❑ **Itasca Consultants (France)**
- ❑ **Géosciences Rennes**
- ❑ **CNRS**

P. Davy, R. Le Goc, C. Darcel, O. Bour, J.-R. de Dreuzy, R. Munier. *Journal of Geophysical Research: Solid Earth.* **2010.**

J.-R. de Dreuzy, G. Pichot, B. Poirriez, J. Erhel. *Computers and Geosciences.* **2012.**

Introduction

Modeling underground fractured media

LabCom *fractory*:
- ❑ **Itasca Consultants (France)**
- ❑ **Géosciences Rennes**
- ❑ **CNRS**

Fractures = two-dimensional flat surfaces (e.g. polygons or disks) immersed in a three-dimensional space.

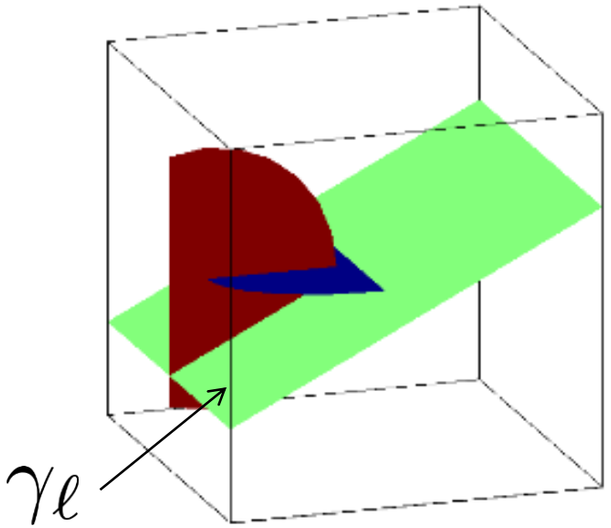

***DFN** with 3 fractures*

P. Davy, R. Le Goc, C. Darcel, O. Bour, J.-R. de Dreuzy, R. Munier. *Journal of Geophysical Research: Solid Earth.* **2010.**

J.-R. de Dreuzy, G. Pichot, B. Poirriez, J. Erhel. *Computers and Geosciences.* **2012.**

Discrete Fracture Network model: 2D only (no rock matrix)

Introduction

Modeling underground fractured media

LabCom *fractory*:
- ❑ **Itasca Consultants (France)**
- ❑ **Géosciences Rennes**
- ❑ **CNRS**

Fractures = two-dimensional flat surfaces (e.g. polygons or disks) immersed in a three-dimensional space.

+ Rock matrix = a three-dimensional domain.

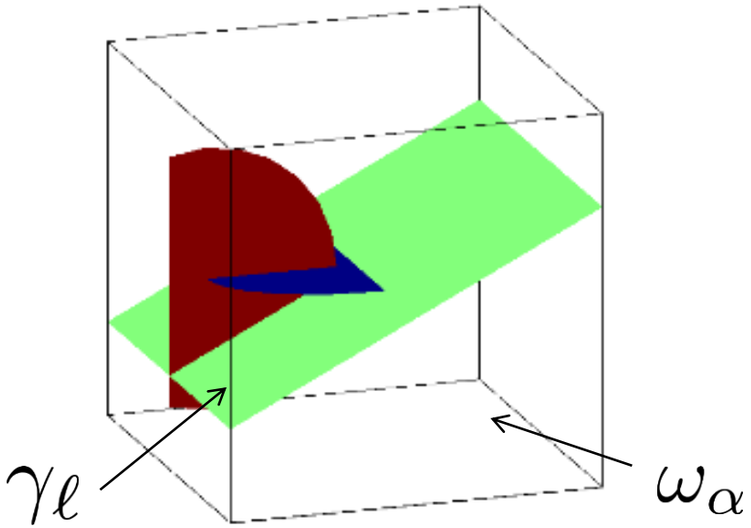

***DFN** with 3 fractures*

P. Davy, R. Le Goc, C. Darcel, O. Bour, J.-R. de Dreuzy, R. Munier. *Journal of Geophysical Research: Solid Earth.* **2010.**

J.-R. de Dreuzy, G. Pichot, B. Poirriez, J. Erhel. *Computers and Geosciences.* **2012.**

Discrete Fracture Network model: 2D only (no rock matrix)

Introduction

Modeling underground fractured media

LabCom *fractory*:
- ❑ **Itasca Consultants (France)**
- ❑ **Géosciences Rennes**
- ❑ **CNRS**

Fractures = two-dimensional flat surfaces (e.g. polygons or disks) immersed in a three-dimensional space.

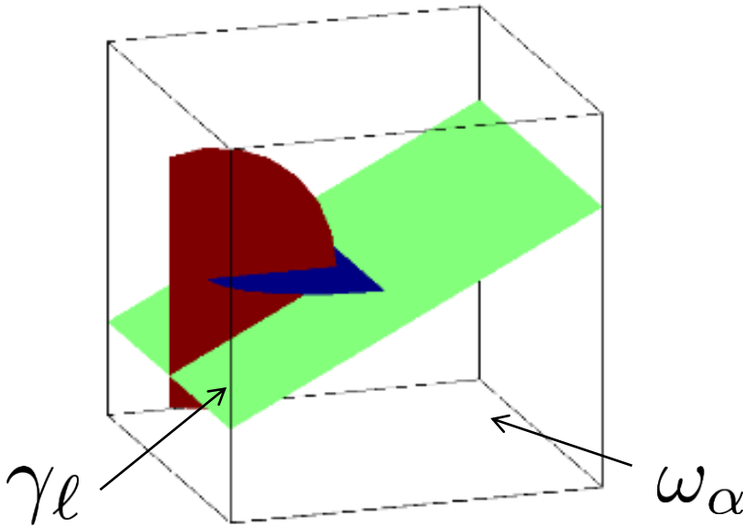

***DFN** with 3 fractures*

P. Davy, R. Le Goc, C. Darcel, O. Bour, J.-R. de Dreuzy, R. Munier. *Journal of Geophysical Research: Solid Earth.* **2010.**

J.-R. de Dreuzy, G. Pichot, B. Poirriez, J. Erhel. *Computers and Geosciences.* **2012.**

+ Rock matrix = a three-dimensional domain.

I. Berre, F. Doster, E. Keilegavlen. *Transport in Porous Media.* **2019.**

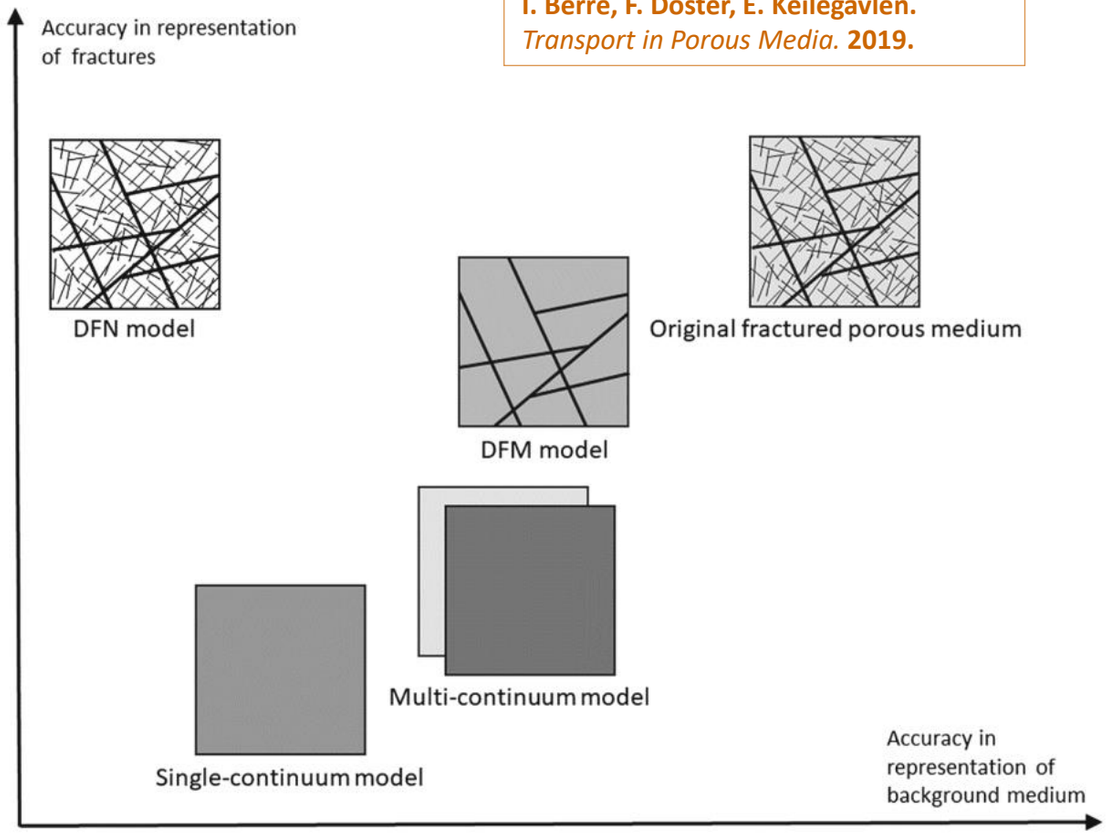

Discrete Fracture Network model: 2D only (no rock matrix)

Introduction

Modeling underground fractured media

LabCom *fractory*:
- ❑ Itasca Consultants (France)
- ❑ Géosciences Rennes
- ❑ CNRS

Fractures = two-dimensional flat surfaces (e.g. polygons or disks) immersed in a three-dimensional space.

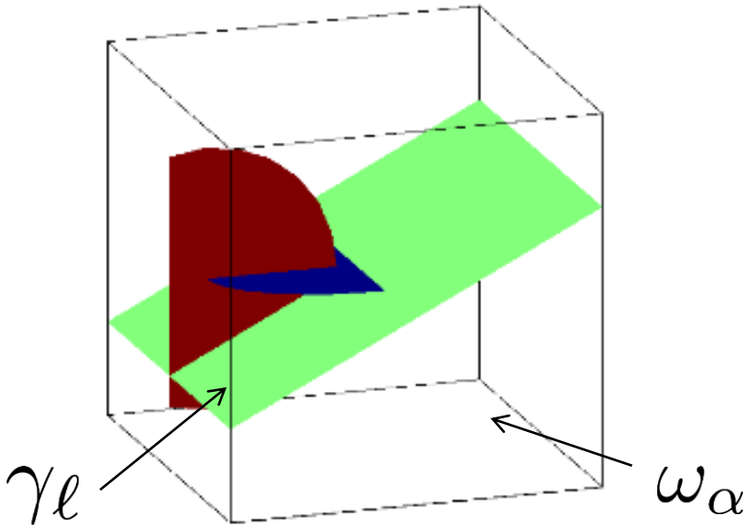

***DFN** with 3 fractures*

P. Davy, R. Le Goc, C. Darcel, O. Bour, J.-R. de Dreuzy, R. Munier. *Journal of Geophysical Research: Solid Earth.* **2010.**

J.-R. de Dreuzy, G. Pichot, B. Poirriez, J. Erhel. *Computers and Geosciences.* **2012.**

Discrete Fracture Network model: 2D only (no rock matrix)

+ Rock matrix = a three-dimensional domain.

I. Berre, F. Doster, E. Keilegavlen. *Transport in Porous Media.* **2019.**

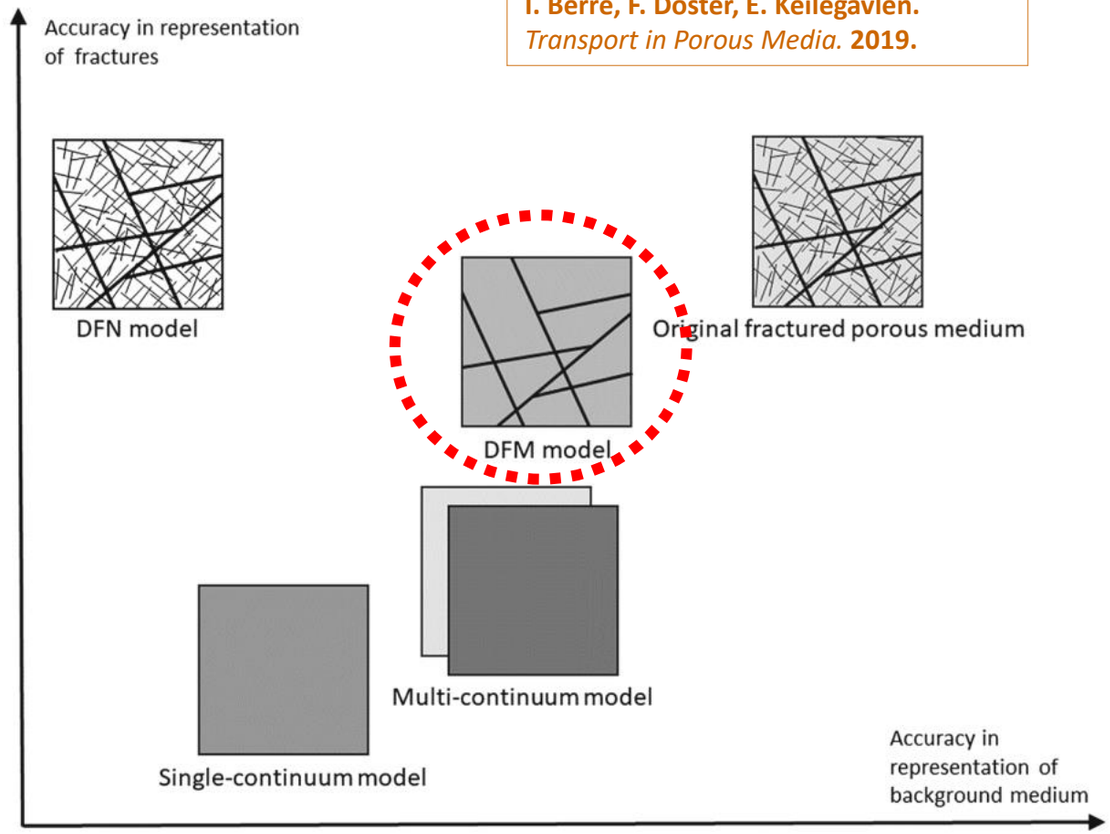

Discrete Fracture Matrix (DFM) model: 2D + 3D

Introduction

Modeling underground fractured media

LabCom *fractory*:
- ❑ Itasca Consultants (France)
- ❑ Géosciences Rennes
- ❑ CNRS

Fractures = two-dimensional flat surfaces (e.g. polygons or disks) immersed in a three-dimensional space.

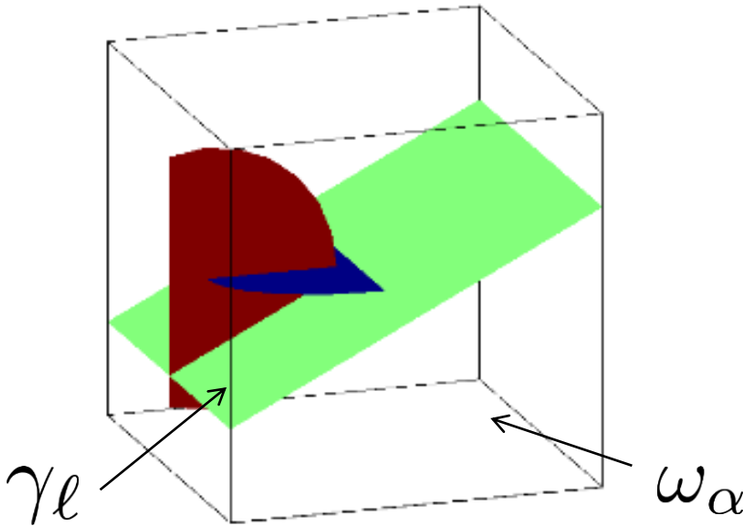

***DFN** with 3 fractures*

P. Davy, R. Le Goc, C. Darcel, O. Bour, J.-R. de Dreuzy, R. Munier. *Journal of Geophysical Research: Solid Earth.* **2010.**

J.-R. de Dreuzy, G. Pichot, B. Poirriez, J. Erhel. *Computers and Geosciences.* **2012.**

Discrete Fracture Network model: 2D only (no rock matrix)

+ Rock matrix = a three-dimensional domain.

I. Berre, F. Doster, E. Keilegavlen. *Transport in Porous Media.* **2019.**

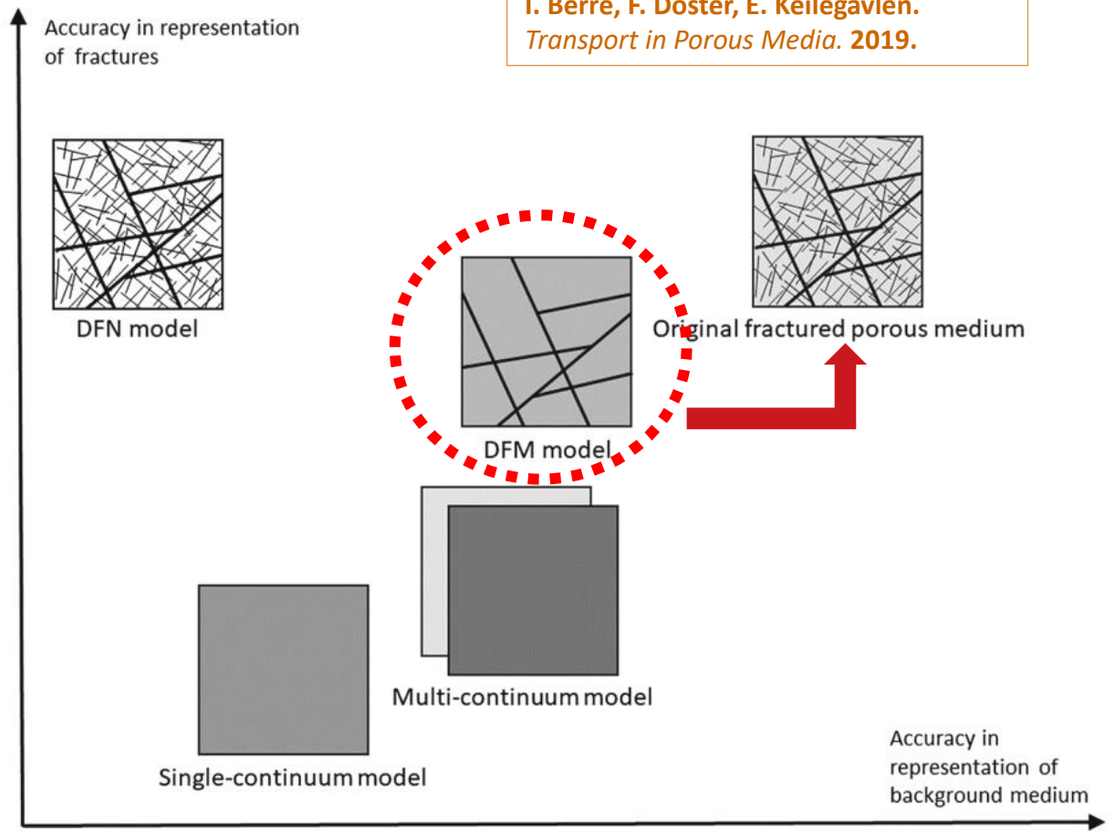

Discrete Fracture Matrix (DFM) model: 2D + 3D

Introduction

Main objective : efficient large-scale simulations

Introduction

Main objective : efficient large-scale simulations

Run efficiently single-phase flow simulations with a large number of fractures with very different sizes.

Introduction

Main objective : efficient large-scale simulations

Run efficiently single-phase flow simulations with a large number of fractures with very different sizes.

Main challenges :

Main objective : efficient large-scale simulations

Run efficiently single-phase flow simulations with a large number of fractures with very different sizes.

Main challenges :

- One simulation must be **cheap** → run several simulations → Monte-Carlo studies.

Main objective : efficient large-scale simulations

Run efficiently single-phase flow simulations with a large number of fractures with very different sizes.

Main challenges :

- One simulation must be **cheap** → run several simulations → Monte-Carlo studies.
- **Highly intricate geometric** entities → dedicated mesh generators.

Main objective : efficient large-scale simulations

Run efficiently single-phase flow simulations with a large number of fractures with very different sizes.

Main challenges :

- One simulation must be **cheap** → run several simulations → Monte-Carlo studies.
- **Highly intricate geometric** entities → dedicated mesh generators.
- **Large-scale simulations** with :

Main objective : efficient large-scale simulations

Run efficiently single-phase flow simulations with a large number of fractures with very different sizes.

Main challenges :

- One simulation must be **cheap** → run several simulations → Monte-Carlo studies.
- **Highly intricate geometric** entities → dedicated mesh generators.
- **Large-scale simulations** with :
  - strong permeability heterogeneities ;

Main objective : efficient large-scale simulations

Run efficiently single-phase flow simulations with a large number of fractures with very different sizes.

Main challenges :

- One simulation must be **cheap** → run several simulations → Monte-Carlo studies.
- **Highly intricate geometric** entities → dedicated mesh generators.
- **Large-scale simulations** with :
  - strong permeability heterogeneities ;
  - a large number of fractures ;

Main objective : efficient large-scale simulations

Run efficiently single-phase flow simulations with a large number of fractures with very different sizes.

Main challenges :

- One simulation must be **cheap** → run several simulations → Monte-Carlo studies.
- **Highly intricate geometric** entities → dedicated mesh generators.
- **Large-scale simulations** with :
  - strong permeability heterogeneities ;
  - a large number of fractures ;
  - many dof (3D).

Main objective : efficient large-scale simulations

Run efficiently single-phase flow simulations with a large number of fractures with very different sizes.

Main challenges :

- One simulation must be **cheap** → run several simulations → Monte-Carlo studies.
- **Highly intricate geometric** entities → dedicated mesh generators.
- **Large-scale simulations** with :
  - strong permeability heterogeneities ;
  - a large number of fractures ;
  - many dof (3D).

J. D. Hyman, S. Karra, N. Makedonska, C. W. Gable, S. L. Painter, H. S. Viswanathan. *Computers and Geosciences.* **2015.**

O. Durán, P. R. B. Devloo, S. M. Gomes, F. Valentin. *Computer Methods in Applied Mechanics and Engineering.* **2019.**

P. F. Antonietti, C. Facciolà, M. Verani. *Computers and Mathematics with Applications.* **2022.**

F. Chave, D. A. Di Pietro, L. Formaggia. *SIAM Journal on Scientific Computing.* **2018.**

B. Noetinger. *Journal of Computational Physics.* **2015.**

J. M. Nordbotten, W. M. Boon, A. Fumagalli, E. Keilegavlen. *Computational Geosciences.* **2019.**

I. Berre, F. Doster, E. Keilegavlen. *Transport in Porous Media.* **2019.**

S. Berrone, S. Pieraccini, S. Scialò. *Journal of Computational Physics.* **2017.**

E. Keilegavlen, R. Berge, A. Fumagalli et al. *Computational Geosciences.* **2021.**

K. Brenner, M. Groza, C. Guichard, G. Lebeau, R. Masson. *Numerische Mathematik.* **2016.**

A. Fumagalli, E. Keilegavlen, S.Scialò. *Journal of Computational Physics.* **2019.**

Outline

Part 1 : Mathematical modeling of single-phase flow

Part 2 : Simulation framework

Part 3: The main bottleneck : solving the linear system

Part 4: The spectral domain decomposition method GenEO as a robust preconditioner

Conclusion and further work

Part 1 :
Mathematical modeling of single-phase flow

M. Kern, G. Pichot and D. Zegarra Vasquez. *Mathematical and numerical analysis of the mixed formulation of single phase flow in three-dimensional fractured porous media.* Pre-print hal-05029638. **2025.**

Part 1: mathematical model

Reduced model for flow in DFM

Part 1: mathematical model

Reduced model for flow in DFM

Fractures

$$\nabla_\tau \cdot u_\ell^{\mathbb{F}} = f_\ell^{\mathbb{F}} \text{ in } \gamma_\ell,$$

Conservation of mass

$$u_\ell^{\mathbb{F}} = -\mathcal{K}_\ell^{\mathbb{F}} \nabla_\tau p_\ell^{\mathbb{F}} \text{ in } \gamma_\ell,$$

Darcy's law

$$\gamma^{\mathbb{F}} p_\ell^{\mathbb{F}} = g_\ell^{\mathbb{F},D} \text{ on } \Sigma_\ell^D,$$

$$\gamma_n^{\mathbb{F}} u_\ell^{\mathbb{F}} = q_\ell^{\mathbb{F},N} \text{ on } \Sigma_\ell^N.$$

M. Vohralík, J. Maryška, O. Severýn. *Applied Numerical Mathematics. An IMACS Journal.* **2007.**

Part 1: mathematical model

Reduced model for flow in DFM

Fractures

$$\nabla_\tau \cdot u_\ell^{\mathbb{f}} = f_\ell^{\mathbb{f}} \text{ in } \gamma_\ell,$$

Conservation of mass

$$u_\ell^{\mathbb{f}} = -\mathcal{K}_\ell^{\mathbb{f}} \nabla_\tau p_\ell^{\mathbb{f}} \text{ in } \gamma_\ell,$$

Darcy's law

$$\gamma^{\mathbb{f}} p_\ell^{\mathbb{f}} = g_\ell^{\mathbb{f},D} \text{ on } \Sigma_\ell^D,$$

$$\gamma_n^{\mathbb{f}} u_\ell^{\mathbb{f}} = q_\ell^{\mathbb{f},N} \text{ on } \Sigma_\ell^N.$$

+ other conditions:

- continuity of the hydraulic head at fracture-fracture intersections

$$\gamma^{\mathbb{f},\sigma} p_\ell^{\mathbb{f}}|_\sigma = \gamma^{\mathbb{f},\sigma} p_k^{\mathbb{f}}|_\sigma \text{ for } (\ell,k) \in \mathcal{I}_\sigma^2,$$

- outgoing flow from a fracture has to be equal to its neighbors incoming flow

$$\sum_{\ell \in \mathcal{I}_\sigma} \gamma_n^{\mathbb{f},\sigma} u_\ell^{\mathbb{f}} = 0, \text{ for each } \sigma \subset \Sigma.$$

- null flux at immersed fracture "tips".

M. Vohralík, J. Maryška, O. Severýn. *Applied Numerical Mathematics. An IMACS Journal.* **2007.**

Part 1: mathematical model

Reduced model for flow in DFM

Fractures

$$\nabla_\tau \cdot u_\ell^{\mathbb{f}} = f_\ell^{\mathbb{f}} \text{ in } \gamma_\ell,$$

Conservation of mass

$$u_\ell^{\mathbb{f}} = -\mathcal{K}_\ell^{\mathbb{f}} \nabla_\tau p_\ell^{\mathbb{f}} \text{ in } \gamma_\ell,$$

Darcy's law

$$\gamma^{\mathbb{f}} p_\ell^{\mathbb{f}} = g_\ell^{\mathbb{f},D} \text{ on } \Sigma_\ell^D,$$

$$\gamma_n^{\mathbb{f}} u_\ell^{\mathbb{f}} = q_\ell^{\mathbb{f},N} \text{ on } \Sigma_\ell^N.$$

Rock matrix

$$\nabla \cdot u_\alpha^{\mathbb{m}} = f_\alpha^{\mathbb{m}} \text{ in } \omega_\alpha,$$

Conservation of mass

$$u_\alpha^{\mathbb{m}} = -\mathcal{K}_\alpha^{\mathbb{m}} \nabla p_\alpha^{\mathbb{m}} \text{ in } \omega_\alpha,$$

Darcy's law

$$\gamma^{\mathbb{m}} p_\alpha^{\mathbb{m}} = g_\alpha^{\mathbb{m},D} \text{ on } \Gamma_\alpha^D,$$

$$\gamma_n^{\mathbb{m}} u^{\mathbb{m}} = q_\alpha^{\mathbb{m},N} \text{ on } \Gamma_\alpha^N.$$

+ other conditions:

- continuity of the hydraulic head at fracture-fracture intersections

$$\gamma^{\mathbb{f},\sigma} p_\ell^{\mathbb{f}}|_\sigma = \gamma^{\mathbb{f},\sigma} p_k^{\mathbb{f}}|_\sigma \text{ for } (\ell, k) \in \mathcal{I}_\sigma^2,$$

- outgoing flow from a fracture has to be equal to its neighbors incoming flow

$$\sum_{\ell \in \mathcal{I}_\sigma} \gamma_n^{\mathbb{f},\sigma} u_\ell^{\mathbb{f}} = 0, \text{ for each } \sigma \subset \Sigma.$$

- null flux at immersed fracture "tips".

M. Vohralík, J. Maryška, O. Severýn. *Applied Numerical Mathematics. An IMACS Journal.* **2007.**

Part 1: mathematical model

Reduced model for flow in DFM

Fractures

$$\nabla_\tau \cdot u_\ell^{\mathbb{f}} = [[u^{\mathbb{m}}]]_{|\gamma_\ell} + f_\ell^{\mathbb{f}} \text{ in } \gamma_\ell,$$

Conservation of mass

$$u_\ell^{\mathbb{f}} = -\mathcal{K}_\ell^{\mathbb{f}} \nabla_\tau p_\ell^{\mathbb{f}} \text{ in } \gamma_\ell,$$

Darcy's law

$$\gamma^{\mathbb{f}} p_\ell^{\mathbb{f}} = g_\ell^{\mathbb{f},D} \text{ on } \Sigma_\ell^D,$$

$$\gamma_n^{\mathbb{f}} u_\ell^{\mathbb{f}} = q_\ell^{\mathbb{f},N} \text{ on } \Sigma_\ell^N.$$

$$[[u^{\mathbb{m}}]]_{|\gamma_\ell} = \gamma_n^{\mathbb{m},+} u^{\mathbb{m}}_{\alpha_\ell^+} + \gamma^{\mathbb{m},-} u^{\mathbb{m}}_{\alpha_\ell^-}$$

Coupling (jump of flux)

Rock matrix

$$\nabla \cdot u_\alpha^{\mathbb{m}} = f_\alpha^{\mathbb{m}} \text{ in } \omega_\alpha,$$

Conservation of mass

$$u_\alpha^{\mathbb{m}} = -\mathcal{K}_\alpha^{\mathbb{m}} \nabla p_\alpha^{\mathbb{m}} \text{ in } \omega_\alpha,$$

Darcy's law

$$\gamma^{\mathbb{m}} p_\alpha^{\mathbb{m}} = g_\alpha^{\mathbb{m},D} \text{ on } \Gamma_\alpha^D,$$

$$\gamma_n^{\mathbb{m}} u^{\mathbb{m}} = q_\alpha^{\mathbb{m},N} \text{ on } \Gamma_\alpha^N.$$

+ other conditions:

- continuity of the hydraulic head at fracture-fracture intersections

$$\gamma^{\mathbb{f},\sigma} p_\ell^{\mathbb{f}}|_\sigma = \gamma^{\mathbb{f},\sigma} p_k^{\mathbb{f}}|_\sigma \text{ for } (\ell,k) \in \mathcal{I}_\sigma^2,$$

- outgoing flow from a fracture has to be equal to its neighbors incoming flow

$$\sum_{\ell \in \mathcal{I}_\sigma} \gamma_n^{\mathbb{f},\sigma} u_\ell^{\mathbb{f}} = 0, \text{ for each } \sigma \subset \Sigma.$$

- null flux at immersed fracture "tips".

M. Vohralík, J. Maryška, O. Severýn. *Applied Numerical Mathematics. An IMACS Journal.* **2007.**

V. Martin, J. Jaffré, J. E. Roberts. *SIAM Journal on Scientific Computing.* **2005.**

K. Brenner, M. Groza, C. Guichard, G. Lebeau, R. Masson. *Numerische Mathematik.* **2016.**

W. M. Boon, J. M. Nordbotten, I. Yotov. *SIAM Journal on Numerical Analysis.* **2018.**

L. Amir, M. Kern, J. E. Roberts, Z. Mghazli. *Applicable Analysis.* **2023**

Part 1: mathematical model

Reduced model for flow in DFM

Fractures

$$\nabla_\tau \cdot u_\ell^{\mathbb{f}} = [[u^{\mathbb{m}}]]_{|\gamma_\ell} + f_\ell^{\mathbb{f}} \text{ in } \gamma_\ell,$$

Conservation of mass

$$u_\ell^{\mathbb{f}} = -\mathcal{K}_\ell^{\mathbb{f}} \nabla_\tau p_\ell^{\mathbb{f}} \text{ in } \gamma_\ell,$$

Darcy's law

$$\gamma^{\mathbb{f}} p_\ell^{\mathbb{f}} = g_\ell^{\mathbb{f},D} \text{ on } \Sigma_\ell^D,$$

$$\gamma_n^{\mathbb{f}} u_\ell^{\mathbb{f}} = q_\ell^{\mathbb{f},N} \text{ on } \Sigma_\ell^N.$$

$$[[u^{\mathbb{m}}]]_{|\gamma_\ell} = \gamma_n^{\mathbb{m},+} u^{\mathbb{m}}_{\alpha_\ell^+} + \gamma^{\mathbb{m},-} u^{\mathbb{m}}_{\alpha_\ell^-}$$

Coupling (jump of flux)

$$\gamma^{\mathbb{m}} p^{\mathbb{m}}_{\alpha_\ell^+} = \gamma^{\mathbb{m}} p^{\mathbb{m}}_{\alpha_\ell^-} = p_\ell^{\mathbb{f}}$$

Continuous hydraulic head model

Rock matrix

$$\nabla \cdot u_\alpha^{\mathbb{m}} = f_\alpha^{\mathbb{m}} \text{ in } \omega_\alpha,$$

Conservation of mass

$$u_\alpha^{\mathbb{m}} = -\mathcal{K}_\alpha^{\mathbb{m}} \nabla p_\alpha^{\mathbb{m}} \text{ in } \omega_\alpha,$$

Darcy's law

$$\gamma^{\mathbb{m}} p_\alpha^{\mathbb{m}} = g_\alpha^{\mathbb{m},D} \text{ on } \Gamma_\alpha^D,$$

$$\gamma_n^{\mathbb{m}} u^{\mathbb{m}} = q_\alpha^{\mathbb{m},N} \text{ on } \Gamma_\alpha^N.$$

+ other conditions:

- continuity of the hydraulic head at fracture-fracture intersections

$$\gamma^{\mathbb{f},\sigma} p_\ell^{\mathbb{f}}|_\sigma = \gamma^{\mathbb{f},\sigma} p_k^{\mathbb{f}}|_\sigma \text{ for } (\ell,k) \in \mathcal{I}_\sigma^2,$$

- outgoing flow from a fracture has to be equal to its neighbors incoming flow

$$\sum_{\ell \in \mathcal{I}_\sigma} \gamma_n^{\mathbb{f},\sigma} u_\ell^{\mathbb{f}} = 0, \text{ for each } \sigma \subset \Sigma.$$

- null flux at immersed fracture "tips".

M. Vohralík, J. Maryška, O. Severýn. *Applied Numerical Mathematics. An IMACS Journal.* **2007.**

V. Martin, J. Jaffré, J. E. Roberts. *SIAM Journal on Scientific Computing.* **2005.**

K. Brenner, M. Groza, C. Guichard, G. Lebeau, R. Masson. *Numerische Mathematik.* **2016.**

W. M. Boon, J. M. Nordbotten, I. Yotov. *SIAM Journal on Numerical Analysis.* **2018.**

L. Amir, M. Kern, J. E. Roberts, Z. Mghazli. *Applicable Analysis.* **2023**

Part 1: mathematical model

Reduced model for flow in DFM

Fractures

$$\nabla_\tau \cdot u_\ell^{\mathbb{f}} = [[u^{\mathbb{m}}]]_{|\gamma_\ell} + f_\ell^{\mathbb{f}} \text{ in } \gamma_\ell,$$

Conservation of mass

$$u_\ell^{\mathbb{f}} = -\mathcal{K}_\ell^{\mathbb{f}} \nabla_\tau p_\ell^{\mathbb{f}} \text{ in } \gamma_\ell,$$

Darcy's law

$$\gamma^{\mathbb{f}} p_\ell^{\mathbb{f}} = g_\ell^{\mathbb{f},D} \text{ on } \Sigma_\ell^D,$$

$$\gamma_n^{\mathbb{f}} u_\ell^{\mathbb{f}} = q_\ell^{\mathbb{f},N} \text{ on } \Sigma_\ell^N.$$

$$[[u^{\mathbb{m}}]]_{|\gamma_\ell} = \gamma_n^{\mathbb{m},+} u^{\mathbb{m}}_{\alpha_\ell^+} + \gamma^{\mathbb{m},-} u^{\mathbb{m}}_{\alpha_\ell^-}$$

Coupling (jump of flux)

$$\gamma^{\mathbb{m}} p^{\mathbb{m}}_{\alpha_\ell^+} = \gamma^{\mathbb{m}} p^{\mathbb{m}}_{\alpha_\ell^-} = p_\ell^{\mathbb{f}}$$

Continuous hydraulic head model

Rock matrix

$$\nabla \cdot u_\alpha^{\mathbb{m}} = f_\alpha^{\mathbb{m}} \text{ in } \omega_\alpha,$$

Conservation of mass

$$u_\alpha^{\mathbb{m}} = -\mathcal{K}_\alpha^{\mathbb{m}} \nabla p_\alpha^{\mathbb{m}} \text{ in } \omega_\alpha,$$

Darcy's law

$$\gamma^{\mathbb{m}} p_\alpha^{\mathbb{m}} = g_\alpha^{\mathbb{m},D} \text{ on } \Gamma_\alpha^D,$$

$$\gamma_n^{\mathbb{m}} u^{\mathbb{m}} = q_\alpha^{\mathbb{m},N} \text{ on } \Gamma_\alpha^N.$$

Weak mixed formulation has a unique solution (u, p).

+ other conditions:

- continuity of the hydraulic head at fracture-fracture intersections

$$\gamma^{\mathbb{f},\sigma} p_\ell^{\mathbb{f}}|_\sigma = \gamma^{\mathbb{f},\sigma} p_k^{\mathbb{f}}|_\sigma \text{ for } (\ell, k) \in \mathcal{I}_\sigma^2,$$

- outgoing flow from a fracture has to be equal to its neighbors incoming flow

$$\sum_{\ell \in \mathcal{I}_\sigma} \gamma_n^{\mathbb{f},\sigma} u_\ell^{\mathbb{f}} = 0, \text{ for each } \sigma \subset \Sigma.$$

- null flux at immersed fracture "tips".

M. Vohralík, J. Maryška, O. Severýn. *Applied Numerical Mathematics. An IMACS Journal.* **2007.**

V. Martin, J. Jaffré, J. E. Roberts. *SIAM Journal on Scientific Computing.* **2005.**

K. Brenner, M. Groza, C. Guichard, G. Lebeau, R. Masson. *Numerische Mathematik.* **2016.**

W. M. Boon, J. M. Nordbotten, I. Yotov. *SIAM Journal on Numerical Analysis.* **2018.**

L. Amir, M. Kern, J. E. Roberts, Z. Mghazli. *Applicable Analysis.* **2023**

Part 1: mathematical model

M FE, unknowns and linear system

Part 1: mathematical model

M FE, unknowns and linear system

Mixed unknowns :

Part 1: mathematical model

M FE, unknowns and linear system

Mixed unknowns :

- Velocity (flux) : Raviart-Thomas-Nédélec lowest order ;

Part 1: mathematical model

M FE, unknowns and linear system

Mixed unknowns :

- Velocity (flux) : Raviart-Thomas-Nédélec lowest order ;
- Hydraulic head : piecewise constant functions ;

Part 1: mathematical model

MHFE, unknowns and linear system

H. Hoteit, A. Firoozabadi. *Advances in Water Resources.* **2008.**

Mixed-hybrid unknowns :

- Velocity (flux) : Raviart-Thomas-Nédélec lowest order ;
- Hydraulic head : piecewise constant functions ;
- Trace of hydraulic head : Lagrange multiplier, piecewise constant functions on the interior faces and all the edges.

Part 1: mathematical model

MHFE, unknowns and linear system

H. Hoteit, A. Firoozabadi. *Advances in Water Resources.* **2008.**

Mixed-hybrid unknowns :

- Velocity (flux) : Raviart-Thomas-Nédélec lowest order ;
- Hydraulic head : piecewise constant functions ;
- Trace of hydraulic head : Lagrange multiplier, piecewise constant functions on the interior faces and all the edges.

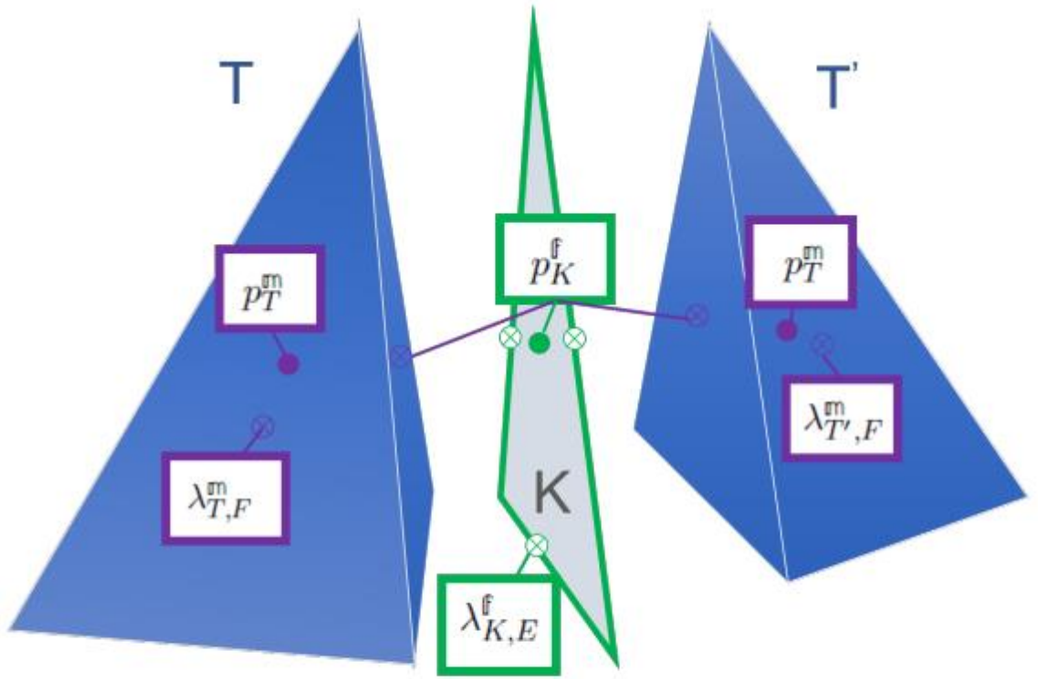

Rock matrix unknowns
Fracture unknowns

- Mean hydraulic head (fracture network)
- Mean hydraulic head (rock matrix)
- Trace of hydraulic head and fluxes (fracture network)
- Trace of hydraulic head and fluxes (rock matrix)

Part 1: mathematical model

MHFE, unknowns and linear system

H. Hoteit, A. Firoozabadi. *Advances in Water Resources.* **2008.**

Mixed-hybrid unknowns :

- Velocity (flux) : Raviart-Thomas-Nédélec lowest order ;
- Hydraulic head : piecewise constant functions ;
- Trace of hydraulic head : Lagrange multiplier, piecewise constant functions on the interior faces and all the edges.

Fluxes are eliminated locally.

Continuous hydraulic head model : $\lambda^{\mathrm{m}}_{T,F} = \lambda^{\mathrm{m}}_{T',F} = p^{\mathrm{f}}_{K}$.

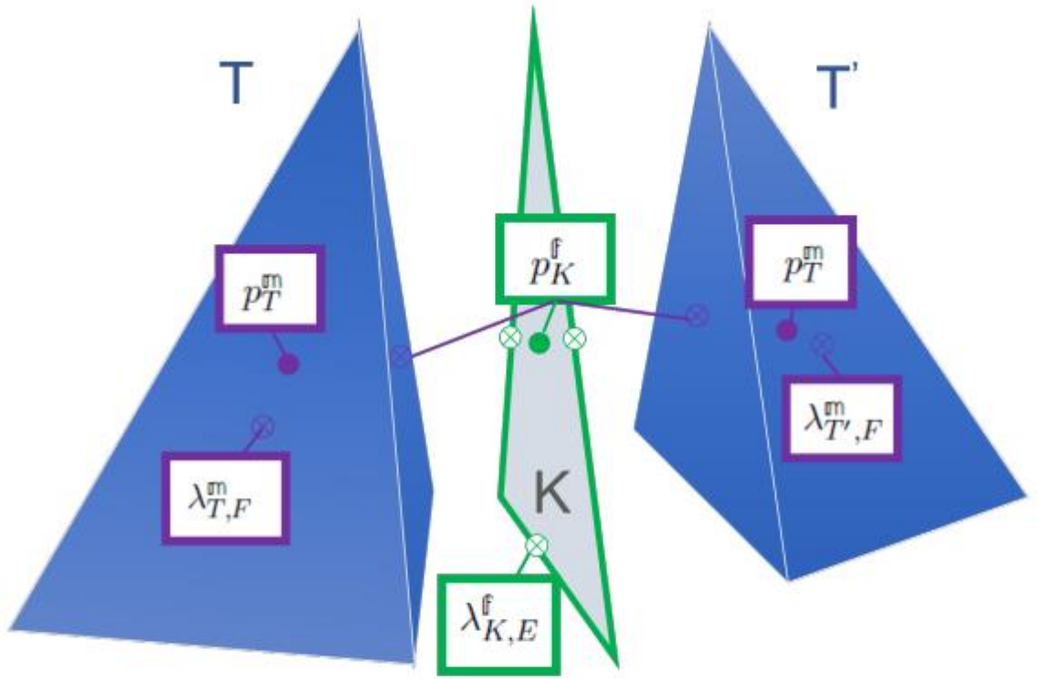

Part 1: mathematical model

MHFE, unknowns and linear system

Mixed-hybrid unknowns :

- Velocity (flux) : Raviart-Thomas-Nédélec lowest order ;
- Hydraulic head : piecewise constant functions ;
- Trace of hydraulic head : Lagrange multiplier, piecewise constant functions on the interior faces and all the edges.

Fluxes are eliminated locally.

Continuous hydraulic head model : $\lambda^{\mathfrak{m}}_{T,F} = \lambda^{\mathfrak{m}}_{T',F} = p^{\mathfrak{f}}_K$.

Schur complement (static condensation) → $\boldsymbol{P}^{\mathfrak{m}}$ **is eliminated.**

$$\begin{pmatrix} A^{\mathfrak{m},\mathfrak{m}} & A^{\mathfrak{m},\mathfrak{f}} & 0 \\ (A^{\mathfrak{m},\mathfrak{f}})^T & A^{\mathfrak{f},\mathfrak{f}} + D^{\mathfrak{f}} & -R^{\mathfrak{f}} \\ 0 & -(R^{\mathfrak{f}})^T & M^{\mathfrak{f}} \end{pmatrix} \begin{pmatrix} \boldsymbol{\Lambda}^{\mathfrak{m}} \\ \boldsymbol{P}^{\mathfrak{f}} \\ \boldsymbol{\Lambda}^{\mathfrak{f}} \end{pmatrix} = \begin{pmatrix} \tilde{\mathscr{F}}^{\mathfrak{m}} + \mathscr{V}^{\mathfrak{m}} \\ \tilde{\mathscr{F}}^{\mathfrak{m},\mathfrak{f}} + V^{\mathfrak{m},\mathfrak{f}} + \mathscr{F}^{\mathfrak{f}} \\ \mathscr{V}^{\mathfrak{f}} \end{pmatrix}$$

Square, sparse, symmetric and positive definite linear system.

H. Hoteit, A. Firoozabadi. *Advances in Water Resources.* **2008.**

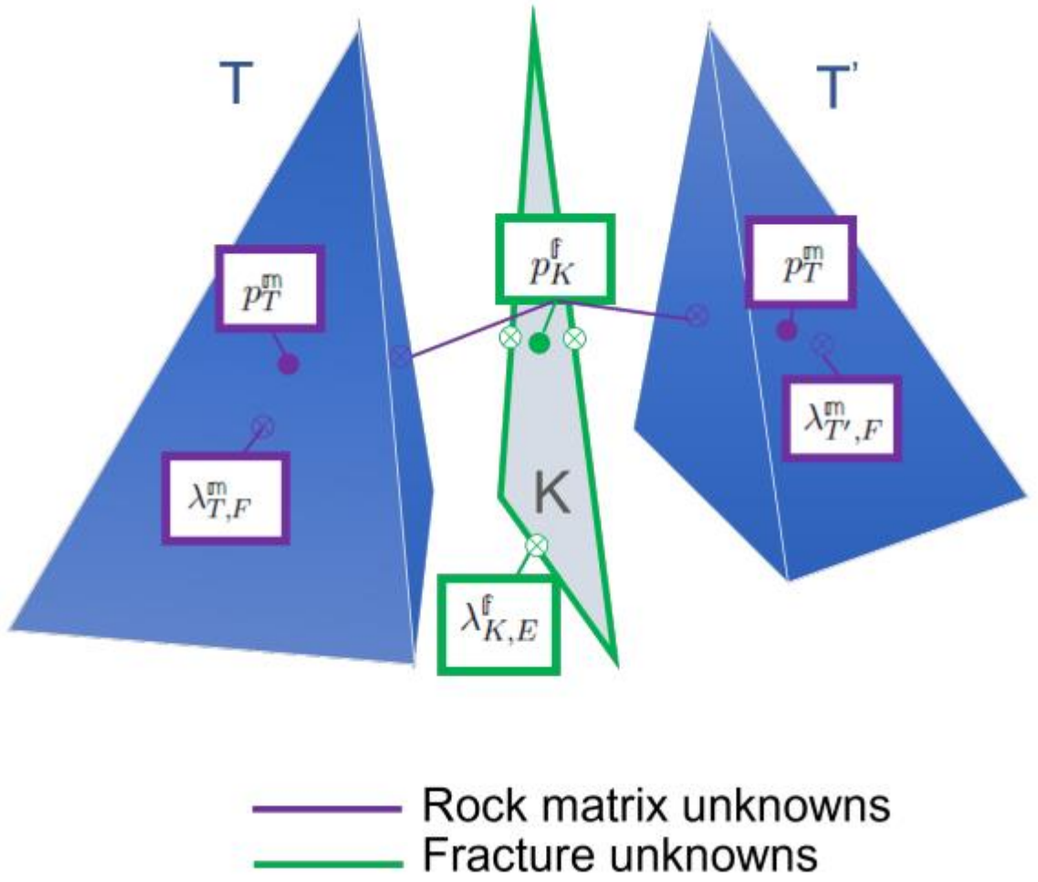

- Mean hydraulic head (fracture network)
- Mean hydraulic head (rock matrix)
- Trace of hydraulic head and fluxes (fracture network)
- Trace of hydraulic head and fluxes (rock matrix)

Part 1: mathematical model

MHFE, unknowns and linear system

H. Hoteit, A. Firoozabadi. *Advances in Water Resources.* **2008.**

Mixed-hybrid unknowns :

- Velocity (flux) : Raviart-Thomas-Nédélec lowest order ;
- Hydraulic head : piecewise constant functions ;
- Trace of hydraulic head : Lagrange multiplier, piecewise constant functions on the interior faces and all the edges.

Fluxes are eliminated locally.

Continuous hydraulic head model : $\lambda^{\mathfrak{m}}_{T,F} = \lambda^{\mathfrak{m}}_{T',F} = p^{\mathfrak{f}}_K$.

Schur complement (static condensation) → $\boldsymbol{P}^{\mathfrak{m}}$ **is eliminated.**

$$\begin{pmatrix} A^{\mathfrak{m},\mathfrak{m}} & A^{\mathfrak{m},\mathfrak{f}} & 0 \\ (A^{\mathfrak{m},\mathfrak{f}})^T & A^{\mathfrak{f},\mathfrak{f}} + D^{\mathfrak{f}} & -R^{\mathfrak{f}} \\ 0 & -(R^{\mathfrak{f}})^T & M^{\mathfrak{f}} \end{pmatrix} \begin{pmatrix} \boldsymbol{\Lambda}^{\mathfrak{m}} \\ \boldsymbol{P}^{\mathfrak{f}} \\ \boldsymbol{\Lambda}^{\mathfrak{f}} \end{pmatrix} = \begin{pmatrix} \tilde{\mathscr{F}}^{\mathfrak{m}} + \mathscr{V}^{\mathfrak{m}} \\ \tilde{\mathscr{F}}^{\mathfrak{m},\mathfrak{f}} + V^{\mathfrak{m},\mathfrak{f}} + \mathscr{F}^{\mathfrak{f}} \\ \mathscr{V}^{\mathfrak{f}} \end{pmatrix}$$

Square, sparse, symmetric and positive definite linear system.

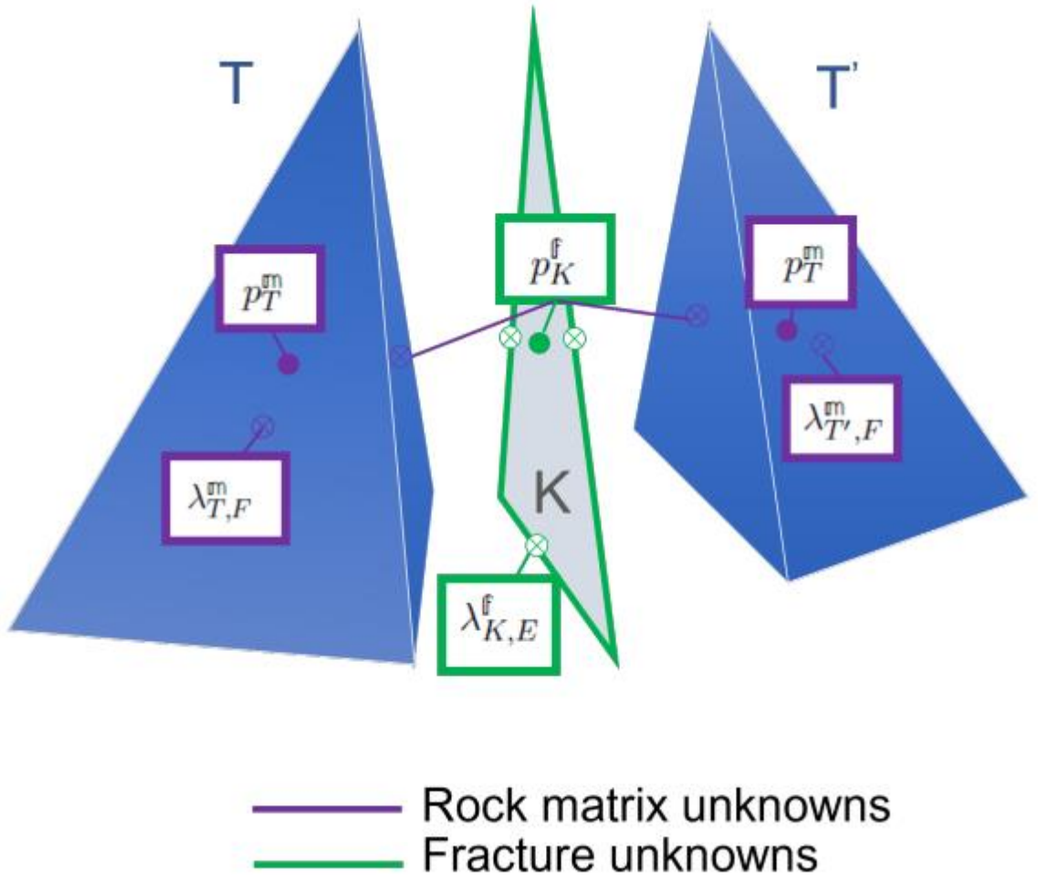

Part 1: mathematical model

MHFE, unknowns and linear system

H. Hoteit, A. Firoozabadi. *Advances in Water Resources.* **2008.**

Mixed-hybrid unknowns :

- Velocity (flux) : Raviart-Thomas-Nédélec lowest order ;
- Hydraulic head : piecewise constant functions ;
- Trace of hydraulic head : Lagrange multiplier, piecewise constant functions on the interior faces and all the edges.

Fluxes are eliminated locally.

Continuous hydraulic head model : $\lambda^{\mathfrak{m}}_{T,F} = \lambda^{\mathfrak{m}}_{T',F} = p^{\mathfrak{f}}_K$.

Schur complement (static condensation) → $\boldsymbol{P}^{\mathfrak{m}}$ **is eliminated.**

$$\begin{pmatrix} A^{\mathfrak{m},\mathfrak{m}} & A^{\mathfrak{m},\mathfrak{f}} & 0 \\ (A^{\mathfrak{m},\mathfrak{f}})^T & A^{\mathfrak{f},\mathfrak{f}} + D^{\mathfrak{f}} & -R^{\mathfrak{f}} \\ 0 & -(R^{\mathfrak{f}})^T & M^{\mathfrak{f}} \end{pmatrix} \begin{pmatrix} \boldsymbol{\Lambda}^{\mathfrak{m}} \\ \boldsymbol{P}^{\mathfrak{f}} \\ \boldsymbol{\Lambda}^{\mathfrak{f}} \end{pmatrix} = \begin{pmatrix} \tilde{\mathscr{F}}^{\mathfrak{m}} + \mathscr{V}^{\mathfrak{m}} \\ \tilde{\mathscr{F}}^{\mathfrak{m},\mathfrak{f}} + V^{\mathfrak{m},\mathfrak{f}} + \mathscr{F}^{\mathfrak{f}} \\ \mathscr{V}^{\mathfrak{f}} \end{pmatrix}$$

Square, sparse, symmetric and positive definite linear system.

Post-processing:

- $\boldsymbol{P}^{\mathfrak{m}}$ and fluxes are recovered on each tetrahedra and triangle.
- Velocity computed using fluxes and mixed FE basis functions.

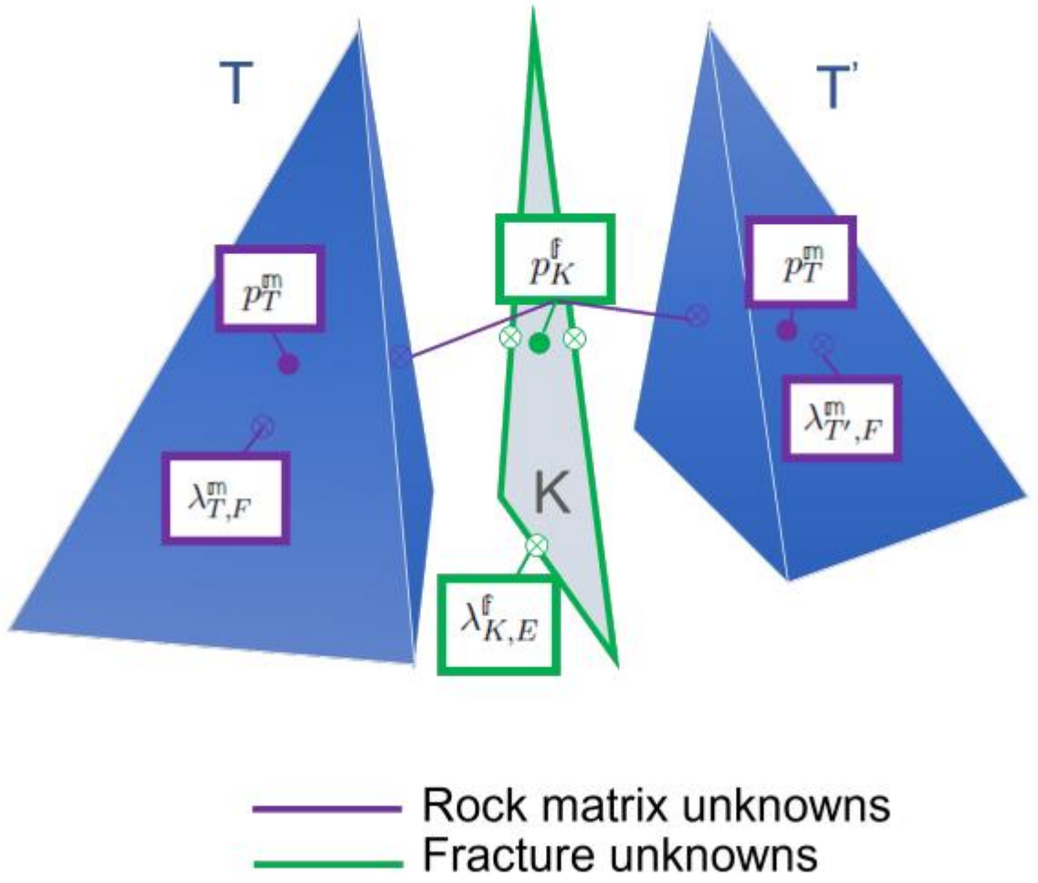

Part 2 :
Simulation framework

M. Kern, G. Pichot and D. Zegarra Vasquez. *Performance of algebraic preconditioners for large-scale simulations of single-phase flow in three-dimensional fractured porous media.* Pre-print hal-05029652. **2025.**

Part 2: simulation framework

Networks with a large number of fractures with a heterogeneous hydraulic conductivity / transmissivity ratio

Part 2: simulation framework

LabCom *fractory*:
- ❑ **Itasca Consultants (France)**
- ❑ **Géosciences Rennes**
- ❑ **CNRS**

Networks with a large number of fractures with a heterogeneous hydraulic conductivity / transmissivity ratio

Fractures = disks.

e.g.: L20 is a cube of side 20 m.

P. Davy, R. Le Goc, C. Darcel, O. Bour, J.-R. de Dreuzy, R. Munier. *Journal of Geophysical Research: Solid Earth.* **2010.**

P. Davy, R. Le Goc, and C. Darcel. *Journal of Geophysical Research: Solid Earth.* **2013.**

Part 2: simulation framework

LabCom *fractory*:
- ❑ Itasca Consultants (France)
- ❑ Géosciences Rennes
- ❑ CNRS

Networks with a large number of fractures with a heterogeneous hydraulic conductivity / transmissivity ratio

Fractures = disks.

e.g.: L20 is a cube of side 20 m.

P. Davy, R. Le Goc, C. Darcel, O. Bour, J.-R. de Dreuzy, R. Munier. *Journal of Geophysical Research: Solid Earth.* **2010.**

P. Davy, R. Le Goc, and C. Darcel. *Journal of Geophysical Research: Solid Earth.* **2013.**

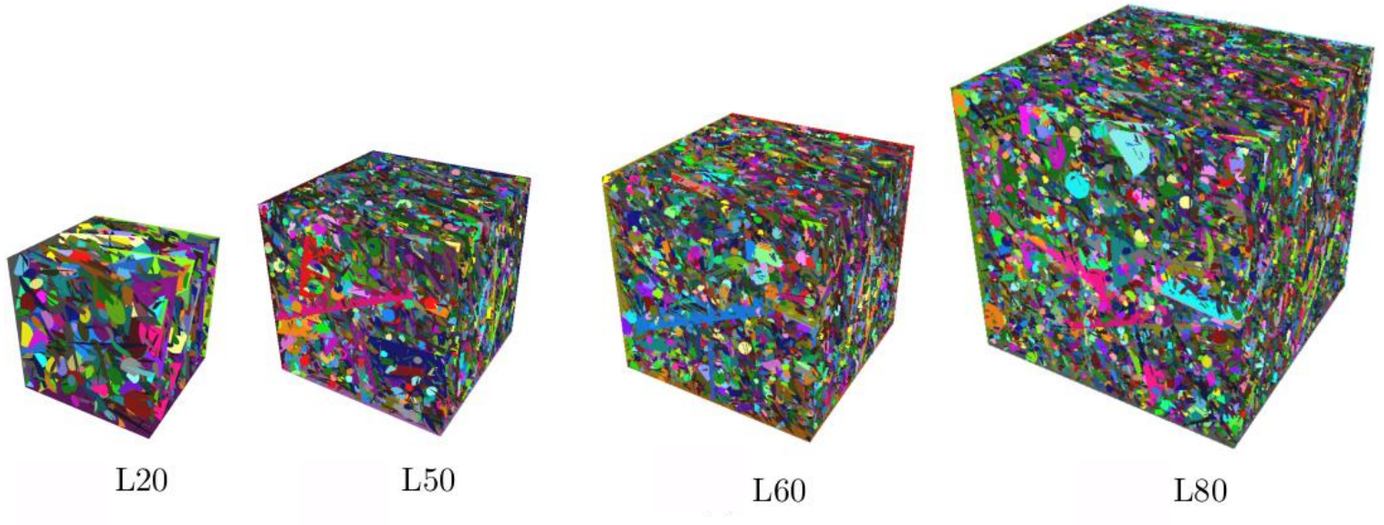

Part 2: simulation framework

LabCom *fractory*:
- ❑ Itasca Consultants (France)
- ❑ Géosciences Rennes
- ❑ CNRS

Networks with a large number of fractures with a heterogeneous hydraulic conductivity / transmissivity ratio

Fractures = disks.

e.g.: L20 is a cube of side 20 m.

P. Davy, R. Le Goc, C. Darcel, O. Bour, J.-R. de Dreuzy, R. Munier. *Journal of Geophysical Research: Solid Earth.* **2010.**

P. Davy, R. Le Goc, and C. Darcel. *Journal of Geophysical Research: Solid Earth.* **2013.**

Geometry name	# frac.
[L20-FPM]	2k
[L50-FPM]	23k
[L60-FPM]	40k
[L80-FPM]	90k
[L100-FPM]	174k
[L130-FPM]	377k
[L160-FPM]	697k

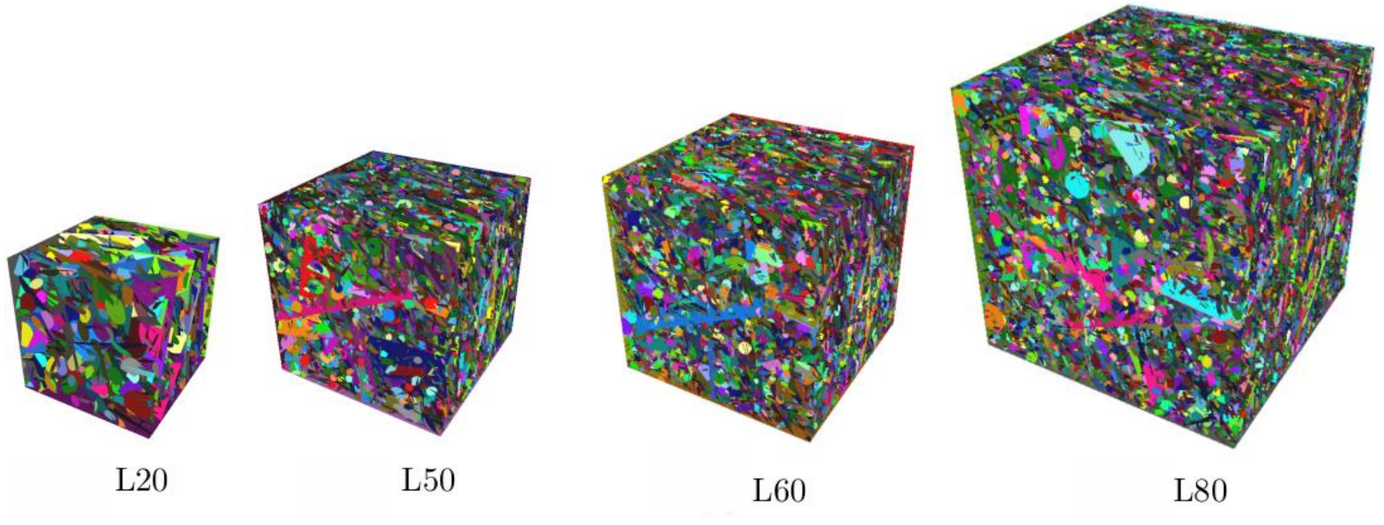

Part 2: simulation framework

LabCom *fractory*:
- ❑ Itasca Consultants (France)
- ❑ Géosciences Rennes
- ❑ CNRS

Networks with a large number of fractures with a heterogeneous hydraulic conductivity / transmissivity ratio

Fractures = disks.

e.g.: L20 is a cube of side 20 m.

P. Davy, R. Le Goc, C. Darcel, O. Bour, J.-R. de Dreuzy, R. Munier. *Journal of Geophysical Research: Solid Earth.* **2010.**

P. Davy, R. Le Goc, and C. Darcel. *Journal of Geophysical Research: Solid Earth.* **2013.**

Geometry name	# frac.
[L20-FPM]	2k
[L50-FPM]	23k
[L60-FPM]	40k
[L80-FPM]	90k
[L100-FPM]	174k
[L130-FPM]	377k
[L160-FPM]	697k

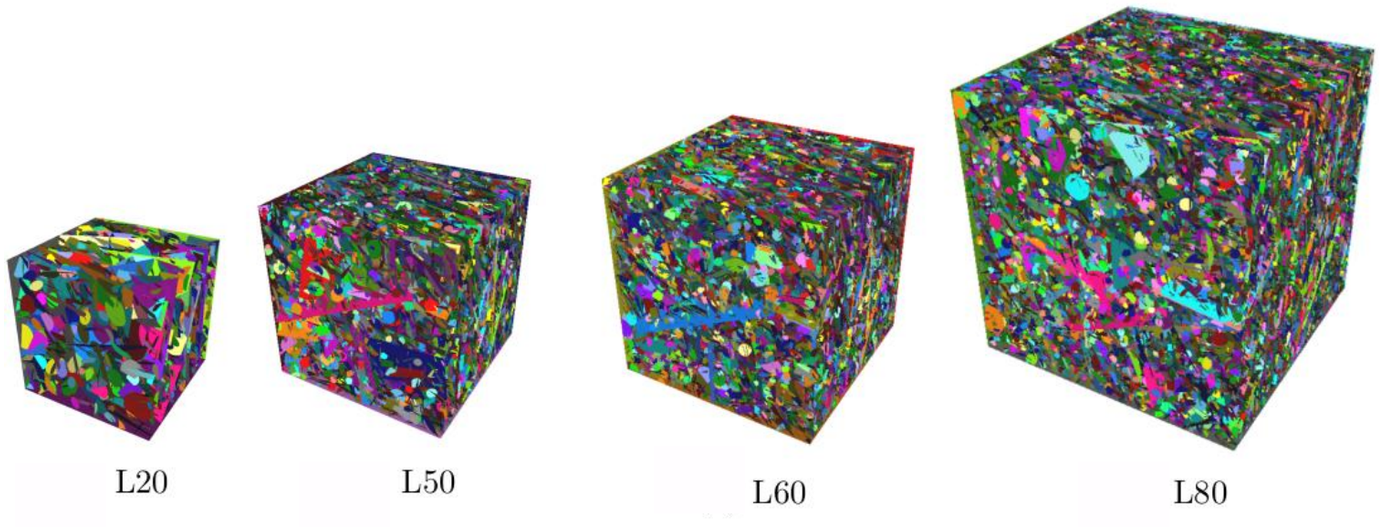

- **"1v100".** Rock matrix: K^m = 1 m/s. Fracture network: K^f = 100 m^2/s (the same for all fractures).

- **"heter".** Rock matrix: $K^m = 10^{-8}$ m/s. Fracture network: K^f takes one value per fracture in the range $[10^{-6}, 20]$ m^2/s (data from **LabCom *fractory***).

Part 2: simulation framework

Mesh generation with dedicated software

Part 2: simulation framework

Mesh generation with dedicated software

2D main challenge. Small angles, up to millions of fractures.

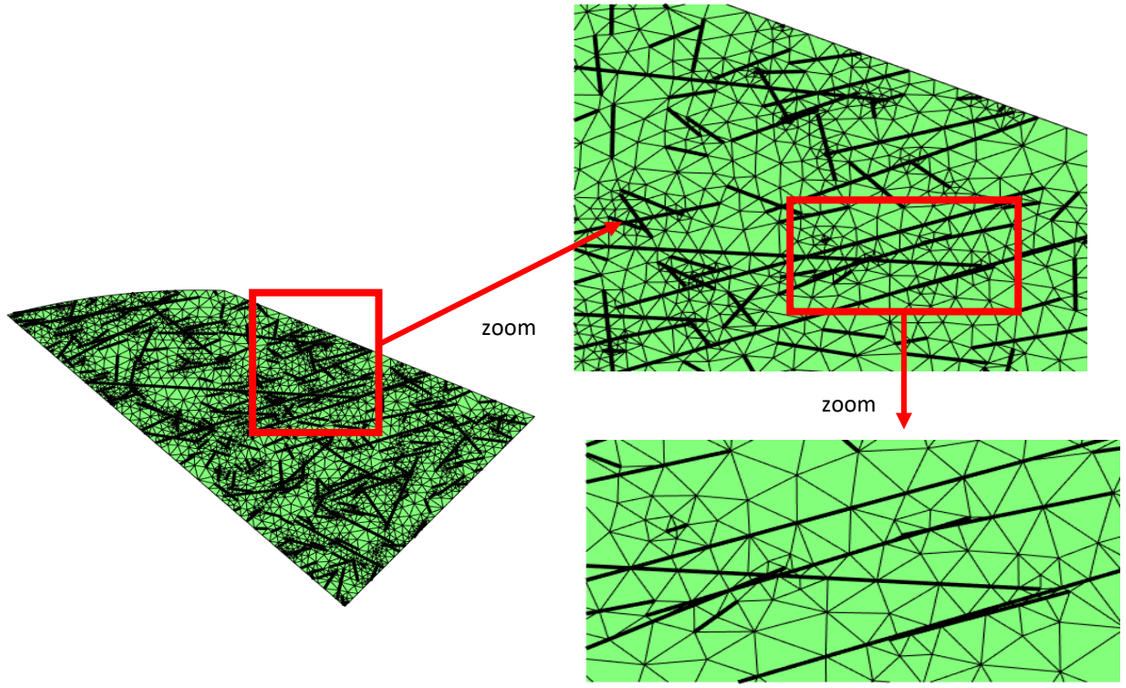

Part 2: simulation framework

Mesh generation with dedicated software

2D main challenge. Small angles, up to millions of fractures.

P. Laug, G. Pichot. *MASCOT IMACS Series in Computational and Applied Mathematics, Vol. 22.* **2018.**

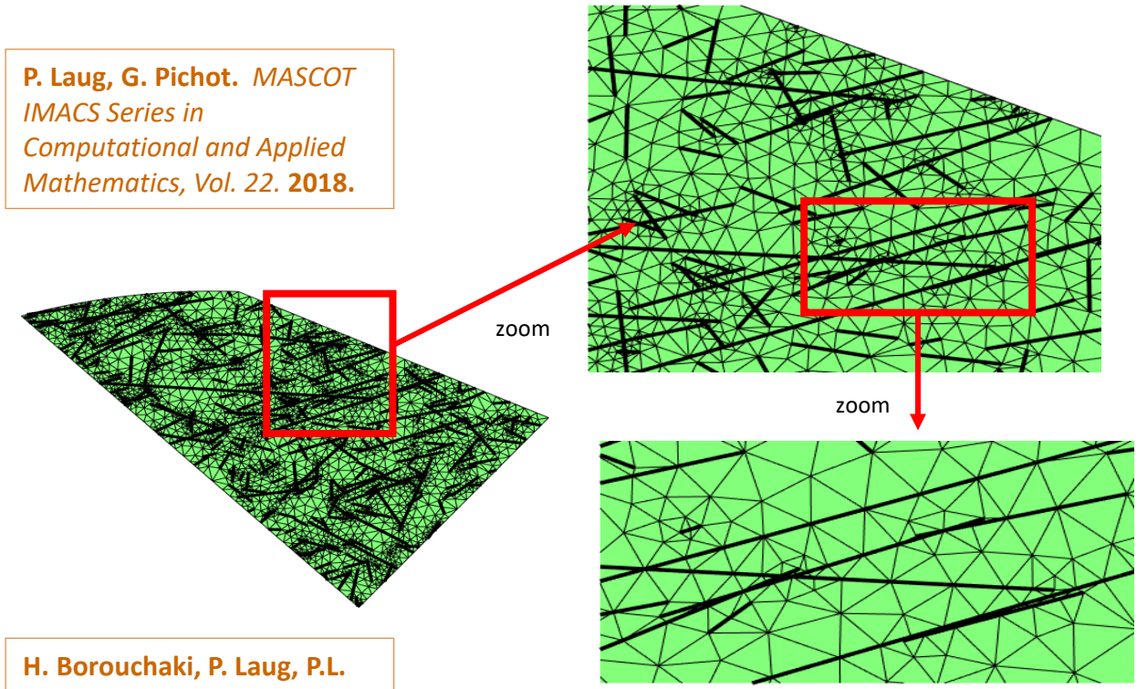

H. Borouchaki, P. Laug, P.L. George. *International Journal for Numerical Methods in Engineering.* **2000.**

MODFRAC

Inria Gamma, Serena & UTT.
Parallel unstructured surface mesh generator
with a user input minimum quality.

Part 2: simulation framework

Mesh generation with dedicated software

2D main challenge. Small angles, up to millions of fractures.

P. Laug, G. Pichot. *MASCOT IMACS Series in Computational and Applied Mathematics, Vol. 22.* **2018.**

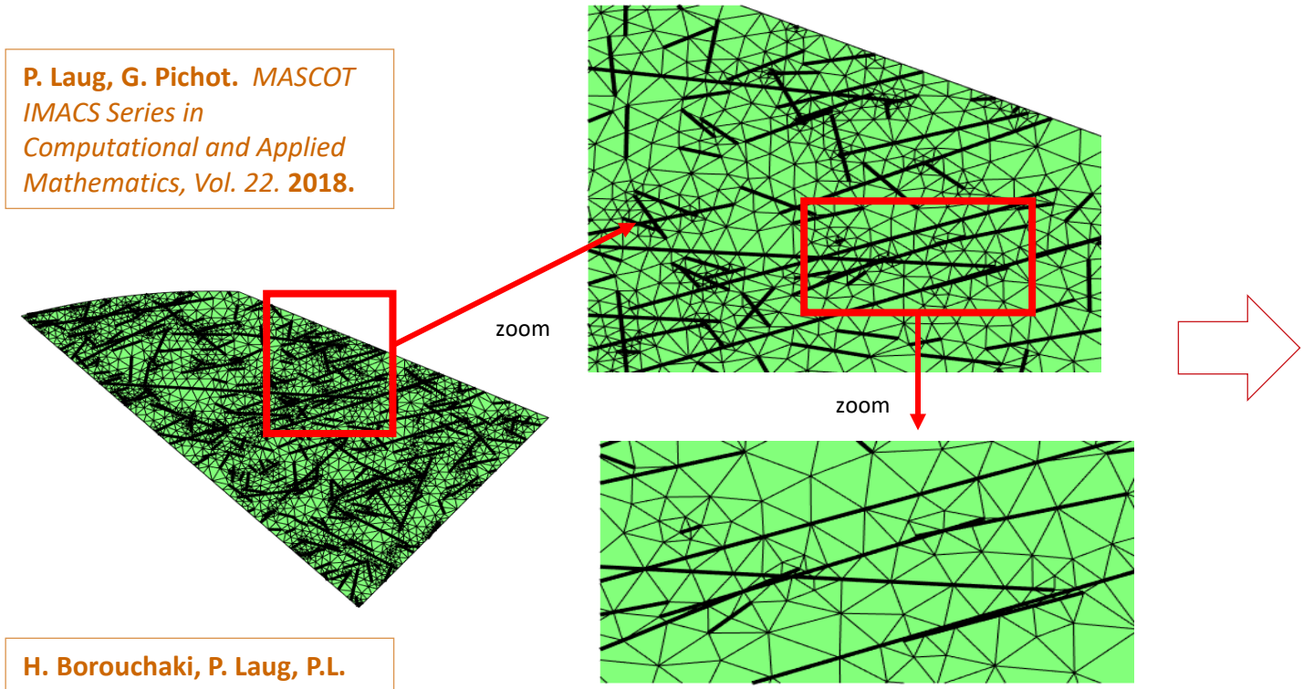

H. Borouchaki, P. Laug, P.L. George. *International Journal for Numerical Methods in Engineering.* **2000.**

MODFRAC

Inria Gamma, Serena & UTT.
Parallel unstructured surface mesh generator
with a user input minimum quality.

Part 2: simulation framework

Mesh generation with dedicated software

2D main challenge. Small angles, up to millions of fractures.

P. Laug, G. Pichot. *MASCOT IMACS Series in Computational and Applied Mathematics, Vol. 22.* **2018.**

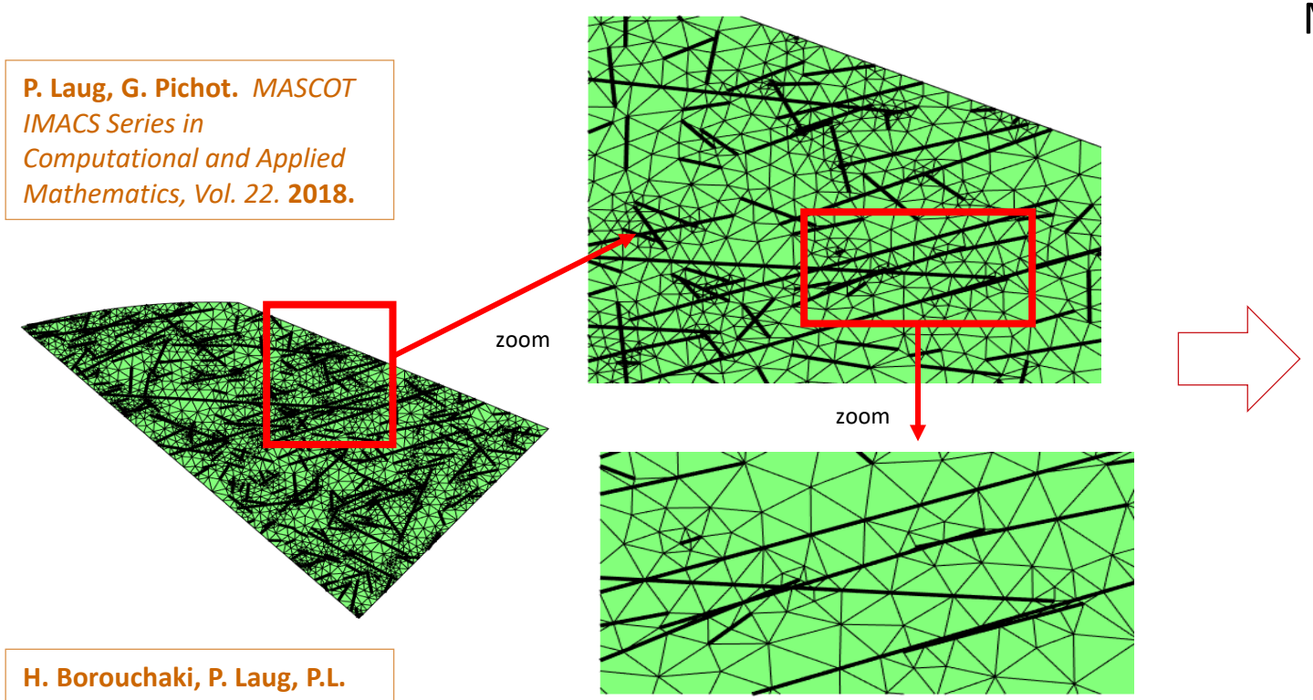

H. Borouchaki, P. Laug, P.L. George. *International Journal for Numerical Methods in Engineering.* **2000.**

MODFRAC

Inria Gamma, Serena & UTT.
Parallel unstructured surface mesh generator with a user input minimum quality.

3D main challenge. Use the triangular mesh generated by MODFRAC as an input to generate the tetrahedral mesh.

Part 2: simulation framework

Mesh generation with dedicated software

P.-L. George, H. Borouchaki, F. Alauzet, A. Loseille, P. Laug, L. Maréchal. *ISTE Group.* **2018.**

2D main challenge. Small angles, up to millions of fractures.

P. Laug, G. Pichot. *MASCOT IMACS Series in Computational and Applied Mathematics, Vol. 22.* **2018.**

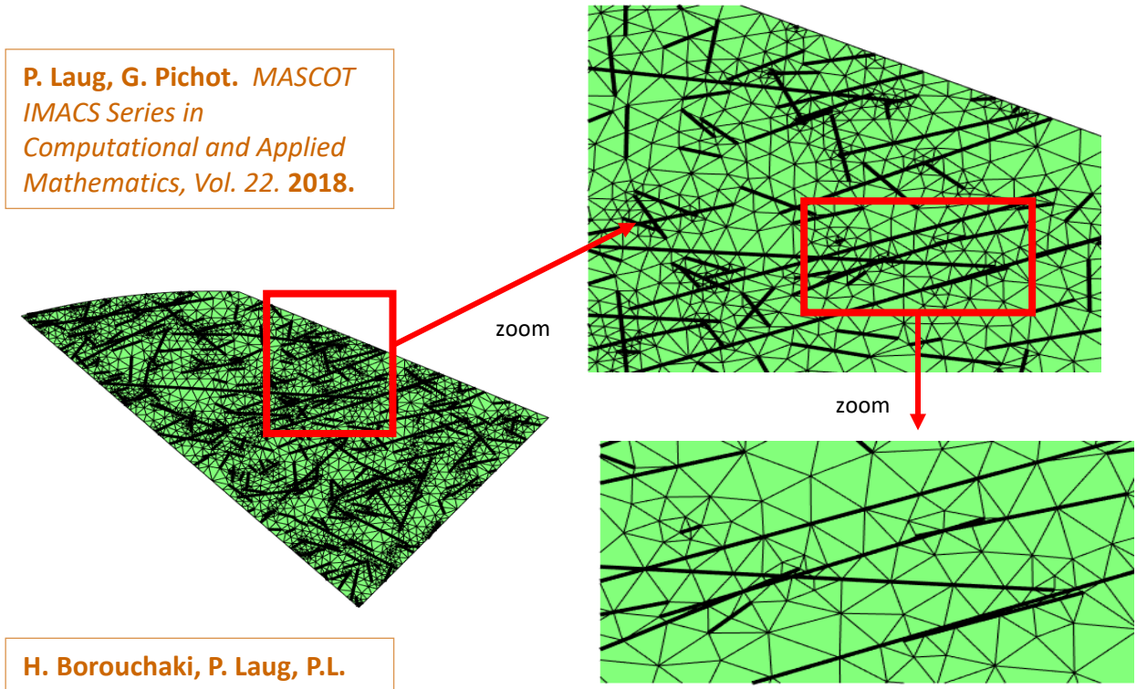

H. Borouchaki, P. Laug, P.L. George. *International Journal for Numerical Methods in Engineering.* **2000.**

MODFRAC

Inria Gamma, Serena & UTT.
Parallel unstructured surface mesh generator with a user input minimum quality.

3D main challenge. Use the triangular mesh generated by MODFRAC as an input to generate the tetrahedral mesh.

GHS3D

Inria Gamma.
Unstructured volume mesh generator.

Part 2: simulation framework

Mesh generation with dedicated software

P.-L. George, H. Borouchaki, F. Alauzet, A. Loseille, P. Laug, L. Maréchal. *ISTE Group.* **2018.**

2D main challenge. Small angles, up to millions of fractures.

P. Laug, G. Pichot. *MASCOT IMACS Series in Computational and Applied Mathematics, Vol. 22.* **2018.**

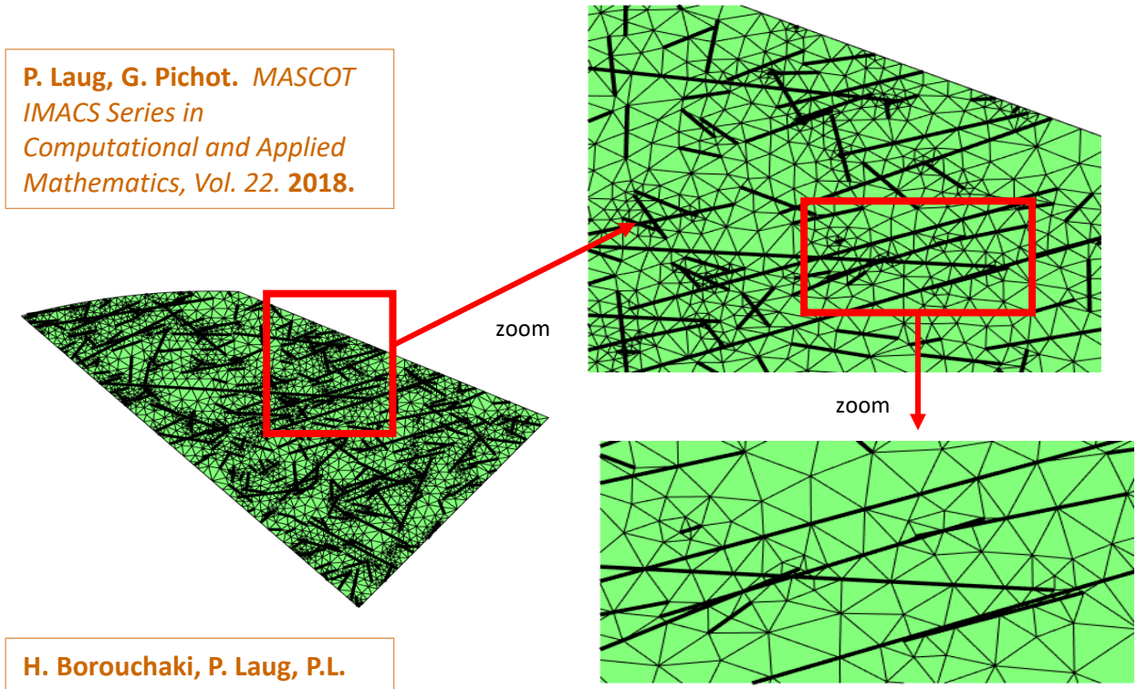

H. Borouchaki, P. Laug, P.L. George. *International Journal for Numerical Methods in Engineering.* **2000.**

MODFRAC

Inria Gamma, Serena & UTT.

Parallel unstructured surface mesh generator with a user input minimum quality.

3D main challenge. Use the triangular mesh generated by MODFRAC as an input to generate the tetrahedral mesh.

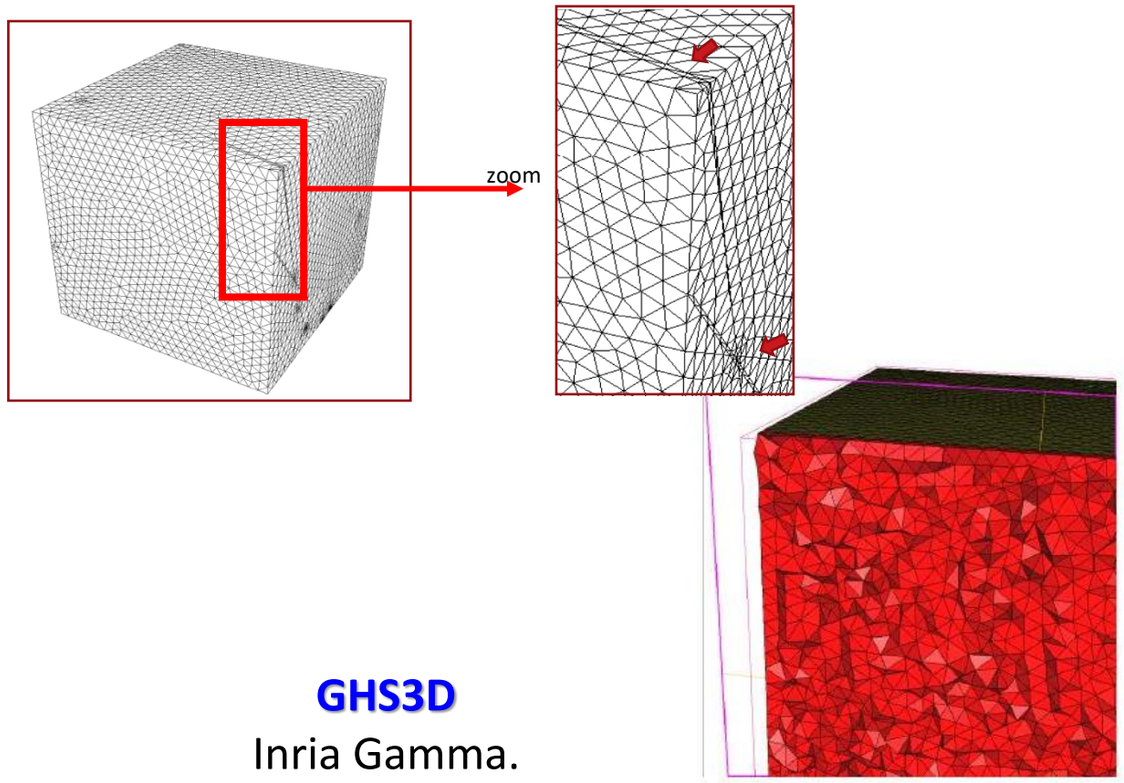

GHS3D

Inria Gamma.

Unstructured volume mesh generator.

Part 2: simulation framework

`nef-flow-fpm`: an MHFE MATLAB code - workflow

Part 2: simulation framework

`nef-flow-fpm`: an MHFE MATLAB code - workflow

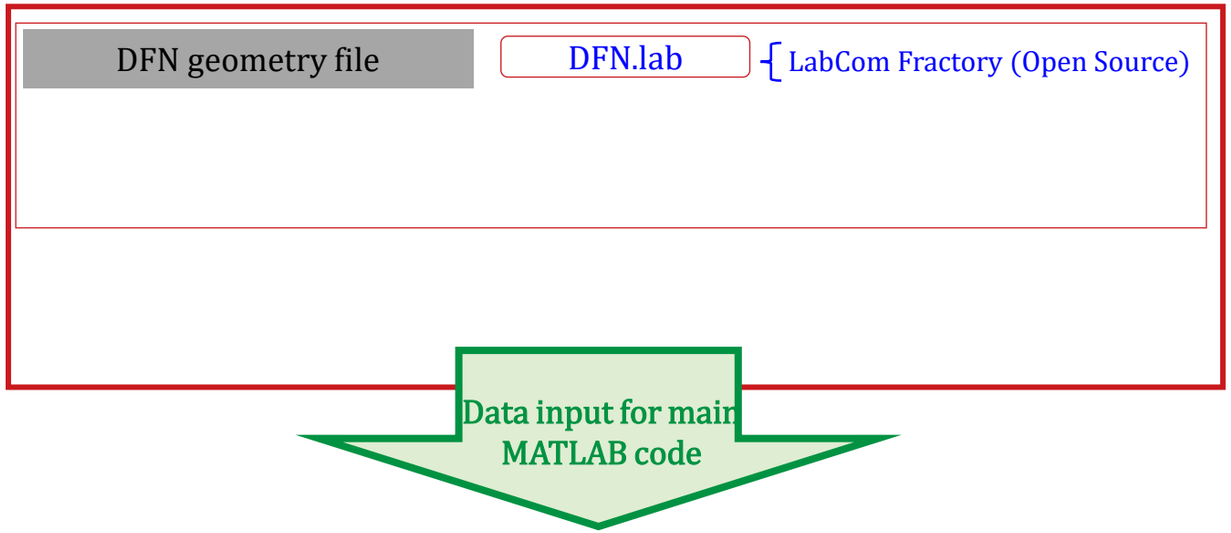

Part 2: simulation framework

`nef-flow-fpm`: an MHFE MATLAB code - workflow

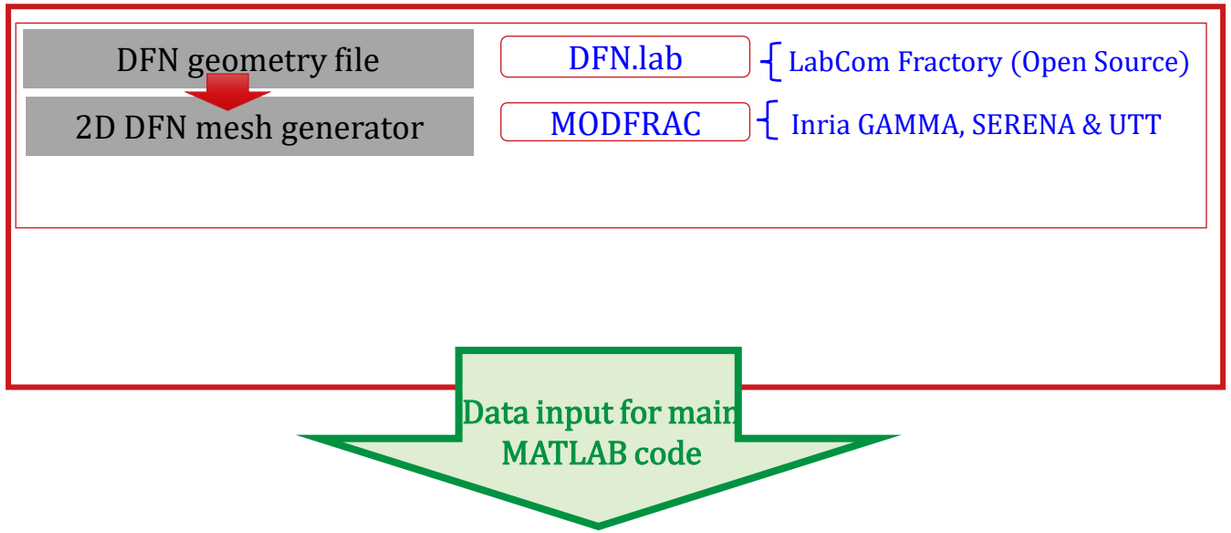

Part 2: simulation framework

`nef-flow-fpm`: an MHFE MATLAB code - workflow

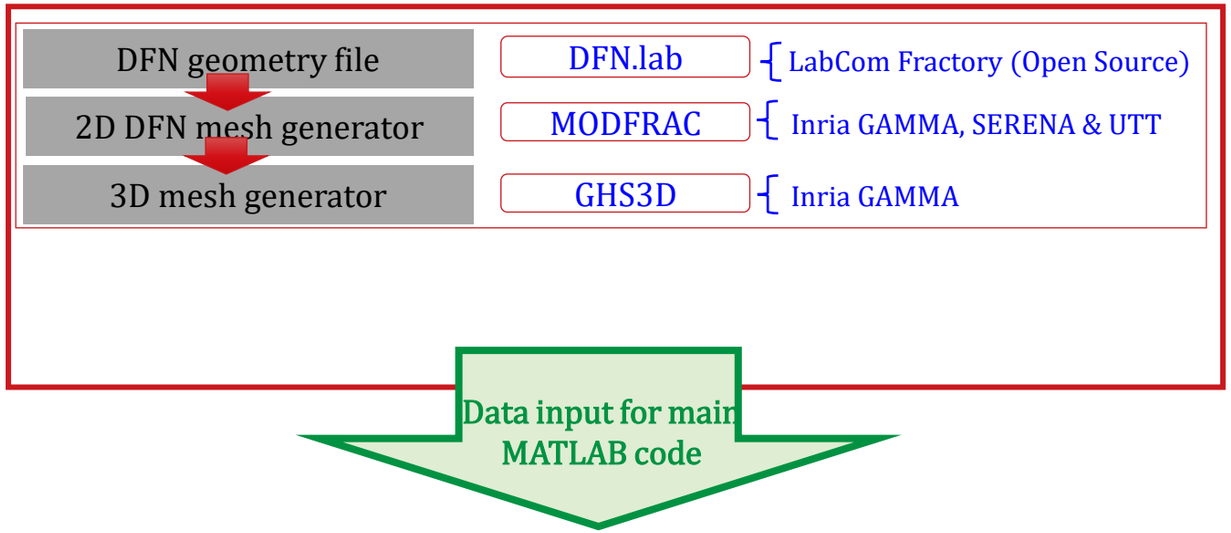

Part 2: simulation framework

`nef-flow-fpm`: an MHFE MATLAB code - workflow

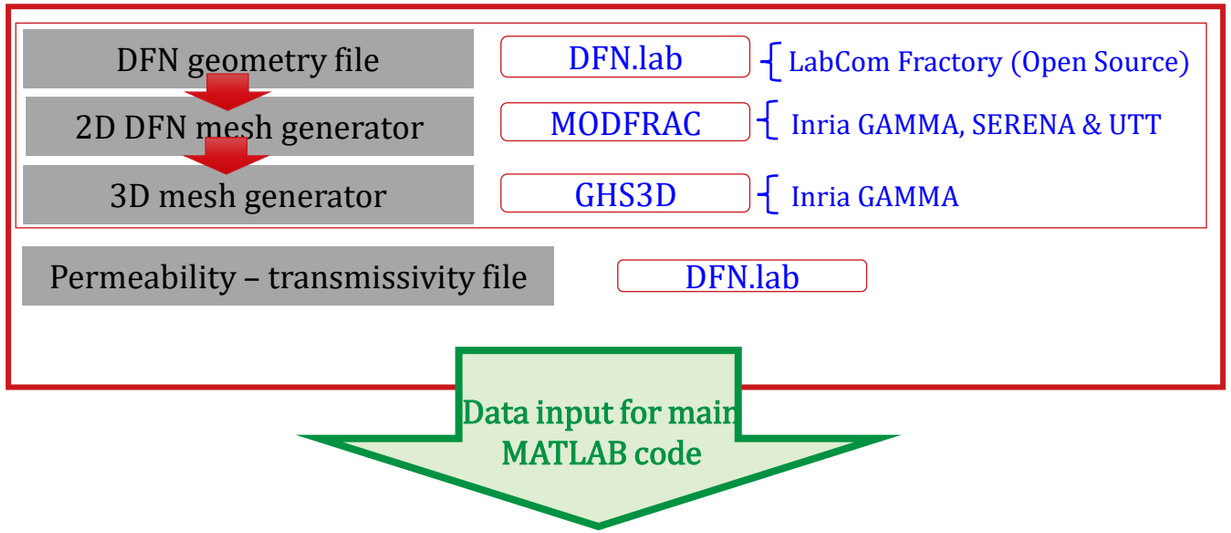

Part 2: simulation framework

`nef-flow-fpm`: an MHFE MATLAB code - workflow

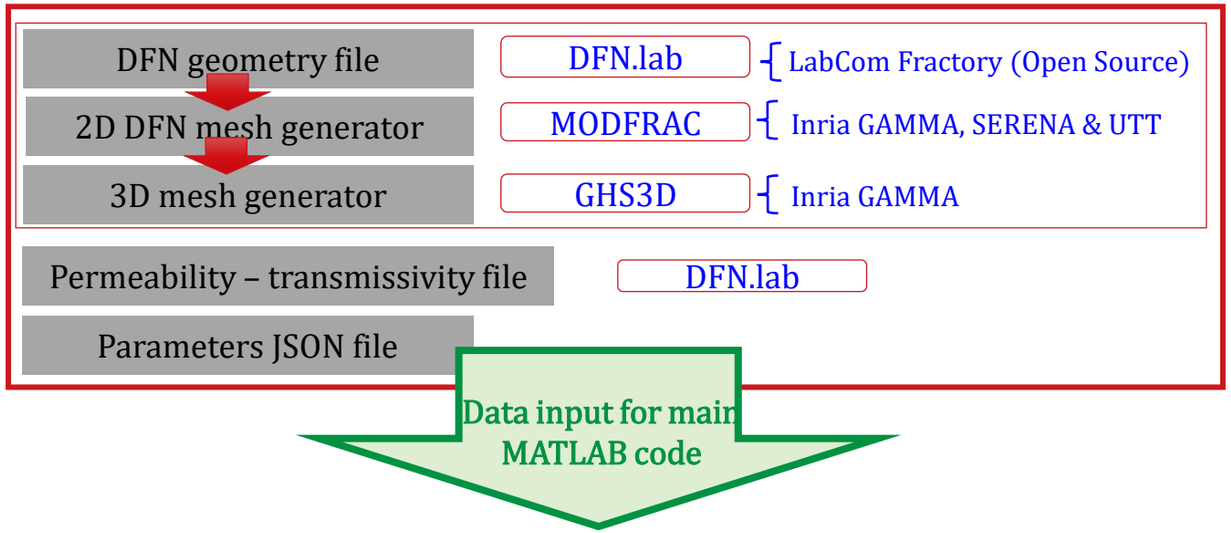

Part 2: simulation framework

`nef-flow-fpm`: an MHFE MATLAB code - workflow

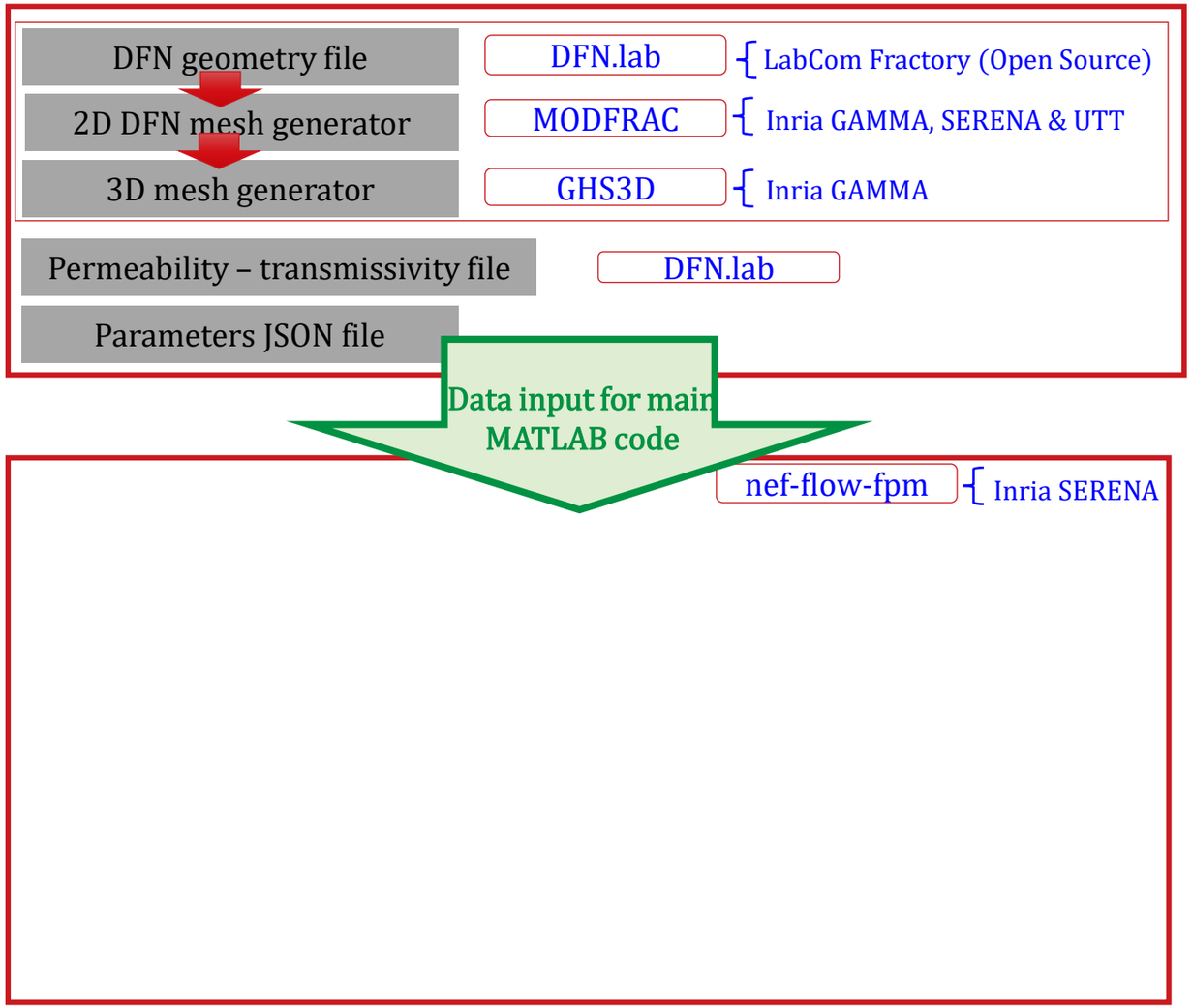

Part 2: simulation framework

`nef-flow-fpm`: an MHFE MATLAB code - workflow

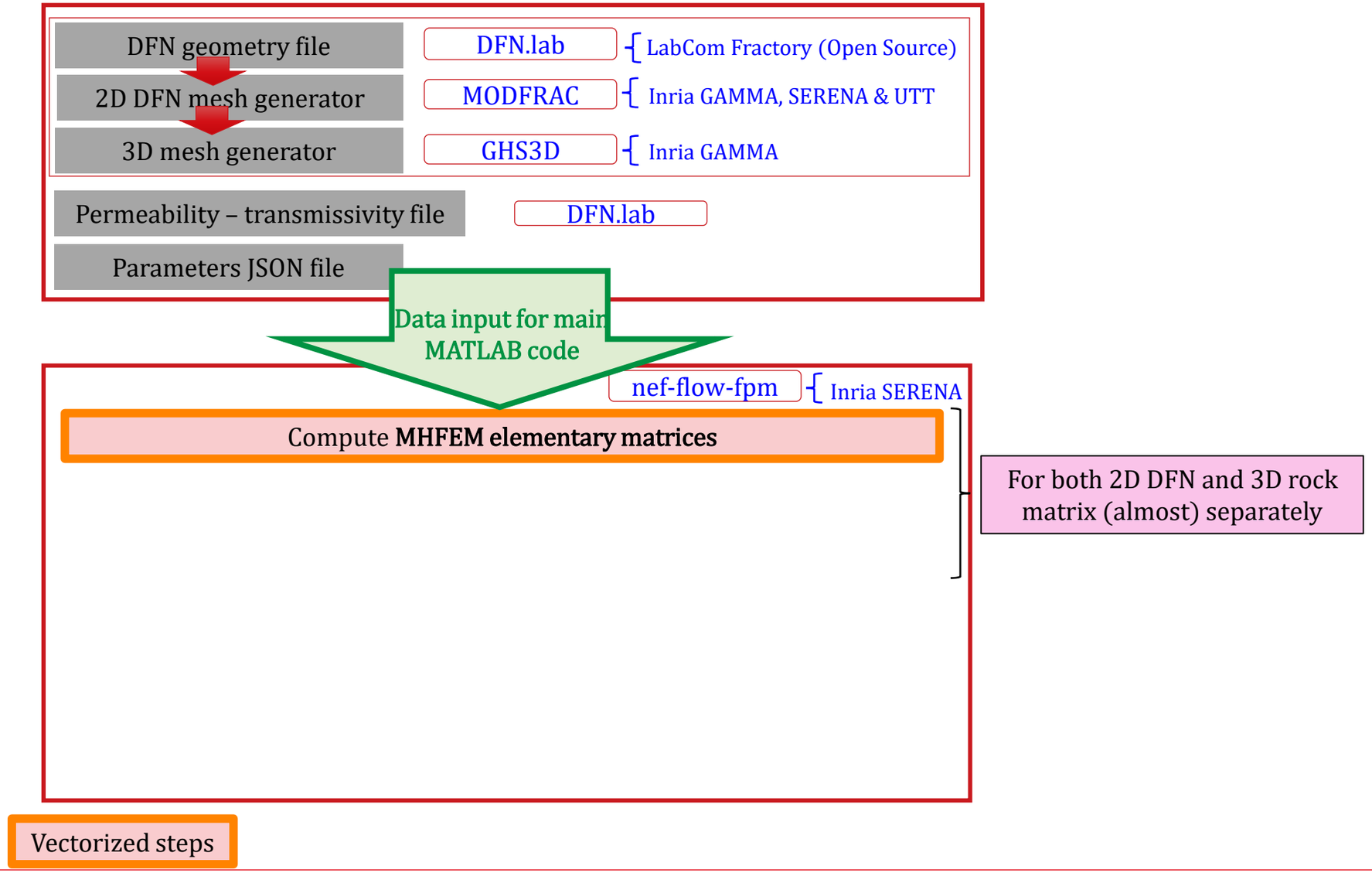

Part 2: simulation framework

`nef-flow-fpm`: an MHFE MATLAB code - workflow

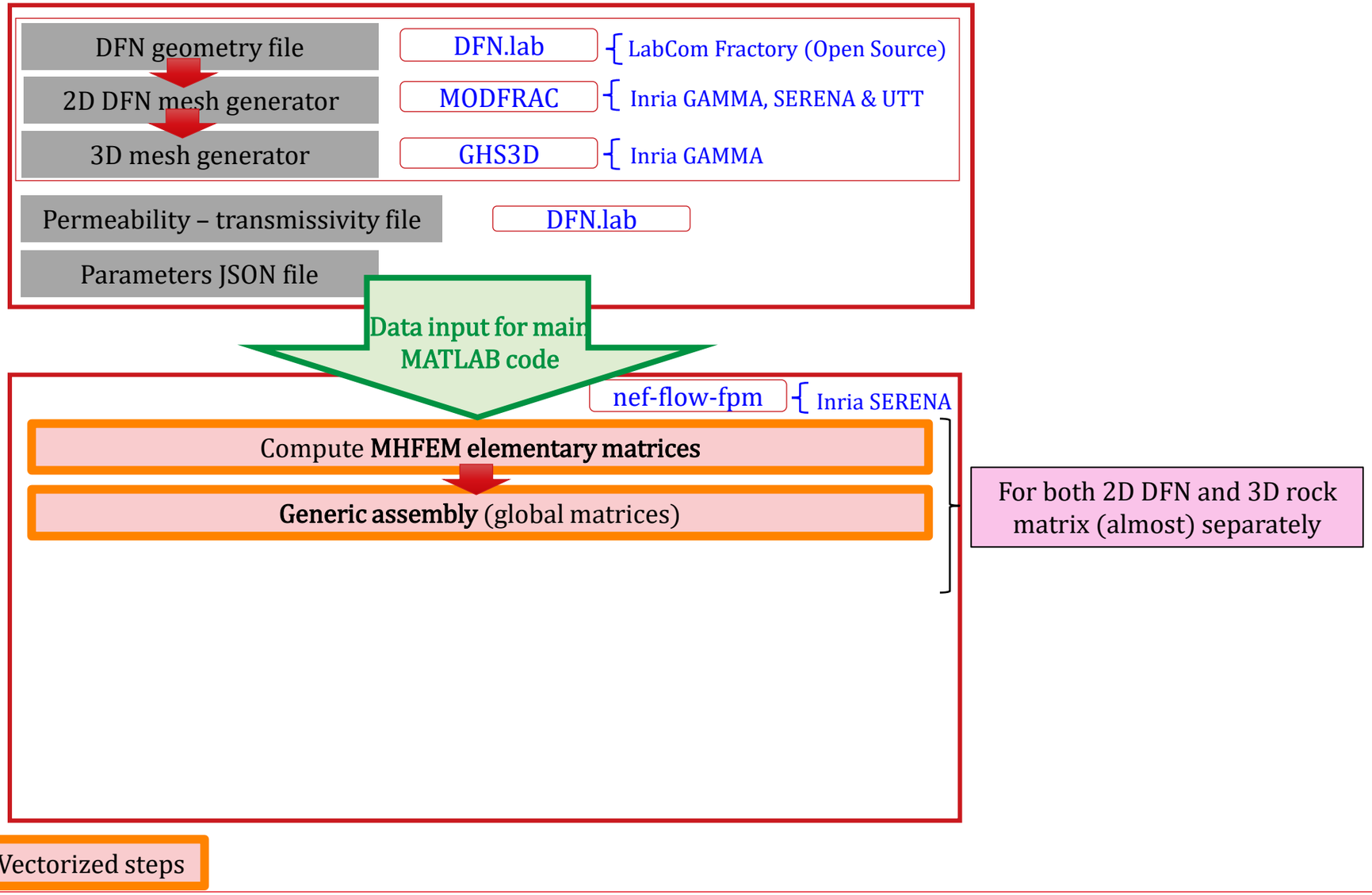

Part 2: simulation framework

`nef-flow-fpm`: an MHFE MATLAB code - workflow

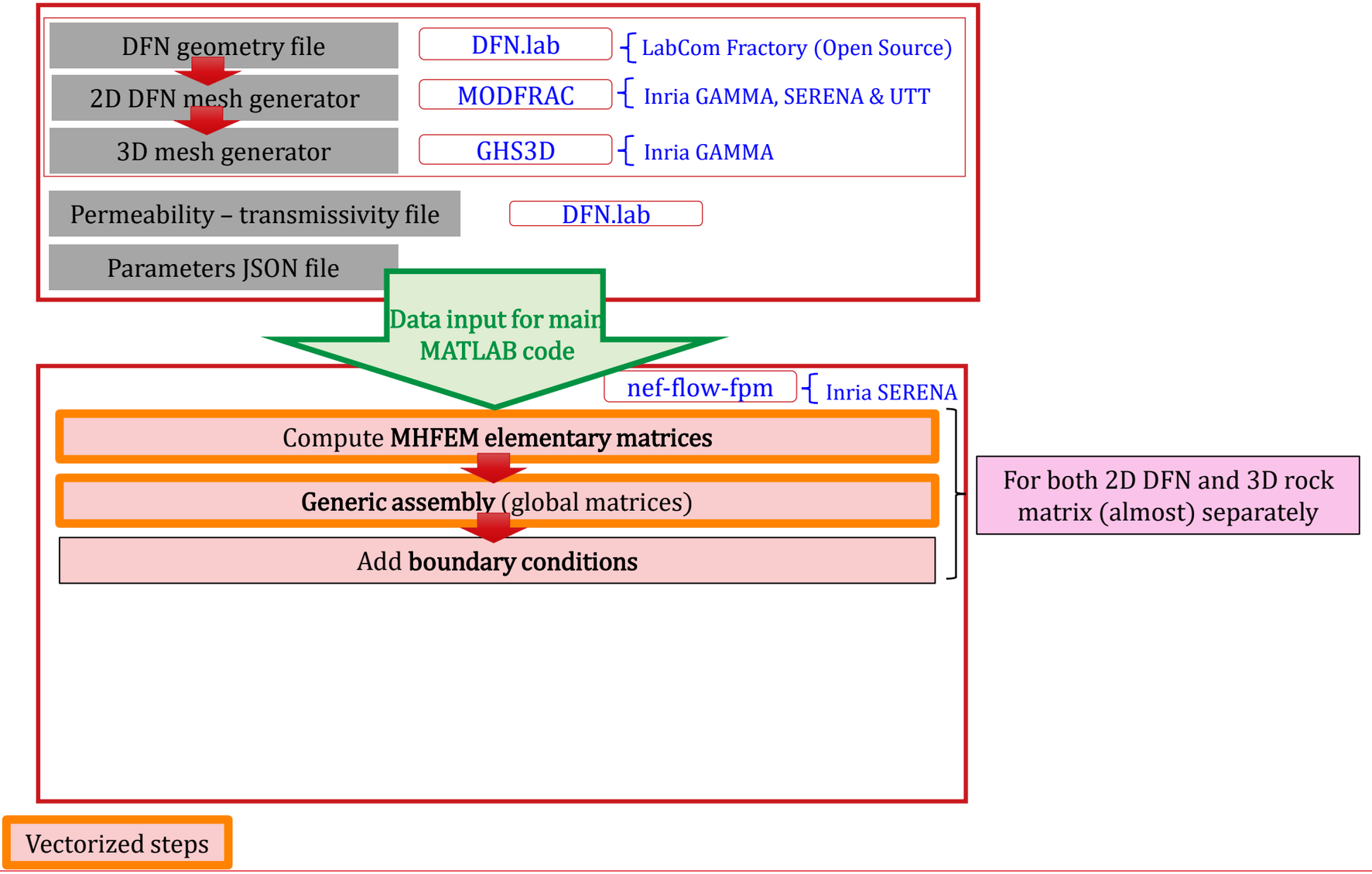

Part 2: simulation framework

`nef-flow-fpm`: an MHFE MATLAB code - workflow

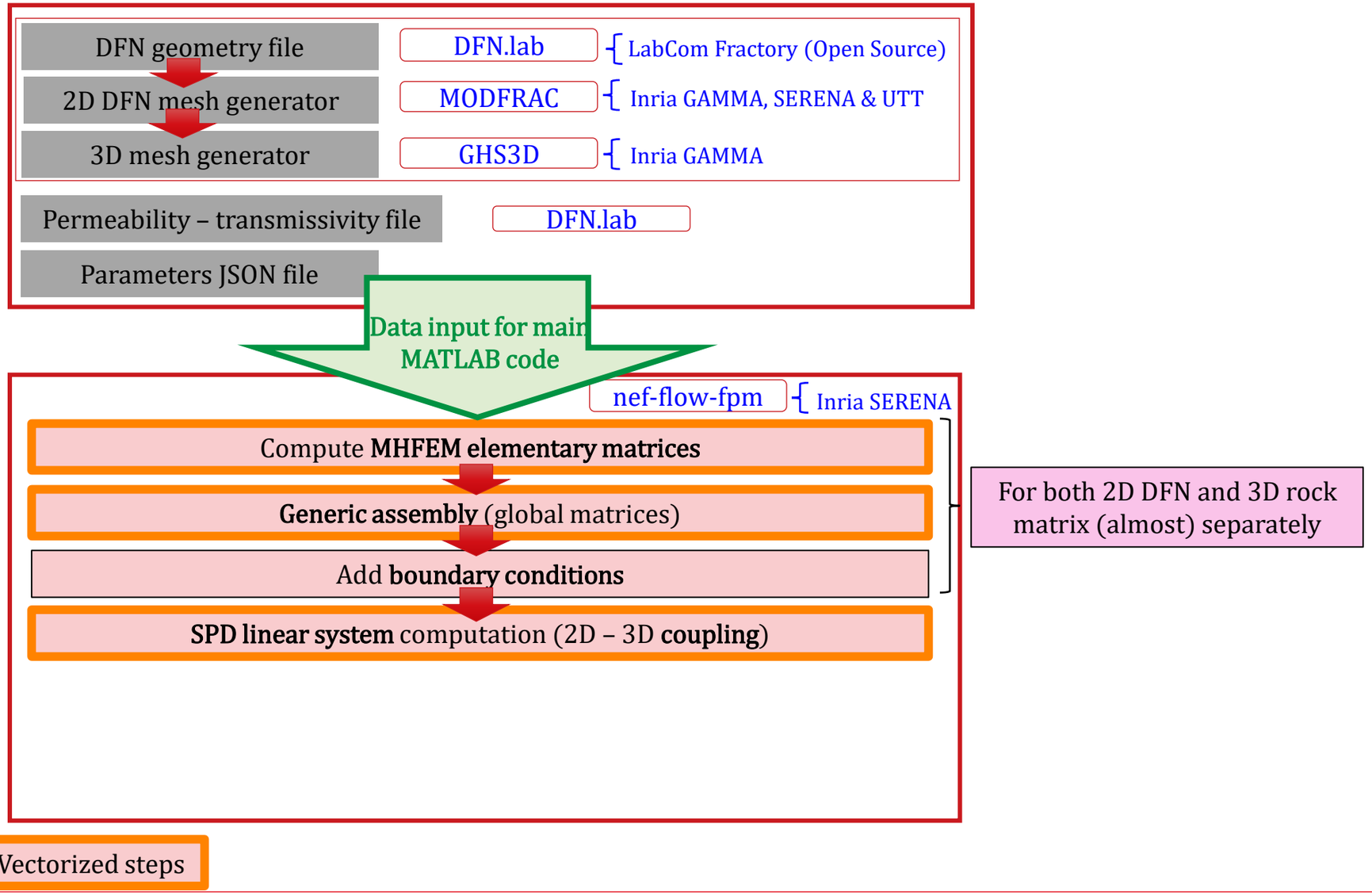

Part 2: simulation framework

`nef-flow-fpm`: an MHFE MATLAB code - workflow

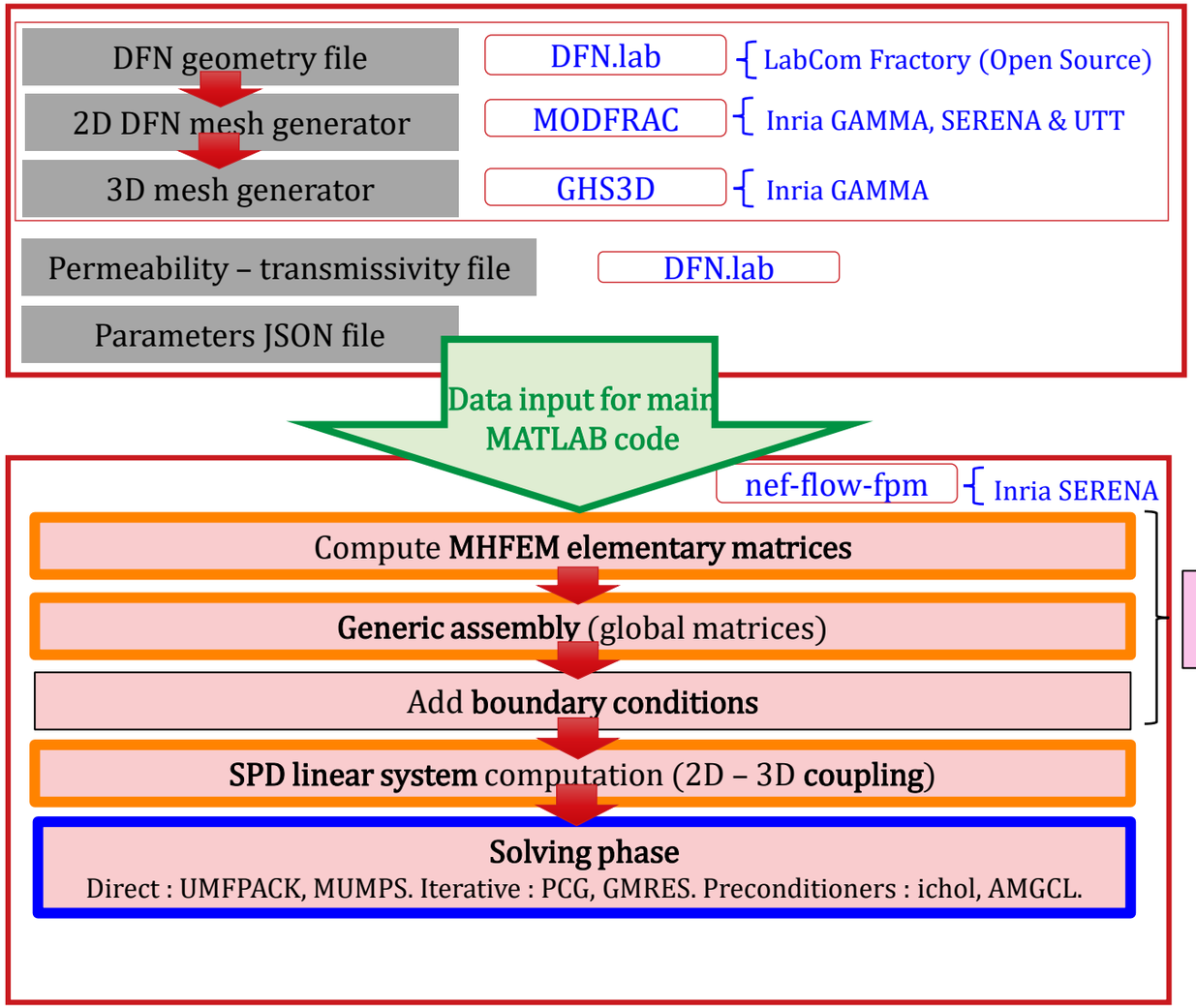

T. A. Davis. *ACM Transactions on Mathematical Software.* **2004.**

P. R. Amestoy, I. S. Duff, J. Koster, J.-Y. l'Excellent. *SIAM Journal on Matrix Analysis and Applications.* **2001.**

D. Demidov. *Lobachevskii Journal of Mathematics.* **2019.**

Part 2: simulation framework

`nef-flow-fpm`: an MHFE MATLAB code - workflow

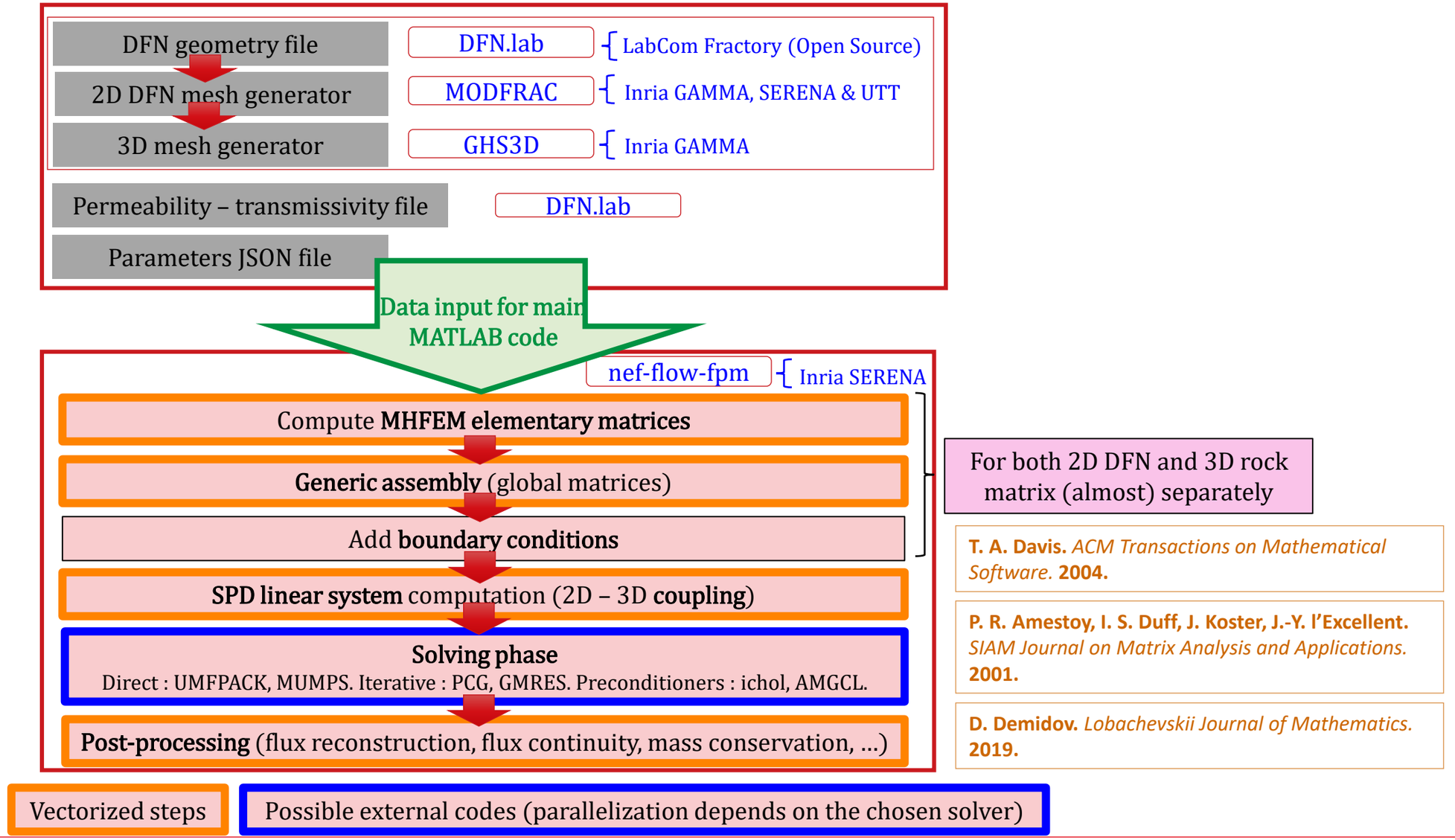

T. A. Davis. *ACM Transactions on Mathematical Software.* **2004.**

P. R. Amestoy, I. S. Duff, J. Koster, J.-Y. l'Excellent. *SIAM Journal on Matrix Analysis and Applications.* **2001.**

D. Demidov. *Lobachevskii Journal of Mathematics.* **2019.**

Part 2: simulation framework

`nef-flow-fpm`: an MHFE MATLAB code - workflow

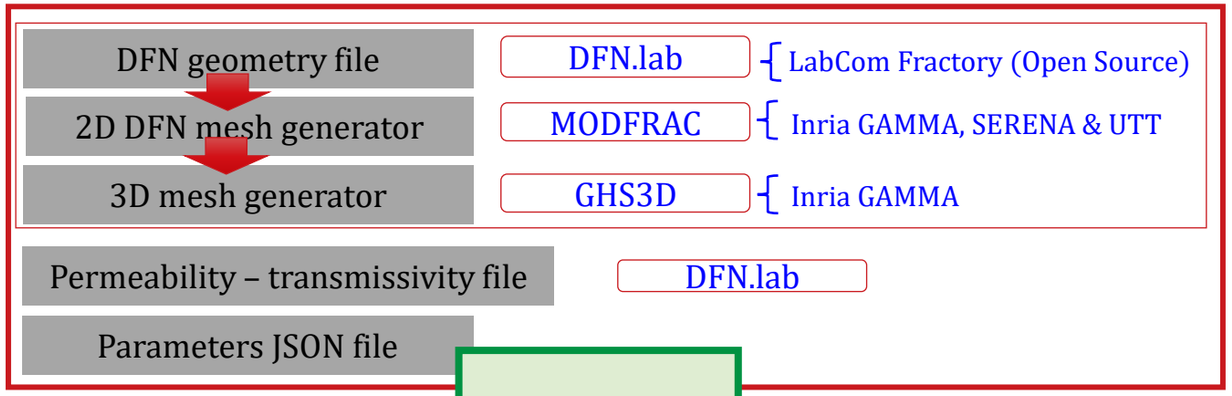

Data input for main MATLAB code

nef-flow-fpm — Inria SERENA

- Compute **MHFEM elementary matrices**
- **Generic assembly** (global matrices)
- Add **boundary conditions**
- **SPD linear system** computation (2D – 3D **coupling**)
- **Solving phase**
  Direct : UMFPACK, MUMPS. Iterative : PCG, GMRES. Preconditioners : ichol, AMGCL.
- **Post-processing** (flux reconstruction, flux continuity, mass conservation, …)

For both 2D DFN and 3D rock matrix (almost) separately

Code validation :

- **T. A. Davis.** *ACM Transactions on Mathematical Software.* **2004.**
- **P. R. Amestoy, I. S. Duff, J. Koster, J.-Y. l'Excellent.** *SIAM Journal on Matrix Analysis and Applications.* **2001.**
- **D. Demidov.** *Lobachevskii Journal of Mathematics.* **2019.**

Vectorized steps

Possible external codes (parallelization depends on the chosen solver)

Part 2: simulation framework

`nef-flow-fpm`: an MHFE MATLAB code - workflow

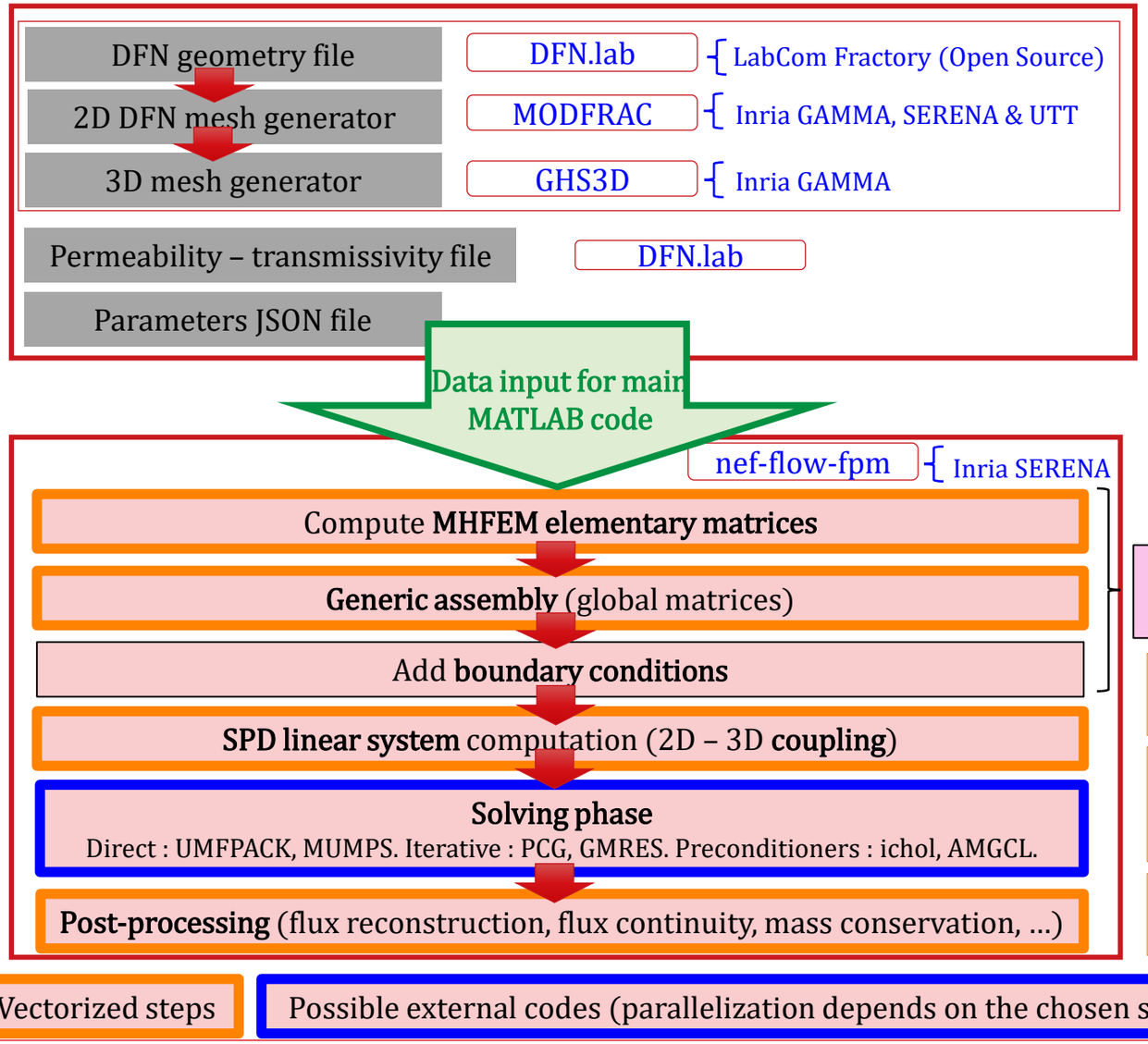

Code validation :
- benchmark ;

I. Berre, W. M. Boon, B. Flemisch, A. Fumagalli, D. Gläser, E. Keilegavlen, A. Scotti, I. Stefansson, A. Tatomir, K. Brenner, S. Burbullah, P. Devloo, O. Duran, M. Favino, J. Hennicker, I. Lee, K. Lipnikov, R. Masson, K. Mosthaf, M. G. C. Nestola, C. Ni, K. Nikitin, P. Schälde, D. Svyatskiy, R. Yanbarisov, P. Zulian. *Advances in Water Resources.* **2021.**

For both 2D DFN and 3D rock matrix (almost) separately

T. A. Davis. *ACM Transactions on Mathematical Software.* **2004.**

P. R. Amestoy, I. S. Duff, J. Koster, J.-Y. l'Excellent. *SIAM Journal on Matrix Analysis and Applications.* **2001.**

D. Demidov. *Lobachevskii Journal of Mathematics.* **2019.**

Part 2: simulation framework

`nef-flow-fpm`: an MHFE MATLAB code - workflow

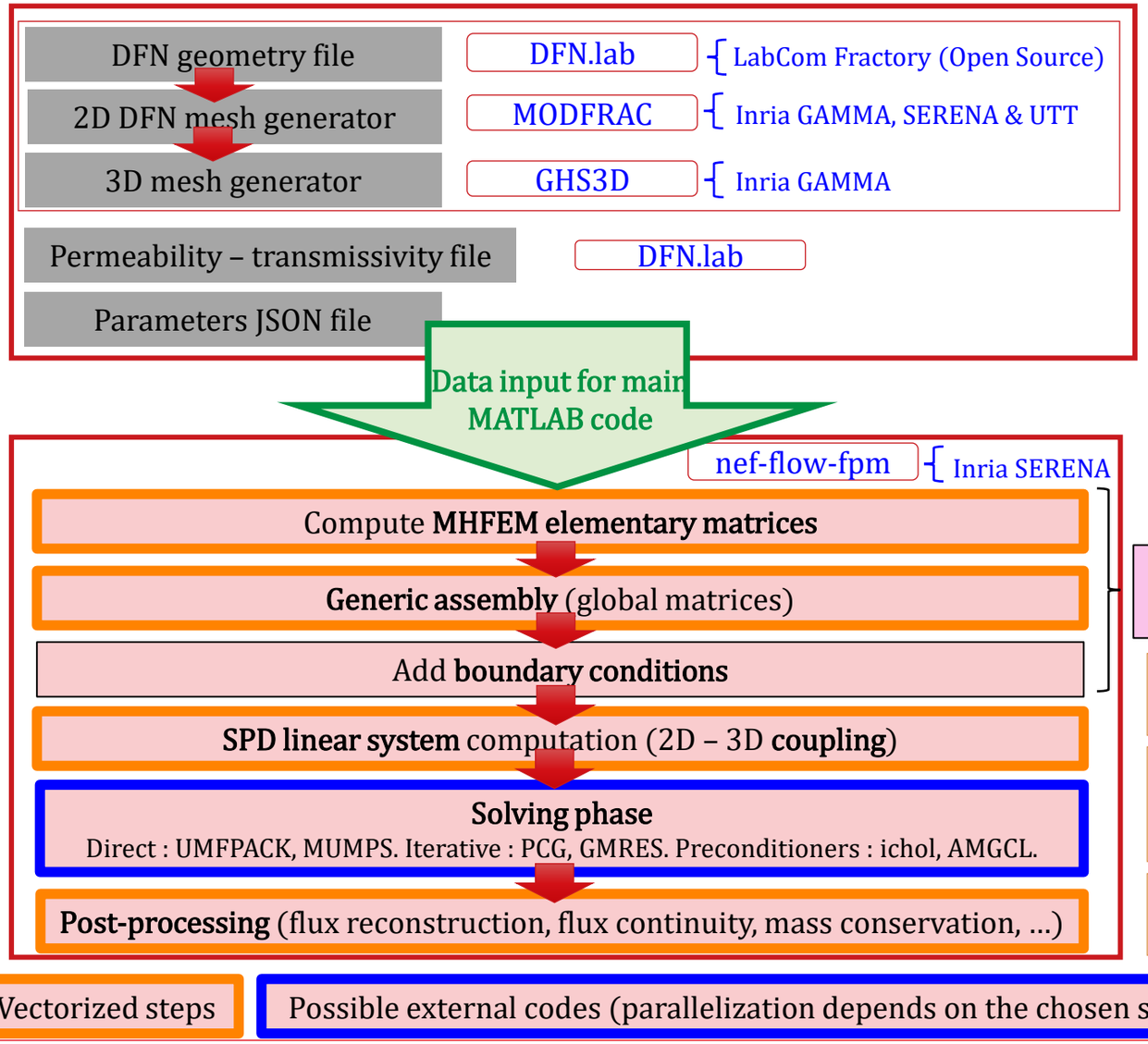

Code validation :
- benchmark ;
- analytical solution.

For both 2D DFN and 3D rock matrix (almost) separately

I. Berre, W. M. Boon, B. Flemisch, A. Fumagalli, D. Gläser, E. Keilegavlen, A. Scotti, I. Stefansson, A. Tatomir, K. Brenner, S. Burbullah, P. Devloo, O. Duran, M. Favino, J. Hennicker, I. Lee, K. Lipnikov, R. Masson, K. Mosthaf, M. G. C. Nestola, C. Ni, K. Nikitin, P. Schälde, D. Svyatskiy, R. Yanbarisov, P. Zulian. *Advances in Water Resources.* **2021.**

K. Brenner, M. Groza, C. Guichard, G. Lebeau, and R. Masson. *Numerische Mathematik.* **2016.**

T. A. Davis. *ACM Transactions on Mathematical Software.* **2004.**

P. R. Amestoy, I. S. Duff, J. Koster, J.-Y. l'Excellent. *SIAM Journal on Matrix Analysis and Applications.* **2001.**

D. Demidov. *Lobachevskii Journal of Mathematics.* **2019.**

Part 3 :
The main bottleneck : solving the linear system

M. Kern, G. Pichot and D. Zegarra Vasquez. *Performance of algebraic preconditioners for large-scale simulations of single-phase flow in three-dimensional fractured porous media.* Pre-print hal-05029652. **2025.**

Part 3: linear system bottleneck

Assessment of “blackbox” linear solvers facing ill-conditioned and large and linear systems

Part 3: linear system bottleneck

Assessment of “blackbox” linear solvers facing ill-conditioned and large and linear systems

- L20-FPM condest :

Part 3: linear system bottleneck

Assessment of “blackbox” linear solvers facing ill-conditioned and large and linear systems

- L20-FPM condest :
  - 1v100 : 1.71e+11 ;

Part 3: linear system bottleneck

Assessment of “blackbox” linear solvers facing ill-conditioned and large and linear systems

- L20-FPM condest :
  - 1v100 : 1.71e+11 ;
  - heter : 6.86e+16.

Part 3: linear system bottleneck

Assessment of “blackbox” linear solvers facing ill-conditioned and large and linear systems

- L20-FPM condest :
  - 1v100 : 1.71e+11 ;
  - heter : 6.86e+16.
- L160-FPM (1v100 and heter) : 697k fractures, 243M dof, 1.8B nnz.

Part 3: linear system bottleneck

Assessment of “blackbox” linear solvers facing ill-conditioned and large and linear systems

- L20-FPM condest :
  - 1v100 : 1.71e+11 ;
  - heter : 6.86e+16.
- L160-FPM (1v100 and heter) : 697k fractures, 243M dof, 1.8B nnz.

- Direct methods suffer from very large RAM consumption + are not scalable.

Part 3: linear system bottleneck

Assessment of “blackbox” linear solvers facing ill-conditioned and large and linear systems

- L20-FPM condest :
  - 1v100 : 1.71e+11 ;
  - heter : 6.86e+16.
- L160-FPM (1v100 and heter) : 697k fractures, 243M dof, 1.8B nnz.

- Direct methods suffer from very large RAM consumption + are not scalable.

- Classic preconditioners suffer from breakdowns or very large iteration count for small test cases (L20).

Part 3: linear system bottleneck

Assessment of “blackbox” linear solvers facing ill-conditioned and large and linear systems

- L20-FPM condest :
  - 1v100 : 1.71e+11 ;
  - heter : 6.86e+16.
- L160-FPM (1v100 and heter) : 697k fractures, 243M dof, 1.8B nnz.

- Direct methods suffer from very large RAM consumption + are not scalable.

- Classic preconditioners suffer from breakdowns or very large iteration count for small test cases (L20).

- AMGCL: Algebraic Multi-Grid preconditioner (MEX-MATLAB) → `nef-flow-fpm`
  → **PCG-AMGCL (sequential).**

D. Demidov. *Lobachevskii Journal of Mathematics.* **2019.**

Part 3: linear system bottleneck

Assessment of “blackbox” linear solvers facing ill-conditioned and large and linear systems

- L20-FPM condest :
  - 1v100 : 1.71e+11 ;
  - heter : 6.86e+16.
- L160-FPM (1v100 and heter) : 697k fractures, 243M dof, 1.8B nnz.

- Direct methods suffer from very large RAM consumption + are not scalable.

- Classic preconditioners suffer from breakdowns or very large iteration count for small test cases (L20).

- AMGCL: Algebraic Multi-Grid preconditioner (MEX-MATLAB) → `nef-flow-fpm`
  → **PCG-AMGCL (sequential).**

D. Demidov. *Lobachevskii Journal of Mathematics.* **2019.**

Source of impact on iterative solver convergence :

Part 3: linear system bottleneck

Assessment of “blackbox” linear solvers facing ill-conditioned and large and linear systems

- L20-FPM condest :
  - 1v100 : 1.71e+11 ;
  - heter : 6.86e+16.
- L160-FPM (1v100 and heter) : 697k fractures, 243M dof, 1.8B nnz.

- Direct methods suffer from very large RAM consumption + are not scalable.

- Classic preconditioners suffer from breakdowns or very large iteration count for small test cases (L20).

- AMGCL: Algebraic Multi-Grid preconditioner (MEX-MATLAB) → `nef-flow-fpm`
  → **PCG-AMGCL (sequential).**

D. Demidov. *Lobachevskii Journal of Mathematics.* **2019.**

Source of impact on iterative solver convergence :
- DFM geometrical complexity (number of fractures → increasing number of fracture-fracture intersections) ;

Part 3: linear system bottleneck

Assessment of “blackbox” linear solvers facing ill-conditioned and large and linear systems

- L20-FPM condest :
  - 1v100 : 1.71e+11 ;
  - heter : 6.86e+16.
- L160-FPM (1v100 and heter) : 697k fractures, 243M dof, 1.8B nnz.

- Direct methods suffer from very large RAM consumption + are not scalable.

- Classic preconditioners suffer from breakdowns or very large iteration count for small test cases (L20).

- AMGCL: Algebraic Multi-Grid preconditioner (MEX-MATLAB) → `nef-flow-fpm`
  → **PCG-AMGCL (sequential).**

D. Demidov. *Lobachevskii Journal of Mathematics.* **2019.**

Source of impact on iterative solver convergence :
- DFM geometrical complexity (number of fractures → increasing number of fracture-fracture intersections) ;
- **mesh quality ;**

Part 3: linear system bottleneck

Assessment of “blackbox” linear solvers facing ill-conditioned and large and linear systems

- L20-FPM condest :
  - 1v100 : 1.71e+11 ;
  - heter : 6.86e+16.
- L160-FPM (1v100 and heter) : 697k fractures, 243M dof, 1.8B nnz.

- Direct methods suffer from very large RAM consumption + are not scalable.

- Classic preconditioners suffer from breakdowns or very large iteration count for small test cases (L20).

- AMGCL: Algebraic Multi-Grid preconditioner (MEX-MATLAB) → `nef-flow-fpm`
  → **PCG-AMGCL (sequential).**

D. Demidov. *Lobachevskii Journal of Mathematics.* **2019.**

Source of impact on iterative solver convergence :
- DFM geometrical complexity (number of fractures → increasing number of fracture-fracture intersections) ;
- **mesh quality ;**
- **contrast of hydraulic conductivity / transmissivity.**

Part 3: linear system bottleneck

Difficult linear solver convergence due to mesh quality

Part 3: linear system bottleneck

Difficult linear solver convergence due to mesh quality

Thanks to *CLEPS* : Inria Paris CLuster pour l'Expérimentation et le Prototypage Scientifique. HOMOGEN partition, 2x Cascade Lake Intel Xeon 5218, 16 cores, 2.4GHz, 192 GB, 2,667 MHz. No hyperthreading.

Part 3: linear system bottleneck

Difficult linear solver convergence due to mesh quality

Test case	# frac.	Min. frac. triang. qual.	Min. rock tetra qual.	# dofs
[L20geo-FPM-1v100]	1.8k	10^{-3}	10^{-5}	4.2M

Thanks to *CLEPS* : Inria Paris CLuster pour l'Expérimentation et le Prototypage Scientifique. HOMOGEN partition, 2x Cascade Lake Intel Xeon 5218, 16 cores, 2.4GHz, 192 GB, 2,667 MHz. No hyperthreading.

Part 3: linear system bottleneck

Difficult linear solver convergence due to mesh quality

Test case	# frac.	Min. frac. triang. qual.	Min. rock tetra qual.	# dofs
[L20geo-FPM-1v100]	1.8k	10^{-3}	10^{-5}	4.2M
[L20geo-PM-LQ-1]	0	—	10^{-5}	3.8M

Thanks to *CLEPS* : Inria Paris CLuster pour l'Expérimentation et le Prototypage Scientifique. HOMOGEN partition, 2x Cascade Lake Intel Xeon 5218, 16 cores, 2.4GHz, 192 GB, 2,667 MHz. No hyperthreading.

Part 3: linear system bottleneck

Difficult linear solver convergence due to mesh quality

Test case	# frac.	Min. frac. triang. qual.	Min. rock tetra qual.	# dofs
[L20geo-FPM-1v100]	1.8k	10^{-3}	10^{-5}	4.2M
[L20geo-PM-LQ-1]	0	—	10^{-5}	3.8M
[L20phy-PM-GQ-1]	0	—	10^{-1}	1M

Thanks to *CLEPS* : Inria Paris CLuster pour l'Expérimentation et le Prototypage Scientifique. HOMOGEN partition, 2x Cascade Lake Intel Xeon 5218, 16 cores, 2.4GHz, 192 GB, 2,667 MHz. No hyperthreading.

Part 3: linear system bottleneck

Difficult linear solver convergence due to mesh quality

Test case	# frac.	Min. frac. triang. qual.	Min. rock tetra qual.	# dofs
[L20geo-FPM-1v100]	1.8k	10^{-3}	10^{-5}	4.2M
[L20geo-PM-LQ-1]	0	—	10^{-5}	3.8M
[L20phy-PM-GQ-1]	0	—	10^{-1}	1M
[L20geo-DFN-100]	1.4k	10^{-3}	—	274k

Thanks to *CLEPS* : Inria Paris CLuster pour l'Expérimentation et le Prototypage Scientifique. HOMOGEN partition, 2x Cascade Lake Intel Xeon 5218, 16 cores, 2.4GHz, 192 GB, 2,667 MHz. No hyperthreading.

Part 3: linear system bottleneck

Difficult linear solver convergence due to mesh quality

Sequential P**CG**-**AMG**CL. Solver tol.: 10^{-14}.

Test case	# frac.	Min. frac. triang. qual.	Min. rock tetra qual.	# dofs
[L20geo-FPM-1v100]	1.8k	10^{-3}	10^{-5}	4.2M
[L20geo-PM-LQ-1]	0	—	10^{-5}	3.8M
[L20phy-PM-GQ-1]	0	—	10^{-1}	1M
[L20geo-DFN-100]	1.4k	10^{-3}	—	274k

Test case	# it.	Solver time hh:mm:ss	RAM (GB)
[L20geo-FPM-1v100]	2.87k	00:28:01	1.6
[L20geo-PM-LQ-1]	2.93k	00:26:18	1.5
[L20phy-PM-GQ-1]	66	00:00:18	0.50
[L20geo-DFN-100]	692	00:00:17	0.08

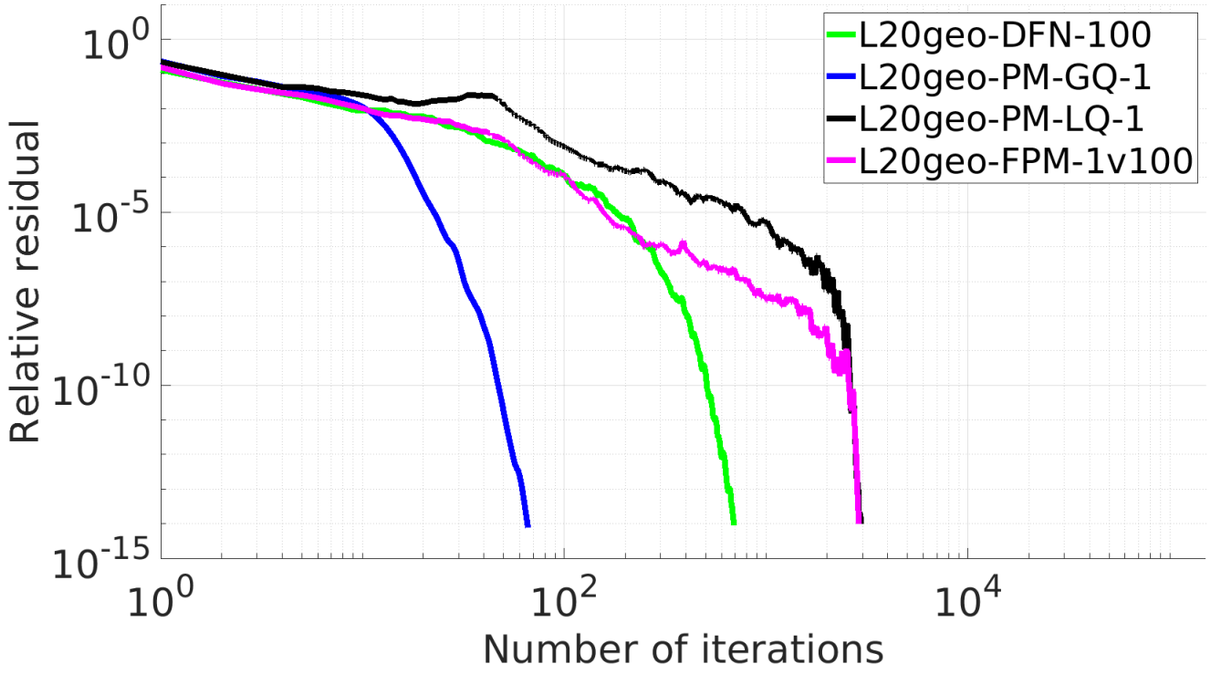

Thanks to *CLEPS* : Inria Paris CLuster pour l'Expérimentation et le Prototypage Scientifique. HOMOGEN partition, 2x Cascade Lake Intel Xeon 5218, 16 cores, 2.4GHz, 192 GB, 2,667 MHz. No hyperthreading.

Part 3: linear system bottleneck

Difficult linear solver convergence due to mesh quality and due to the heterogeneity of hydraulic conductivity/transmissivity

Sequential P**CG**-**AMG**CL. Solver tol.: 10^{-14}.

Test case	# frac.	Min. frac. triang. qual.	Min. rock tetra qual.	# dofs
[L20geo-FPM-1v100]	1.8k	10^{-3}	10^{-5}	4.2M
[L20geo-PM-LQ-1]	0	—	10^{-5}	3.8M
[L20phy-PM-GQ-1]	0	—	10^{-1}	1M
[L20geo-DFN-100]	1.4k	10^{-3}	—	274k

Test case	# it.	Solver time hh:mm:ss	RAM (GB)
[L20geo-FPM-1v100]	2.87k	00:28:01	1.6
[L20geo-PM-LQ-1]	2.93k	00:26:18	1.5
[L20phy-PM-GQ-1]	66	00:00:18	0.50
[L20geo-DFN-100]	692	00:00:17	0.08

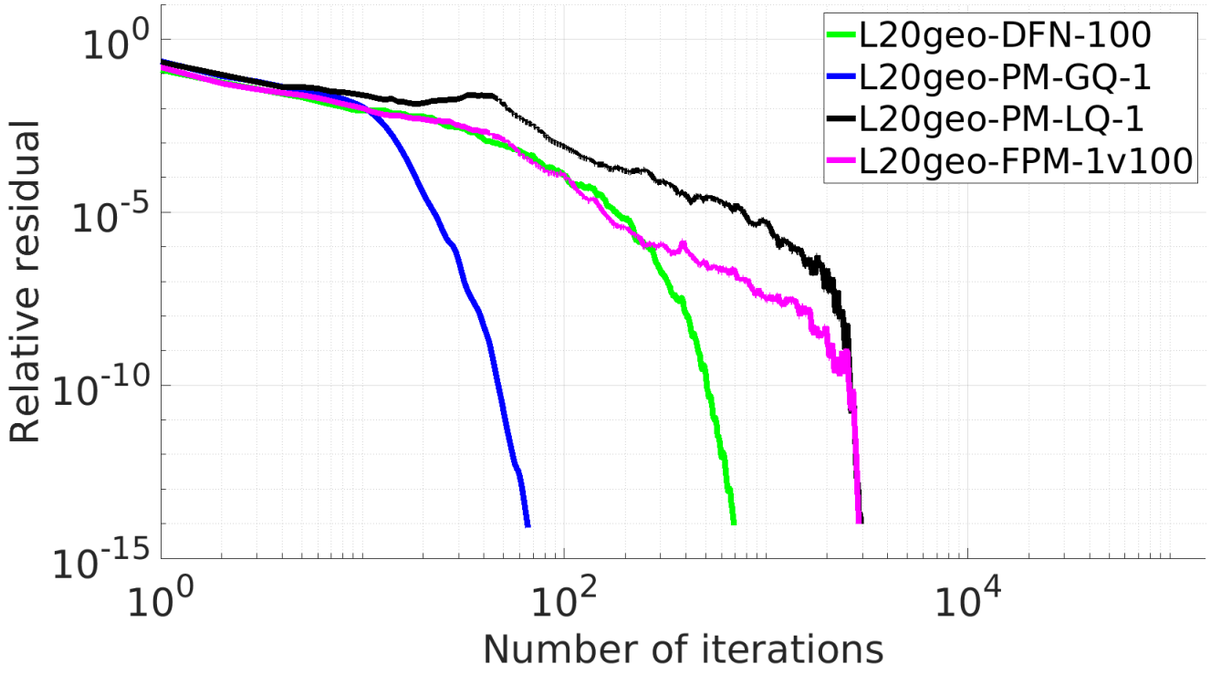

Thanks to *CLEPS* : Inria Paris CLuster pour l'Expérimentation et le Prototypage Scientifique. HOMOGEN partition, 2x Cascade Lake Intel Xeon 5218, 16 cores, 2.4GHz, 192 GB, 2,667 MHz. No hyperthreading.

Part 3: linear system bottleneck

Difficult linear solver convergence due to mesh quality and due to the heterogeneity of hydraulic conductivity/transmissivity

Sequential P**CG**-**AMG**CL. Solver tol.: 10^{-14}.

Test case	# frac.	Min. frac. triang. qual.	Min. rock tetra qual.	# dofs
[L20geo-FPM-heter]	1.8k	10^{-3}	10^{-5}	4.2M
[L20geo-FPM-1v100]	1.8k	10^{-3}	10^{-5}	4.2M
[L20geo-PM-LQ-1]	0	—	10^{-5}	3.8M
[L20phy-PM-GQ-1]	0	—	10^{-1}	1M
[L20geo-DFN-100]	1.4k	10^{-3}	—	274k

Test case	# it.	Solver time hh:mm:ss	RAM (GB)
[L20geo-FPM-1v100]	2.87k	00:28:01	1.6
[L20geo-PM-LQ-1]	2.93k	00:26:18	1.5
[L20phy-PM-GQ-1]	66	00:00:18	0.50
[L20geo-DFN-100]	692	00:00:17	0.08

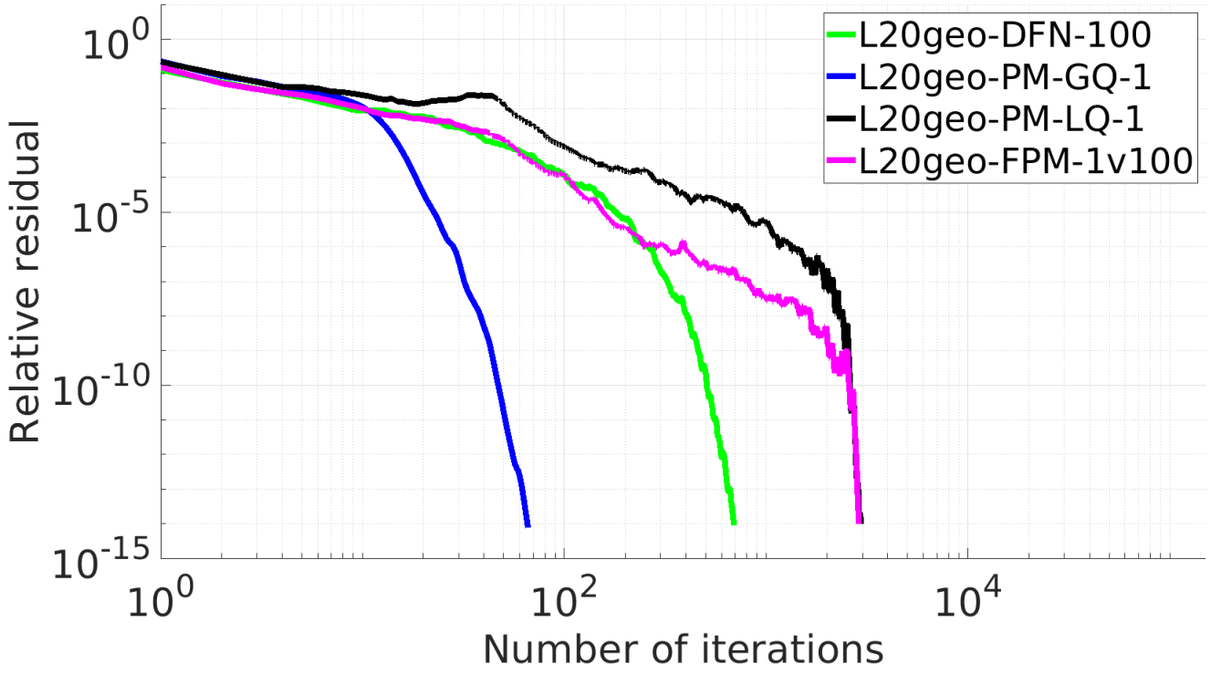

Thanks to *CLEPS* : Inria Paris CLuster pour l'Expérimentation et le Prototypage Scientifique. HOMOGEN partition, 2x Cascade Lake Intel Xeon 5218, 16 cores, 2.4GHz, 192 GB, 2,667 MHz. No hyperthreading.

Part 3: linear system bottleneck

Difficult linear solver convergence due to mesh quality and due to the heterogeneity of hydraulic conductivity/transmissivity

Sequential P**CG**-**AMG**CL. Solver tol.: 10^{-14}.

Test case	# frac.	Min. frac. triang. qual.	Min. rock tetra qual.	# dofs
[L20geo-FPM-heter]	1.8k	10^{-3}	10^{-5}	4.2M
[L20geo-FPM-1v100]	1.8k	10^{-3}	10^{-5}	4.2M
[L20geo-PM-LQ-1]	0	—	10^{-5}	3.8M
[L20phy-PM-GQ-1]	0	—	10^{-1}	1M
[L20geo-DFN-100]	1.4k	10^{-3}	—	274k

Test case	# it.	Solver time hh:mm:ss	RAM (GB)
[L20geo-FPM-heter]	123k	20:01:26	1.7
[L20geo-FPM-1v100]	2.87k	00:28:01	1.6
[L20geo-PM-LQ-1]	2.93k	00:26:18	1.5
[L20phy-PM-GQ-1]	66	00:00:18	0.50
[L20geo-DFN-100]	692	00:00:17	0.08

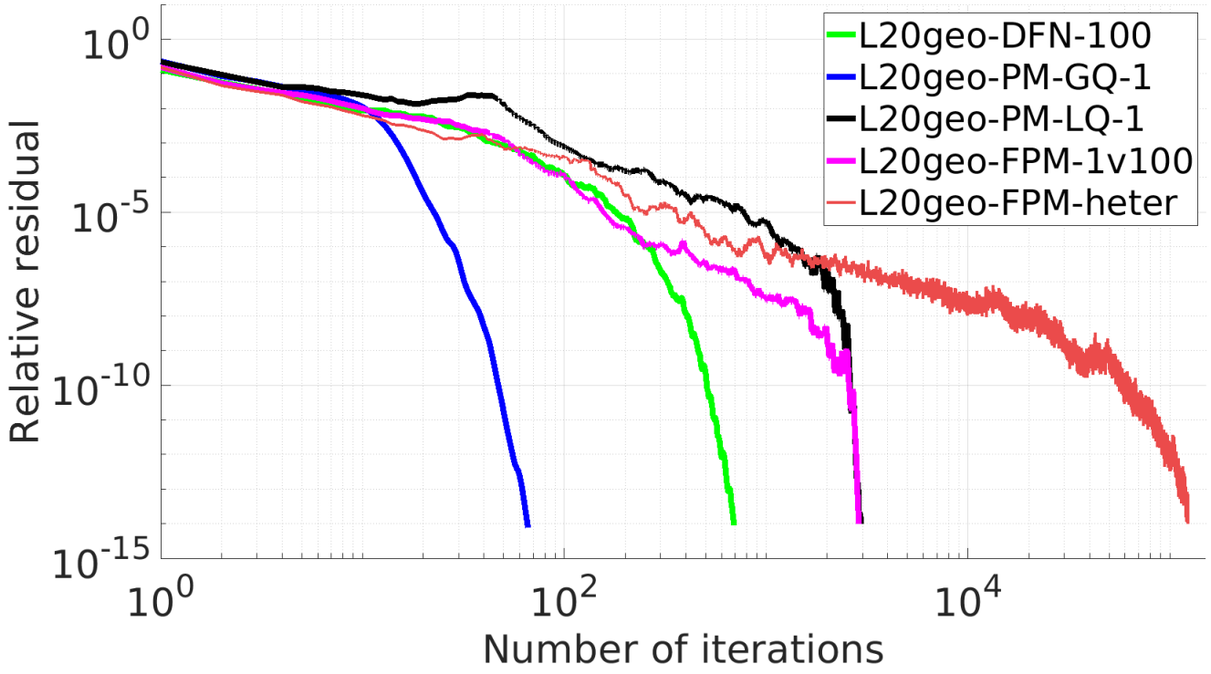

Thanks to *CLEPS* : Inria Paris CLuster pour l'Expérimentation et le Prototypage Scientifique. HOMOGEN partition, 2x Cascade Lake Intel Xeon 5218, 16 cores, 2.4GHz, 192 GB, 2,667 MHz. No hyperthreading.

Part 3: linear system bottleneck

Difficult linear solver convergence due to mesh quality and due to the heterogeneity of hydraulic conductivity/transmissivity

Sequential P**CG**-**AMG**CL. Solver tol.: 10^{-14}.

Test case	# frac.	Min. frac. triang. qual.	Min. rock tetra qual.	# dofs
[L20geo-FPM-heter]	1.8k	10^{-3}	10^{-5}	4.2M
[L20geo-FPM-1v100]	1.8k	10^{-3}	10^{-5}	4.2M
[L20geo-PM-LQ-1]	0	—	10^{-5}	3.8M
[L20phy-PM-GQ-1]	0	—	10^{-1}	1M
[L20geo-DFN-100]	1.4k	10^{-3}	—	274k

Test case	# it.	Solver time hh:mm:ss	RAM (GB)
[L20geo-FPM-heter]	123k	20:01:26	1.7
[L20geo-FPM-1v100]	2.87k	00:28:01	1.6
[L20geo-PM-LQ-1]	2.93k	00:26:18	1.5
[L20phy-PM-GQ-1]	66	00:00:18	0.50
[L20geo-DFN-100]	692	00:00:17	0.08

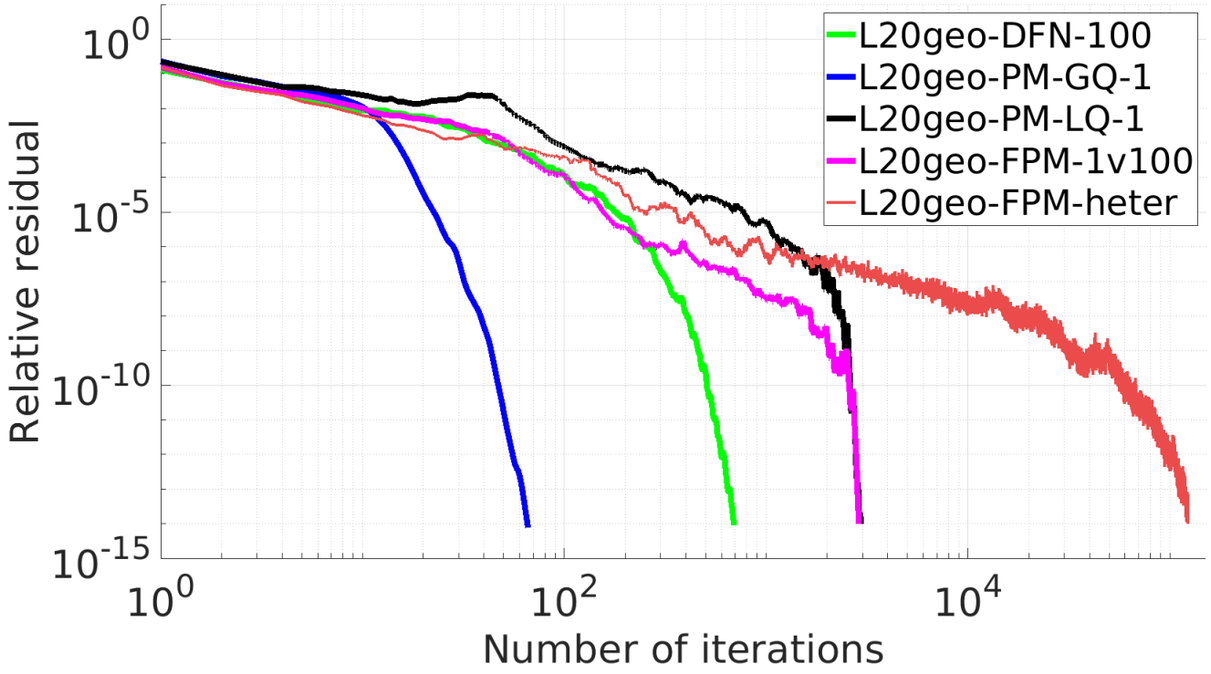

Thanks to *CLEPS* : Inria Paris CLuster pour l'Expérimentation et le Prototypage Scientifique. HOMOGEN partition, 2x Cascade Lake Intel Xeon 5218, 16 cores, 2.4GHz, 192 GB, 2,667 MHz. No hyperthreading.

Y. Chen and G. N. Wells. *Pre-print doi:10.48550/arXiv.2402.12947* . **2024.**

J. Gopalakrishnan and S. Tan. *Numerical Linear Algebra with Applications.* **2009.**

S. C. Brenner. *SIAM Journal on Numerical Analysis.* **1992.**

Part 4 :
The spectral domain decomposition method GenEO as a robust preconditioner

P. Jolivet, M. Kern, F. Nataf, G. Pichot and D. Zegarra Vasquez. *Spectral domain decomposition methods as robust preconditioners for single-phase flow in fractured porous media.* Pre-print hal-05029676. **2025.**

Part 4: DD preconditioner GenEO

Domain decomposition (DD) methods with minimal overlap

Part 4: DD preconditioner GenEO

Domain decomposition (DD) methods with minimal overlap

One-level methods:

Additive Schwarz Method (**ASM**) or restrictive ASM (**RAS**).

$$M_{\mathrm{ASM}}^{-1} = \sum_{i=1}^{N} R_i^T (A_i)^{-1} R_i, \qquad M_{\mathrm{RAS}}^{-1} = \sum_{i=1}^{N} \widetilde{R}_i^T (A_i)^{-1} R_i.$$

V. Dolean, P. Jolivet, and F. Nataf. *Society for Industrial and Applied Mathematics, Philadelphia, PA.* **2015.**

Part 4: DD preconditioner GenEO

Domain decomposition (DD) methods with minimal overlap

One-level methods: not scalable

Additive Schwarz Method (**ASM**) or restrictive ASM (**RAS**).

$$M_{\mathrm{ASM}}^{-1} = \sum_{i=1}^{N} R_i^T (A_i)^{-1} R_i, \qquad M_{\mathrm{RAS}}^{-1} = \sum_{i=1}^{N} \widetilde{R}_i^T (A_i)^{-1} R_i.$$

V. Dolean, P. Jolivet, and F. Nataf. *Society for Industrial and Applied Mathematics, Philadelphia, PA.* **2015.**

Part 4: DD preconditioner GenEO

Domain decomposition (DD) methods with minimal overlap

One-level methods: not scalable

Additive Schwarz Method (**ASM**) or restrictive ASM (**RAS**).

$$M_{\mathrm{ASM}}^{-1} = \sum_{i=1}^{N} R_i^T (A_i)^{-1} R_i, \qquad M_{\mathrm{RAS}}^{-1} = \sum_{i=1}^{N} \widetilde{R}_i^T (A_i)^{-1} R_i.$$

"HPDDM GenEO" M^{-1}, a **two-level** scalable method, sum of:

V. Dolean, P. Jolivet, and F. Nataf. *Society for Industrial and Applied Mathematics, Philadelphia, PA.* **2015.**

P. Jolivet, F. Hecht, F. Nataf, and C. Prud'homme. *In Proceedings of the International Conference on High Performance Computing, Networking, Storage and Analysis, SC '13, New York, USA.* **2013.**

N. Spillane, V. Dolean, P. Hauret, F. Nataf, C. Pechstein, and R. Scheichl. *Numerische Mathematik.* **2014.**

P. Jolivet, J.E. Roman, and S. Zampini. *Computers and Mathematics with Applications.* **2021.**

Part 4: DD preconditioner GenEO

Domain decomposition (DD) methods with minimal overlap

One-level methods: not scalable

Additive Schwarz Method (**ASM**) or restrictive ASM (**RAS**).

$$M_{\mathrm{ASM}}^{-1} = \sum_{i=1}^{N} R_i^T (A_i)^{-1} R_i, \qquad M_{\mathrm{RAS}}^{-1} = \sum_{i=1}^{N} \widetilde{R}_i^T (A_i)^{-1} R_i.$$

"HPDDM GenEO" M^{-1}, a **two-level** scalable method, sum of:

- a fine level, **ASM** or **RAS** ;

V. Dolean, P. Jolivet, and F. Nataf. *Society for Industrial and Applied Mathematics, Philadelphia, PA.* **2015.**

P. Jolivet, F. Hecht, F. Nataf, and C. Prud'homme. *In Proceedings of the International Conference on High Performance Computing, Networking, Storage and Analysis, SC '13, New York, USA.* **2013.**

N. Spillane, V. Dolean, P. Hauret, F. Nataf, C. Pechstein, and R. Scheichl. *Numerische Mathematik.* **2014.**

P. Jolivet, J.E. Roman, and S. Zampini. *Computers and Mathematics with Applications.* **2021.**

Part 4: DD preconditioner GenEO

Domain decomposition (DD) methods with minimal overlap

One-level methods: not scalable

Additive Schwarz Method (**ASM**) or restrictive ASM (**RAS**).

$$M_{\mathrm{ASM}}^{-1} = \sum_{i=1}^{N} R_i^T (A_i)^{-1} R_i, \qquad M_{\mathrm{RAS}}^{-1} = \sum_{i=1}^{N} \widetilde{R}_i^T (A_i)^{-1} R_i.$$

"HPDDM GenEO" M^{-1}, a **two-level** scalable method, sum of:

- a fine level, **ASM** or **RAS** ;
- a coarse level, a global correction operator built from local **GenEO** ("Generalized Eigenvalue problems on the Overlap"):

$$\text{Find the } \mu_i \in \mathbb{N}^* \text{ smallest eigenpairs } \{y_{i,j}, \rho_{i,j}\}_{j=1}^{\mu_i} \text{ up to the desired tolerance } \nu \in]0,1[\text{ (i.e., } \rho_{i,j} \leq \nu) \text{ such that: } A_i^{\delta} y_{i,j} = \rho_{i,j} \widetilde{R}_i (R_i)^T A_i R_i (\widetilde{R}_i)^T y_{i,j}.$$

V. Dolean, P. Jolivet, and F. Nataf. *Society for Industrial and Applied Mathematics, Philadelphia, PA.* **2015.**

P. Jolivet, F. Hecht, F. Nataf, and C. Prud'homme. *In Proceedings of the International Conference on High Performance Computing, Networking, Storage and Analysis, SC '13, New York, USA.* **2013.**

N. Spillane, V. Dolean, P. Hauret, F. Nataf, C. Pechstein, and R. Scheichl. *Numerische Mathematik.* **2014.**

P. Jolivet, J.E. Roman, and S. Zampini. *Computers and Mathematics with Applications.* **2021.**

Part 4: DD preconditioner GenEO

Domain decomposition (DD) methods with minimal overlap

One-level methods: not scalable

Additive Schwarz Method (**ASM**) or restrictive ASM (**RAS**).

$$M_{\mathrm{ASM}}^{-1} = \sum_{i=1}^{N} R_i^T (A_i)^{-1} R_i, \qquad M_{\mathrm{RAS}}^{-1} = \sum_{i=1}^{N} \widetilde{R}_i^T (A_i)^{-1} R_i.$$

"HPDDM GenEO" M^{-1}, a **two-level** scalable method, sum of:

- a fine level, **ASM** or **RAS** ;
- a coarse level, a global correction operator built from local **GenEO** ("Generalized Eigenvalue problems on the Overlap"):

$$\text{Find the } \mu_i \in \mathbb{N}^* \text{ smallest eigenpairs } \{y_{i,j}, \rho_{i,j}\}_{j=1}^{\mu_i} \text{ up to the desired tolerance } \nu \in]0,1[\text{ (i.e., } \rho_{i,j} \leq \nu) \text{ such that: } A_i^{\delta} y_{i,j} = \rho_{i,j} \widetilde{R}_i (R_i)^T A_i R_i (\widetilde{R}_i)^T y_{i,j}.$$

Neumann matrix

V. Dolean, P. Jolivet, and F. Nataf. *Society for Industrial and Applied Mathematics, Philadelphia, PA.* **2015.**

P. Jolivet, F. Hecht, F. Nataf, and C. Prud'homme. *In Proceedings of the International Conference on High Performance Computing, Networking, Storage and Analysis, SC '13, New York, USA.* **2013.**

N. Spillane, V. Dolean, P. Hauret, F. Nataf, C. Pechstein, and R. Scheichl. *Numerische Mathematik.* **2014.**

P. Jolivet, J.E. Roman, and S. Zampini. *Computers and Mathematics with Applications.* **2021.**

Part 4: DD preconditioner GenEO

Domain decomposition (DD) methods with minimal overlap

One-level methods: not scalable

Additive Schwarz Method (**ASM**) or restrictive ASM (**RAS**).

$$M_{\mathrm{ASM}}^{-1} = \sum_{i=1}^{N} R_i^T (A_i)^{-1} R_i, \qquad M_{\mathrm{RAS}}^{-1} = \sum_{i=1}^{N} \widetilde{R}_i^T (A_i)^{-1} R_i.$$

"HPDDM GenEO" M^{-1}, a **two-level** scalable method, sum of:

- a fine level, **ASM** or **RAS** ;
- a coarse level, a global correction operator built from local **GenEO** ("Generalized Eigenvalue problems on the Overlap"):

$$\text{Find the } \mu_i \in \mathbb{N}^* \text{ smallest eigenpairs } \{y_{i,j}, \rho_{i,j}\}_{j=1}^{\mu_i} \text{ up to the desired tolerance } \nu \in]0,1[\text{ (i.e., } \rho_{i,j} \leq \nu) \text{ such that: } A_i^{\delta} y_{i,j} = \rho_{i,j} \widetilde{R}_i (R_i)^T A_i R_i (\widetilde{R}_i)^T y_{i,j}.$$

Neumann matrix

Theoretical bound on the condition number of the preconditioned matrix independent of the mesh parameters and the number of subdomains.

V. Dolean, P. Jolivet, and F. Nataf. *Society for Industrial and Applied Mathematics, Philadelphia, PA.* **2015.**

P. Jolivet, F. Hecht, F. Nataf, and C. Prud'homme. *In Proceedings of the International Conference on High Performance Computing, Networking, Storage and Analysis, SC '13, New York, USA.* **2013.**

N. Spillane, V. Dolean, P. Hauret, F. Nataf, C. Pechstein, and R. Scheichl. *Numerische Mathematik.* **2014.**

P. Jolivet, J.E. Roman, and S. Zampini. *Computers and Mathematics with Applications.* **2021.**

Part 4: DD preconditioner GenEO

Domain decomposition (DD) methods with minimal overlap

One-level methods: not scalable

Additive Schwarz Method (**ASM**) or restrictive ASM (**RAS**).

$$M_{\mathrm{ASM}}^{-1} = \sum_{i=1}^{N} R_i^T (A_i)^{-1} R_i, \qquad M_{\mathrm{RAS}}^{-1} = \sum_{i=1}^{N} \widetilde{R}_i^T (A_i)^{-1} R_i.$$

"HPDDM GenEO" M^{-1}, a **two-level** scalable method, sum of:

- a fine level, **ASM** or **RAS** ;
- a coarse level, a global correction operator built from local **GenEO** ("Generalized Eigenvalue problems on the Overlap"):

$$\text{Find the } \mu_i \in \mathbb{N}^* \text{ smallest eigenpairs } \{y_{i,j}, \rho_{i,j}\}_{j=1}^{\mu_i} \text{ up to the desired tolerance } \nu \in]0,1[\text{ (i.e., } \rho_{i,j} \leq \nu) \text{ such that: } A_i^{\delta} y_{i,j} = \rho_{i,j} \widetilde{R}_i (R_i)^T A_i R_i (\widetilde{R}_i)^T y_{i,j}.$$

Neumann matrix

Theoretical bound on the condition number of the preconditioned matrix independent of the mesh parameters and the number of subdomains.

These methods are implemented in the HPDDM library from PETSc.

V. Dolean, P. Jolivet, and F. Nataf. *Society for Industrial and Applied Mathematics, Philadelphia, PA.* **2015.**

P. Jolivet, F. Hecht, F. Nataf, and C. Prud'homme. *In Proceedings of the International Conference on High Performance Computing, Networking, Storage and Analysis, SC '13, New York, USA.* **2013.**

N. Spillane, V. Dolean, P. Hauret, F. Nataf, C. Pechstein, and R. Scheichl. *Numerische Mathematik.* **2014.**

P. Jolivet, J.E. Roman, and S. Zampini. *Computers and Mathematics with Applications.* **2021.**

S. Balay et. al. *PETSc/TAO users manual.* **2024.**

Part 4: DD preconditioner GenEO

Application of DD methods to flow in DFM

Part 4: DD preconditioner GenEO

Application of DD methods to flow in DFM

1. MHFE single-phase flow context **fits** GenEO theory.

Part 4: DD preconditioner GenEO

Application of DD methods to flow in DFM

1. MHFE single-phase flow context **fits** GenEO theory.
2. **Decomposition** of 2D-3D DFM mesh.

Part 4: DD preconditioner GenEO

Application of DD methods to flow in DFM

1. MHFE single-phase flow context **fits** GenEO theory.
2. **Decomposition** of 2D-3D DFM mesh.

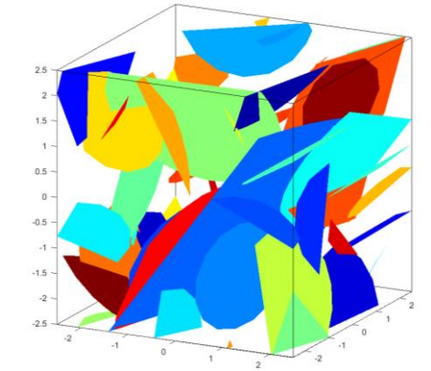

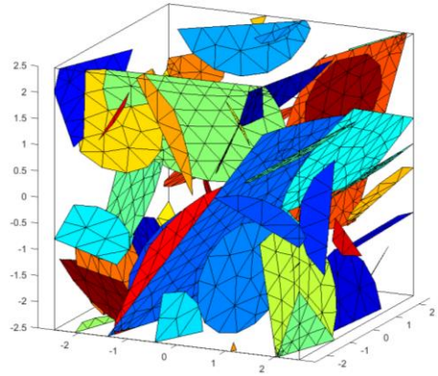

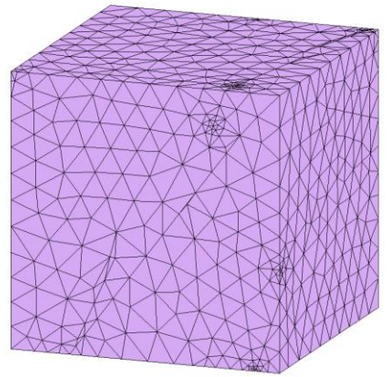

L5 test case: 55 fractures, 14k tetras, 2k triangles

Part 4: DD preconditioner GenEO

Application of DD methods to flow in DFM

1. MHFE single-phase flow context **fits** GenEO theory.
2. **Decomposition** of 2D-3D DFM mesh.

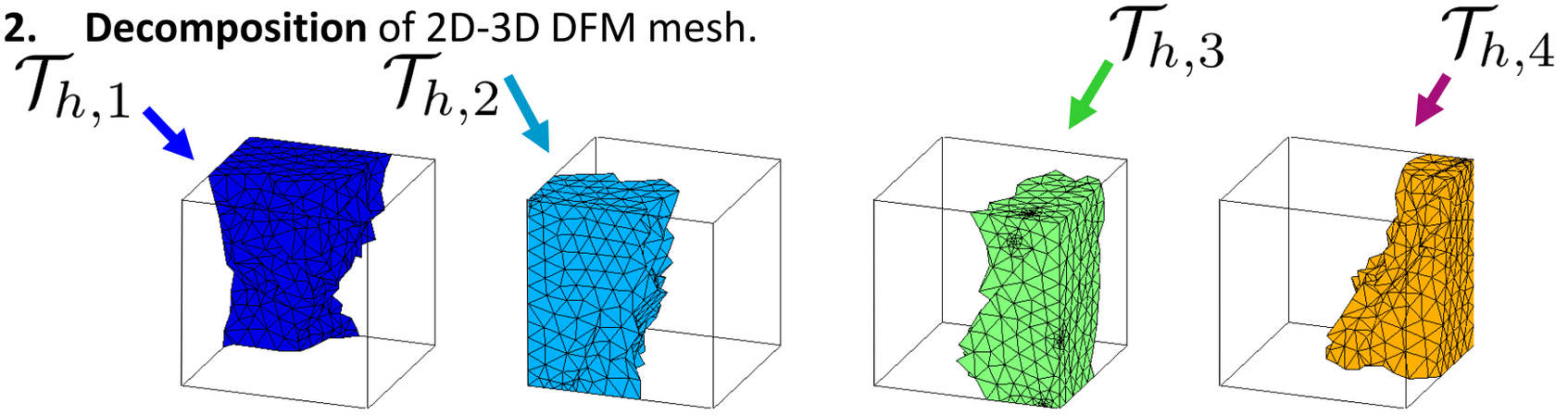

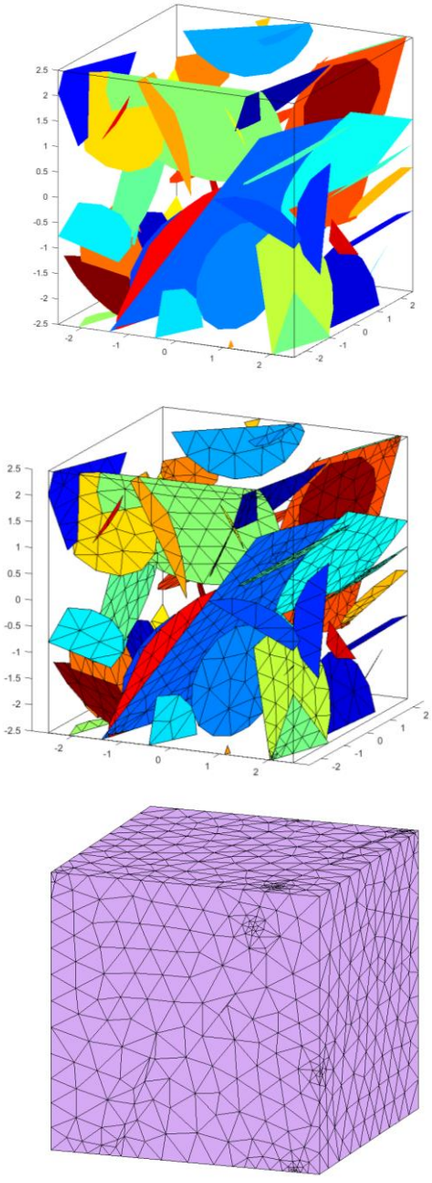

L5 test case: 55 fractures, 14k tetras, 2k triangles

Part 4: DD preconditioner GenEO

Application of DD methods to flow in DFM

1. MHFE single-phase flow context **fits** GenEO theory.
2. **Decomposition** of 2D-3D DFM mesh.

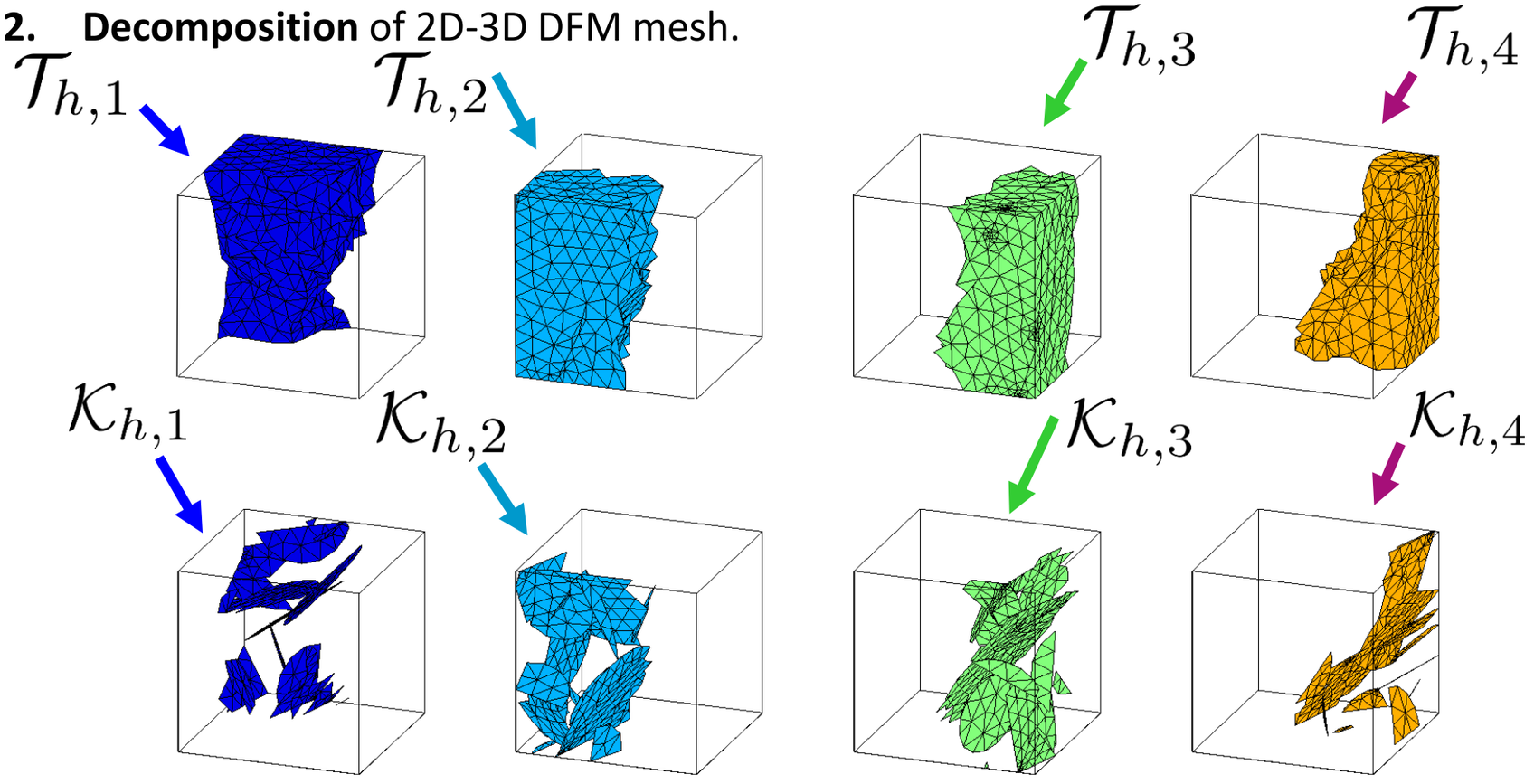

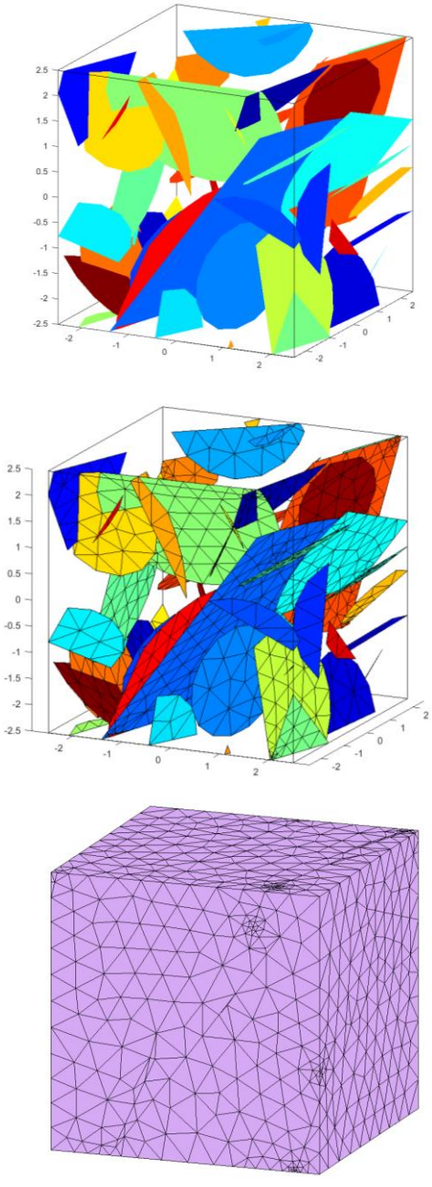

L5 test case: 55 fractures, 14k tetras, 2k triangles

Part 4: DD preconditioner GenEO

Application of DD methods to flow in DFM

1. MHFE single-phase flow context **fits** GenEO theory.
2. **Decomposition** of 2D-3D DFM mesh.

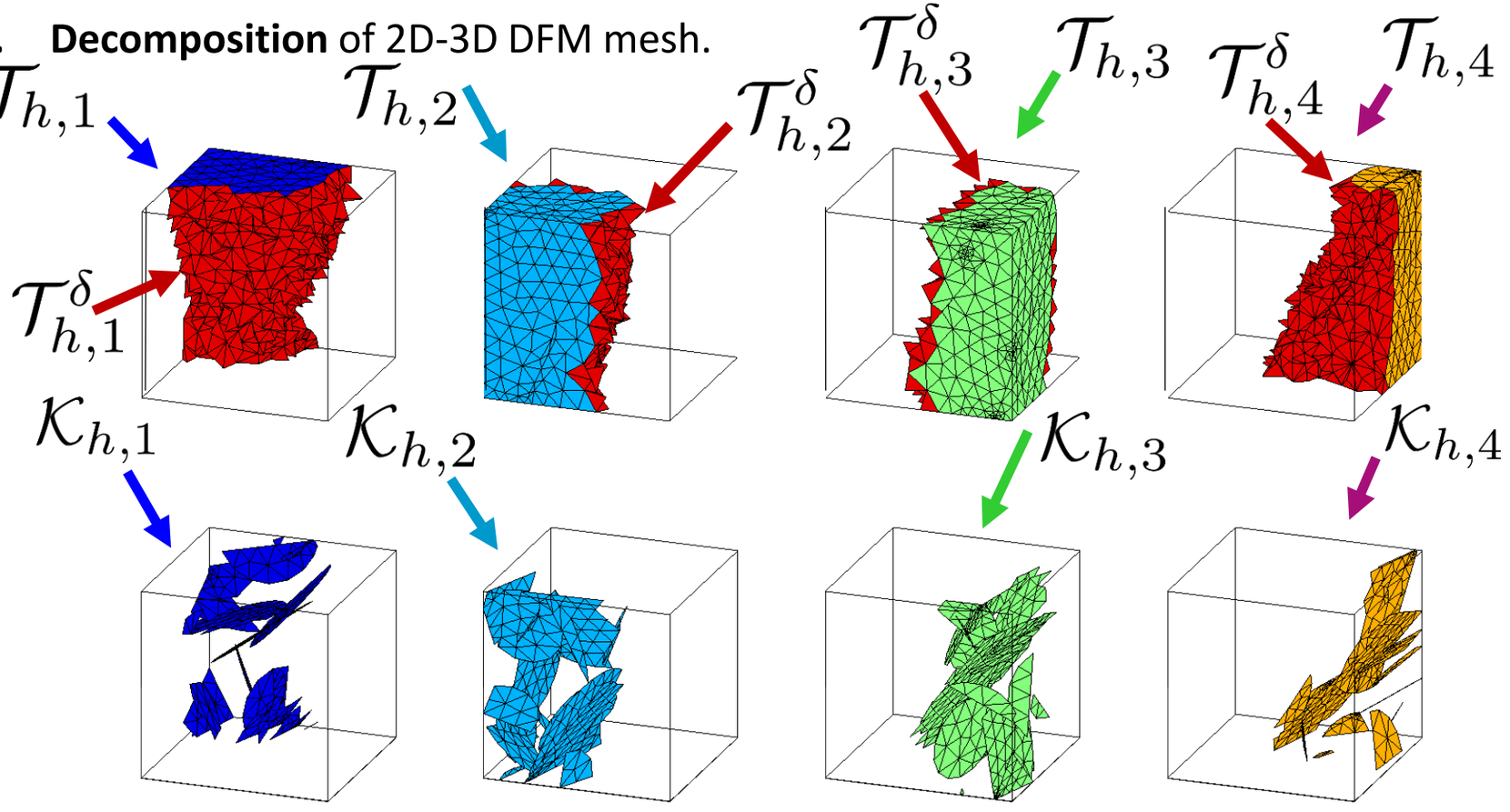

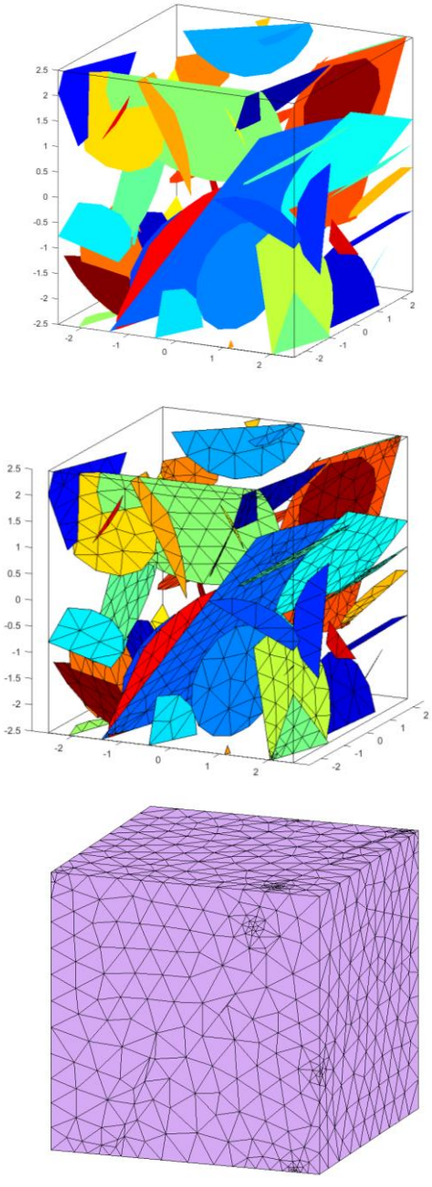

L5 test case: 55 fractures, 14k tetras, 2k triangles

Application of DD methods to flow in DFM

1. MHFE single-phase flow context **fits** GenEO theory.
2. **Decomposition** of 2D-3D DFM mesh.

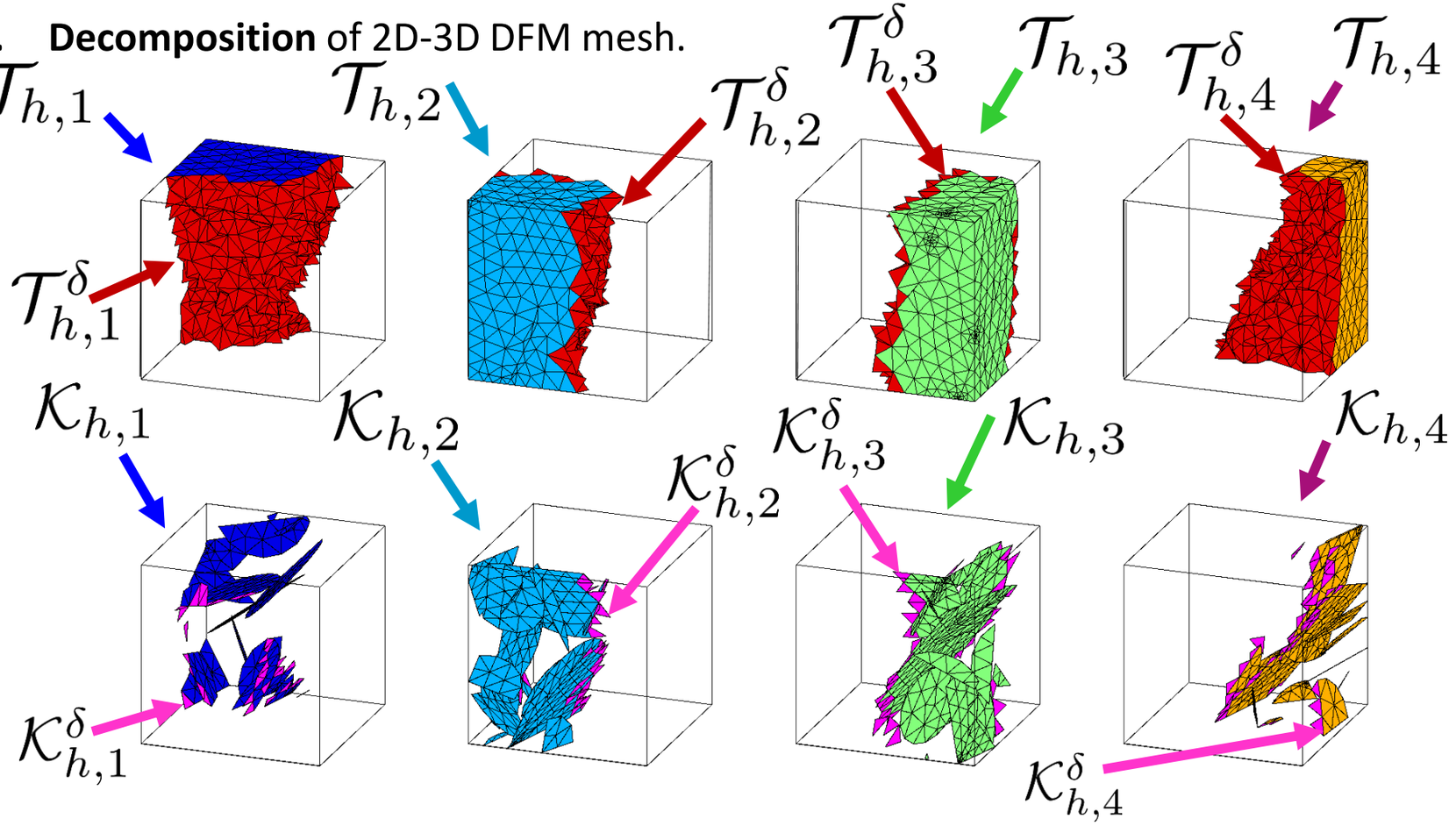

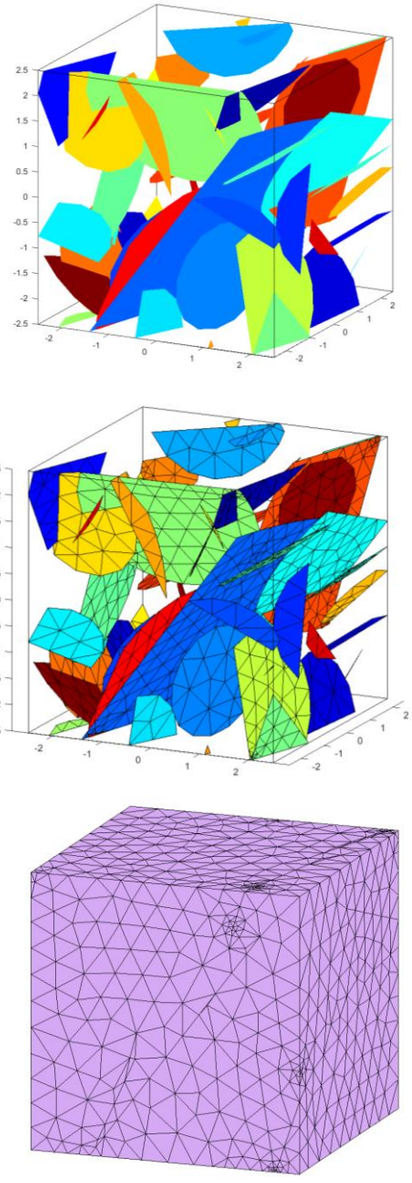

L5 test case: 55 fractures, 14k tetras, 2k triangles

Part 4: DD preconditioner GenEO

Application of DD methods to flow in DFM

1. MHFE single-phase flow context **fits** GenEO theory.
2. **Decomposition** of 2D-3D DFM mesh.

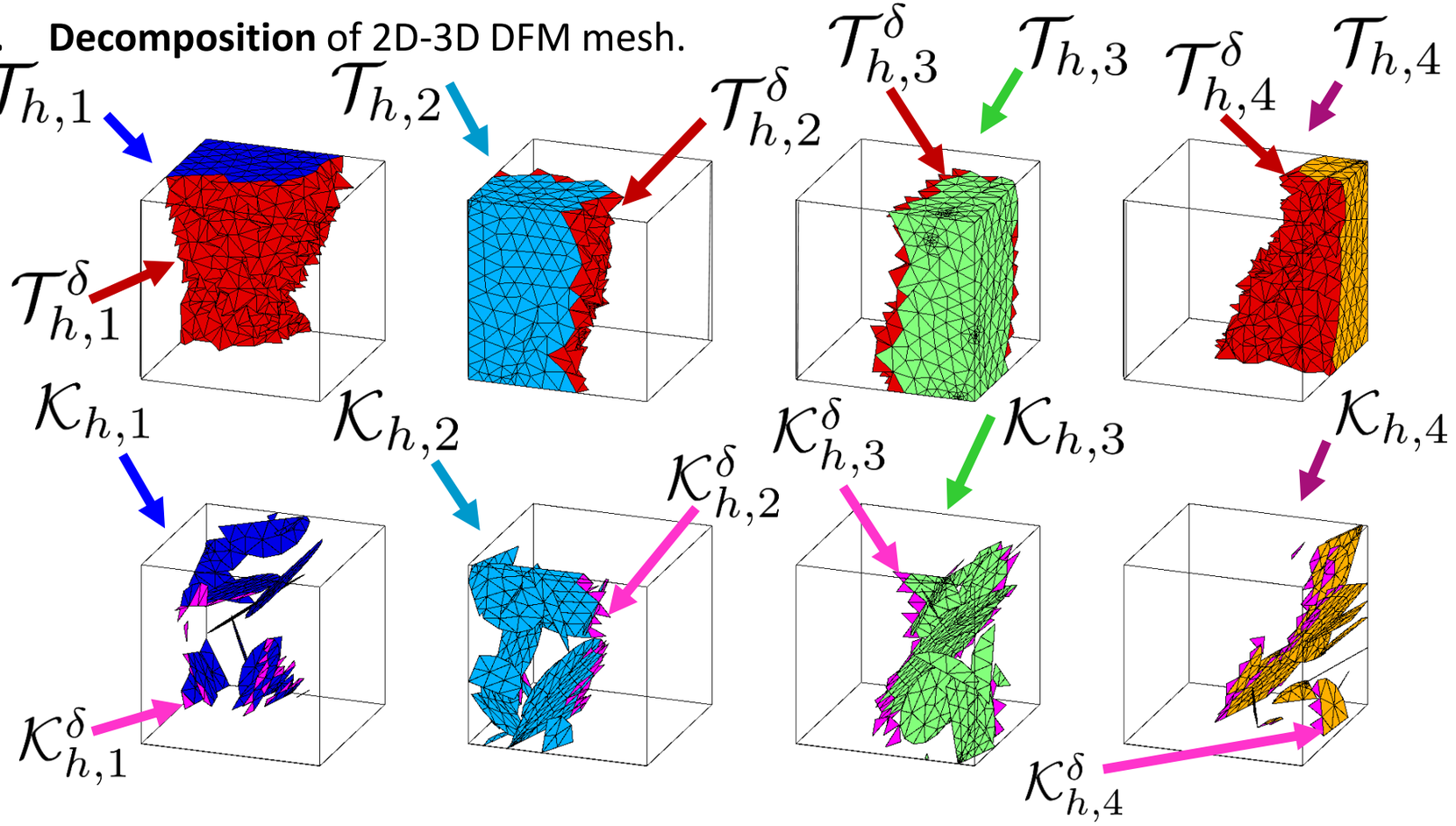

3. **Workflow** in `nef-flow-fpm` for assembling Neumann matrices A_i^{δ}.

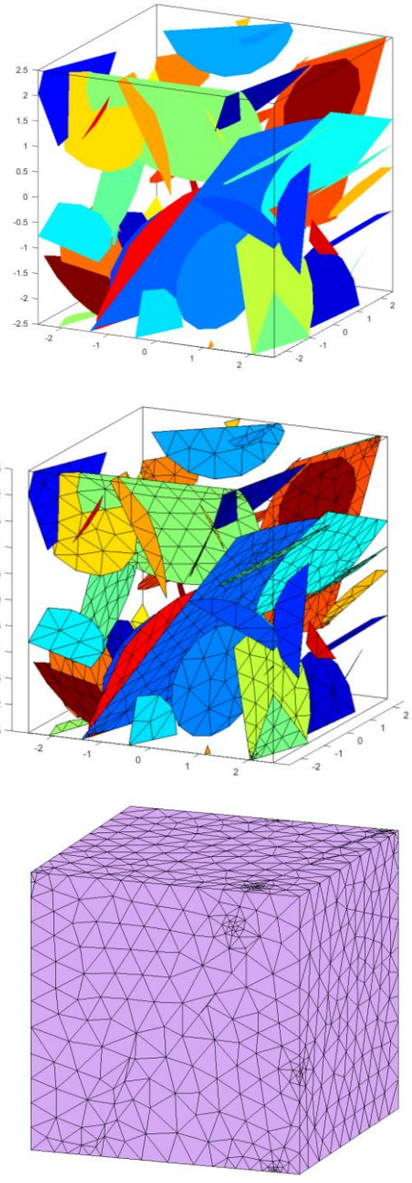

L5 test case: 55 fractures, 14k tetras, 2k triangles

Part 4: DD preconditioner GenEO

Selection of the best Krylov method and preconditioner

Part 4: DD preconditioner GenEO

Thanks to: CEA's Very Large Computing Center (TGCC), AMD Irene, 2292 dual-processor AMD Epyc Rome computer nodes at 2.6 GHz with 64 cores per processor, total of 293,376 computing cores and a power of 11.75 Pflop/s, 256 GB DDR4 memory/node. No hyperthreading.

Selection of the best Krylov method and preconditioner

Part 4: DD preconditioner GenEO

Thanks to: CEA's Very Large Computing Center (TGCC), AMD Irene, 2292 dual-processor AMD Epyc Rome computer nodes at 2.6 GHz with 64 cores per processor, total of 293,376 computing cores and a power of 11.75 Pflop/s, 256 GB DDR4 memory/node. No hyperthreading.

Selection of the best Krylov method and preconditioner

Conjugate Gradient (**CG**)

Part 4: DD preconditioner GenEO

Thanks to: CEA's Very Large Computing Center (TGCC), AMD Irene, 2292 dual-processor AMD Epyc Rome computer nodes at 2.6 GHz with 64 cores per processor, total of 293,376 computing cores and a power of 11.75 Pflop/s, 256 GB DDR4 memory/node. No hyperthreading.

Selection of the best Krylov method and preconditioner

Conjugate Gradient (**CG**)
and Generalized Minimal RESidual (**GMRES**)

Part 4: DD preconditioner GenEO

Thanks to: CEA's Very Large Computing Center (TGCC), AMD Irene, 2292 dual-processor AMD Epyc Rome computer nodes at 2.6 GHz with 64 cores per processor, total of 293,376 computing cores and a power of 11.75 Pflop/s, 256 GB DDR4 memory/node. No hyperthreading.

Selection of the best Krylov method and preconditioner

Conjugate Gradient (**CG**)
and Generalized Minimal RESidual (**GMRES**)
Solver tol.: 10^{-14}. Max. it.: 10,000. GMRES restart : 90. Preconditioners:

Part 4: DD preconditioner GenEO

Thanks to: CEA's Very Large Computing Center (TGCC), AMD Irene, 2292 dual-processor AMD Epyc Rome computer nodes at 2.6 GHz with 64 cores per processor, total of 293,376 computing cores and a power of 11.75 Pflop/s, 256 GB DDR4 memory/node. No hyperthreading.

Selection of the best Krylov method and preconditioner

Conjugate Gradient (**CG**)
and Generalized Minimal RESidual (**GMRES**)
Solver tol.: 10^{-14}. Max. it.: 10,000. GMRES restart : 90. Preconditioners:

- DD: ASM, RAS, HPDDM GenEO – ASM and HPDDM GenEO – RAS ;

Part 4: DD preconditioner GenEO

Thanks to: CEA's Very Large Computing Center (TGCC), AMD Irene, 2292 dual-processor AMD Epyc Rome computer nodes at 2.6 GHz with 64 cores per processor, total of 293,376 computing cores and a power of 11.75 Pflop/s, 256 GB DDR4 memory/node. No hyperthreading.

Selection of the best Krylov method and preconditioner

Conjugate Gradient (**CG**)
and Generalized Minimal RESidual (**GMRES**)
Solver tol.: 10^{-14}. Max. it.: 10,000. GMRES restart : 90. Preconditioners:

- DD: ASM, RAS, HPDDM GenEO – ASM and HPDDM GenEO – RAS ;
- AMG: GAMG, BoomerAMG.

Part 4: DD preconditioner GenEO

Thanks to: CEA's Very Large Computing Center (TGCC), AMD Irene, 2292 dual-processor AMD Epyc Rome computer nodes at 2.6 GHz with 64 cores per processor, total of 293,376 computing cores and a power of 11.75 Pflop/s, 256 GB DDR4 memory/node. No hyperthreading.

Selection of the best Krylov method and preconditioner

Conjugate Gradient (**CG**)
and Generalized Minimal RESidual (**GMRES**)
Solver tol.: 10^{-14}. Max. it.: 10,000. GMRES restart : 90. Preconditioners:

- DD: ASM, RAS, HPDDM GenEO – ASM and HPDDM GenEO – RAS ;
- AMG: GAMG, BoomerAMG.

Parallel simulations, 522 MPI processes (= subdomains for DD).
Test case: `[L60geo-FPM-heter]`: 40k fractures, 18.5M dofs.

Part 4: DD preconditioner GenEO

Thanks to: CEA's Very Large Computing Center (TGCC), AMD Irene, 2292 dual-processor AMD Epyc Rome computer nodes at 2.6 GHz with 64 cores per processor, total of 293,376 computing cores and a power of 11.75 Pflop/s, 256 GB DDR4 memory/node. No hyperthreading.

Selection of the best Krylov method and preconditioner

Conjugate Gradient (**CG**)
and Generalized Minimal RESidual (**GMRES**)
Solver tol.: 10^{-14}. Max. it.: 10,000. GMRES restart : 90. Preconditioners:

- DD: ASM, RAS, HPDDM GenEO – ASM and HPDDM GenEO – RAS ;
- AMG: GAMG, BoomerAMG.

Parallel simulations, 522 MPI processes (= subdomains for DD).
Test case: `[L60geo-FPM-heter]`: 40k fractures, 18.5M dofs.

Preconditioner	CG			GMRES		
	# it.	PCSetUp	KSPSolve	# it.	PCSetUp	KSPSolve
GAMG	2,303	00:15	02:28	!!!	!!! 00:15	!!! 12:23
BoomerAMG	4,621	00:12	17:43	!!!	!!! 00:12	!!! 38:40
ASM	635	00:02	00:23	1,396	00:02	01:00
RAS	—	—	—	924	00:02	00:41
HPDDM GenEO - ASM	59	00:32	00:15	58	00:33	00:09
HPDDM GenEO - RAS	—	—	—	38	00:33	00:06

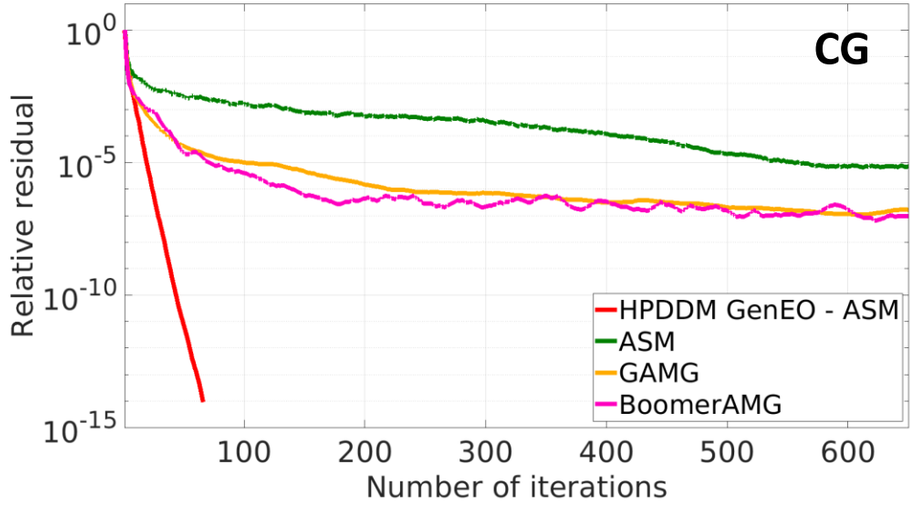

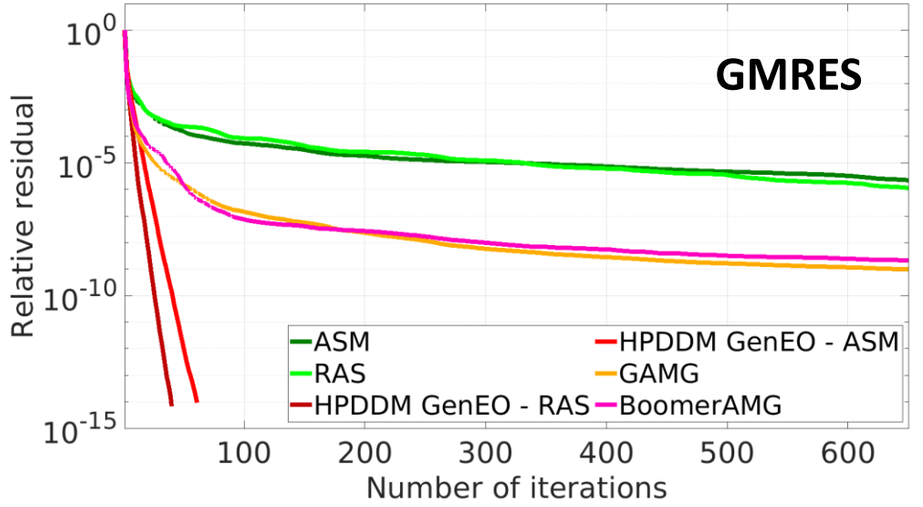

Part 4: DD preconditioner GenEO

Thanks to: CEA's Very Large Computing Center (TGCC), AMD Irene, 2292 dual-processor AMD Epyc Rome computer nodes at 2.6 GHz with 64 cores per processor, total of 293,376 computing cores and a power of 11.75 Pflop/s, 256 GB DDR4 memory/node. No hyperthreading.

Selection of the best Krylov method and preconditioner

Conjugate Gradient (**CG**)
and Generalized Minimal RESidual (**GMRES**)
Solver tol.: 10^{-14}. Max. it.: 10,000. GMRES restart : 90. Preconditioners:

- DD: ASM, RAS, HPDDM GenEO – ASM and HPDDM GenEO – RAS ;
- AMG: GAMG, BoomerAMG.

Parallel simulations, 522 MPI processes (= subdomains for DD).
Test case: `[L60geo-FPM-heter]`: 40k fractures, 18.5M dofs.

Preconditioner	CG			GMRES		
	# it.	PCSetUp	KSPSolve	# it.	PCSetUp	KSPSolve
~~GAMG~~	~~2,303~~	~~00:15~~	~~02:28~~	~~!!!~~	~~!!! 00:15~~	~~!!! 12:23~~
~~BoomerAMG~~	~~4,621~~	~~00:12~~	~~17:43~~	~~!!!~~	~~!!! 00:12~~	~~!!! 38:40~~
ASM	635	00:02	00:23	1,396	00:02	01:00
RAS	—	—	—	924	00:02	00:41
HPDDM GenEO - ASM	59	00:32	00:15	58	00:33	00:09
HPDDM GenEO - RAS	—	—	—	38	00:33	00:06

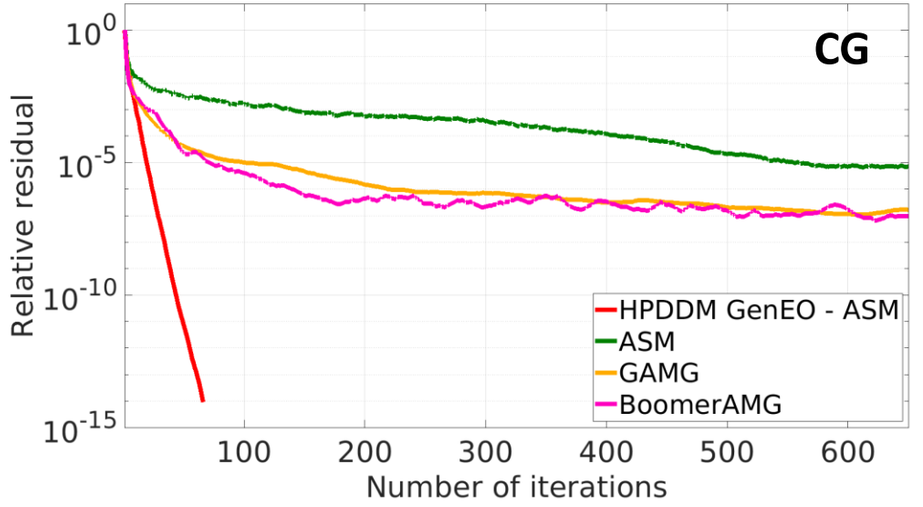

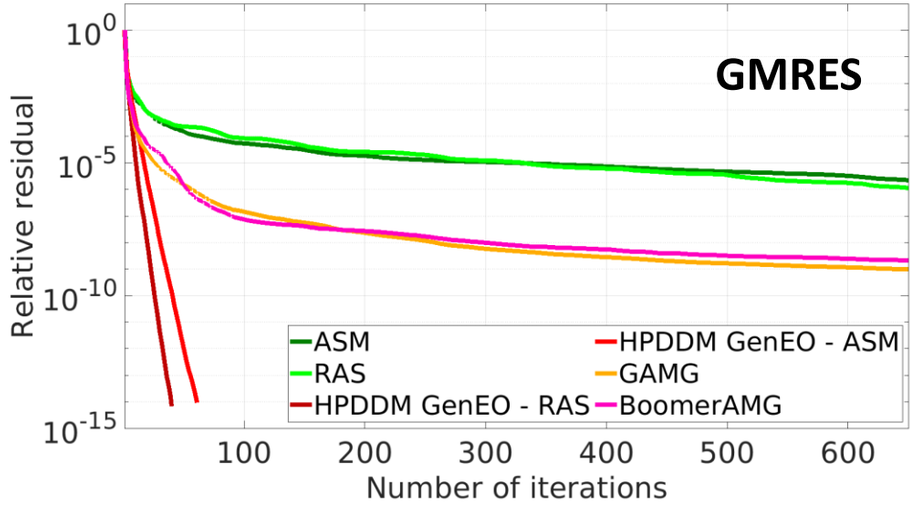

Part 4: DD preconditioner GenEO

Thanks to: CEA's Very Large Computing Center (TGCC), AMD Irene, 2292 dual-processor AMD Epyc Rome computer nodes at 2.6 GHz with 64 cores per processor, total of 293,376 computing cores and a power of 11.75 Pflop/s, 256 GB DDR4 memory/node. No hyperthreading.

Selection of the best Krylov method and preconditioner

Conjugate Gradient (**CG**)
and Generalized Minimal RESidual (**GMRES**)
Solver tol.: 10^{-14}. Max. it.: 10,000. GMRES restart : 90. Preconditioners:

- DD: ASM, RAS, HPDDM GenEO – ASM and HPDDM GenEO – RAS ;
- AMG: GAMG, BoomerAMG.

Parallel simulations, 522 MPI processes (= subdomains for DD).
Test case: `[L60geo-FPM-heter]`: 40k fractures, 18.5M dofs.

Preconditioner	CG			GMRES		
	# it.	PCSetUp	KSPSolve	# it.	PCSetUp	KSPSolve
GAMG	2,303	00:15	02:28	!!!	!!! 00:15	!!! 12:23
BoomerAMG	4,621	00:12	17:43	!!!	!!! 00:12	!!! 38:40
ASM	635	00:02	00:23	1,396	00:02	01:00
RAS				924	00:02	00:41
HPDDM GenEO - ASM	59	00:32	00:15	58	00:33	00:09
HPDDM GenEO - RAS	—	—	—	38	00:33	00:06

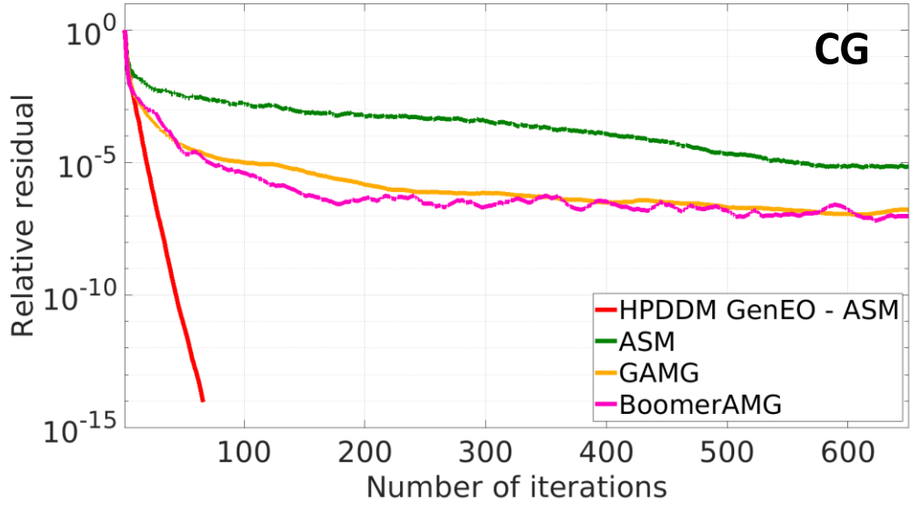

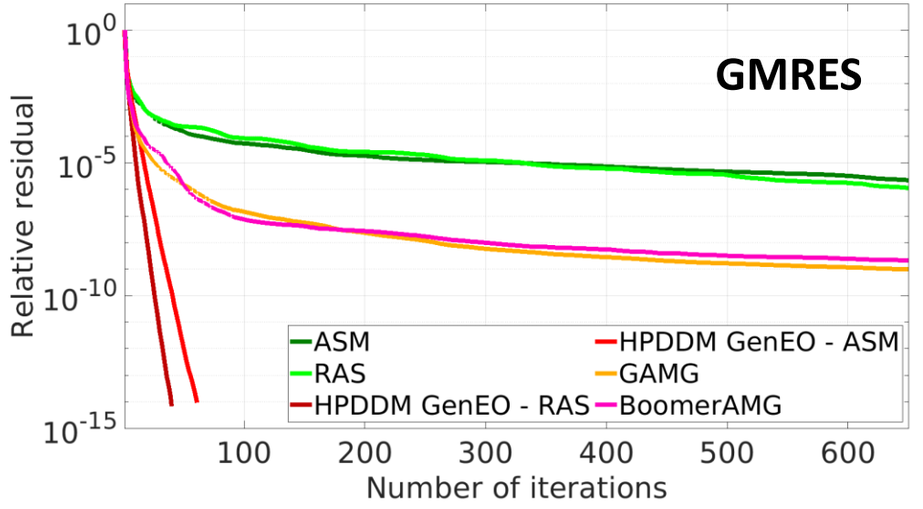

Part 4: DD preconditioner GenEO

Thanks to: CEA's Very Large Computing Center (TGCC), AMD Irene, 2292 dual-processor AMD Epyc Rome computer nodes at 2.6 GHz with 64 cores per processor, total of 293,376 computing cores and a power of 11.75 Pflop/s, 256 GB DDR4 memory/node. No hyperthreading.

Selection of the best Krylov method and preconditioner

Conjugate Gradient (**CG**)
and Generalized Minimal RESidual (**GMRES**)
Solver tol.: 10^{-14}. Max. it.: 10,000. GMRES restart : 90. Preconditioners:

- DD: ASM, RAS, HPDDM GenEO – ASM and HPDDM GenEO – RAS ;
- AMG: GAMG, BoomerAMG.

Parallel simulations, 522 MPI processes (= subdomains for DD).
Test case: `[L60geo-FPM-heter]`: 40k fractures, 18.5M dofs.

Preconditioner	CG			GMRES		
	# it.	PCSetUp	KSPSolve	# it.	PCSetUp	KSPSolve
GAMG	2,303	00.15	02.28	!!!	!!! 00.15	!!! 12.23
BoomerAMG	4,621	00.12	17.43	!!!	!!! 00.12	!!! 38.40
ASM	635	00.02	00.23	1,396	00.02	01.00
RAS				924	00.02	00.41
HPDDM GenEO – ASM	59	00.32	00.15	58	00.33	00.09
HPDDM GenEO - RAS	—	—	—	38	00:33	00:06

GMRES + HPDDM GenEO – RAS → best performance.

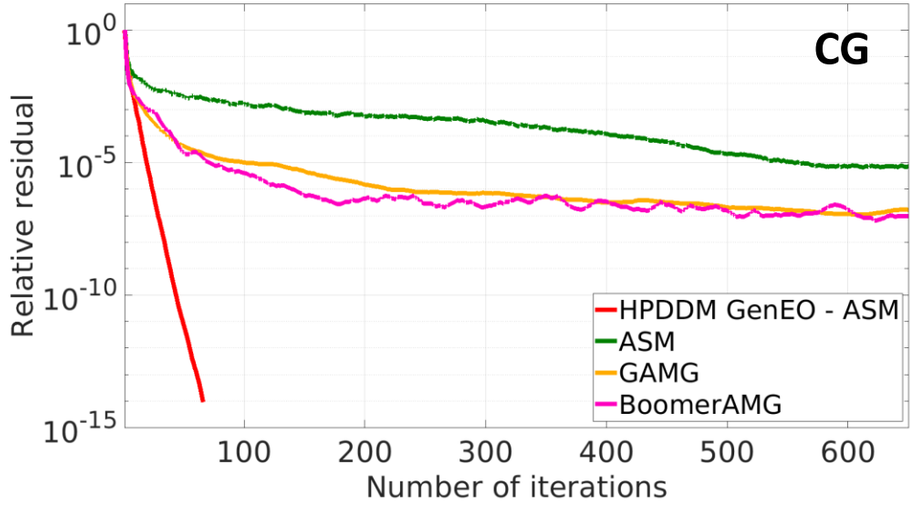

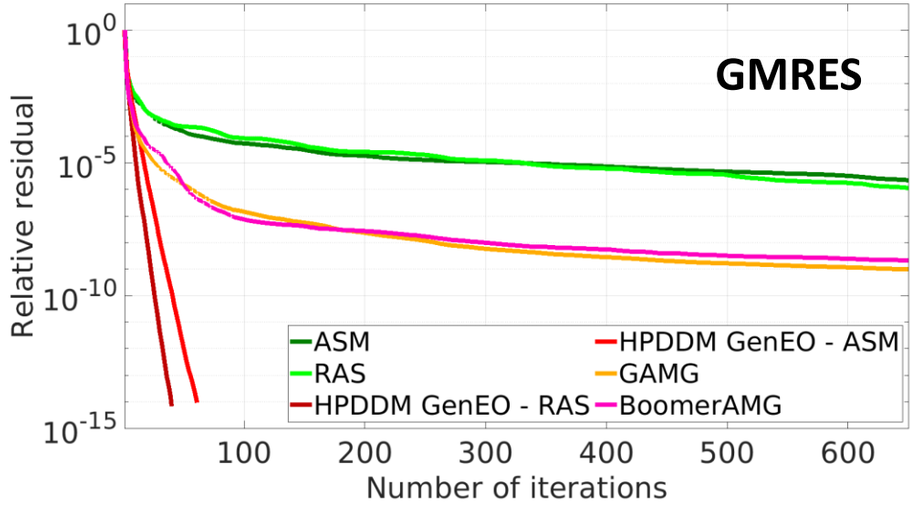

Part 4: DD preconditioner GenEO

Thanks to: CEA's Very Large Computing Center (TGCC), AMD Irene, 2292 dual-processor AMD Epyc Rome computer nodes at 2.6 GHz with 64 cores per processor, total of 293,376 computing cores and a power of 11.75 Pflop/s, 256 GB DDR4 memory/node. No hyperthreading.

Selection of the best Krylov method and preconditioner

Conjugate Gradient (**CG**)
and Generalized Minimal RESidual (**GMRES**)
Solver tol.: 10^{-14}. Max. it.: 10,000. GMRES restart : 90. Preconditioners:

- DD: ASM, RAS, HPDDM GenEO – ASM and HPDDM GenEO – RAS ;
- AMG: GAMG, BoomerAMG.

Parallel simulations, 522 MPI processes (= subdomains for DD).
Test case: `[L60geo-FPM-heter]`: 40k fractures, 18.5M dofs.

Preconditioner	CG			GMRES		
	# it.	PCSetUp	KSPSolve	# it.	PCSetUp	KSPSolve
GAMG	2,303	00.15	02.28	!!!	!!! 00.15	!!! 12.23
BoomerAMG	4,621	00.12	17.43	!!!	!!! 00.12	!!! 38.40
ASM	635	00.02	00.23	1,396	00.02	01.00
RAS				924	00.02	00.41
HPDDM GenEO – ASM	59	00.32	00.15	58	00.33	00.09
HPDDM GenEO - RAS	—	—	—	38	00:33	00:06

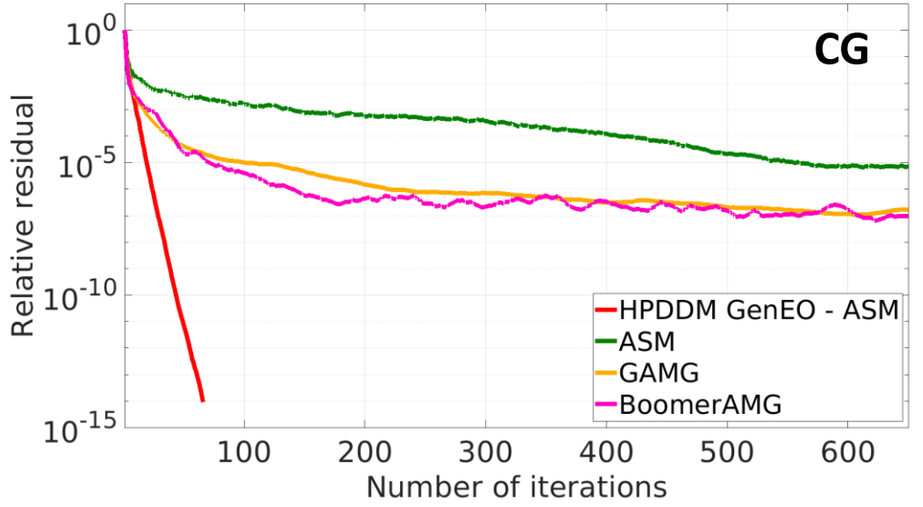

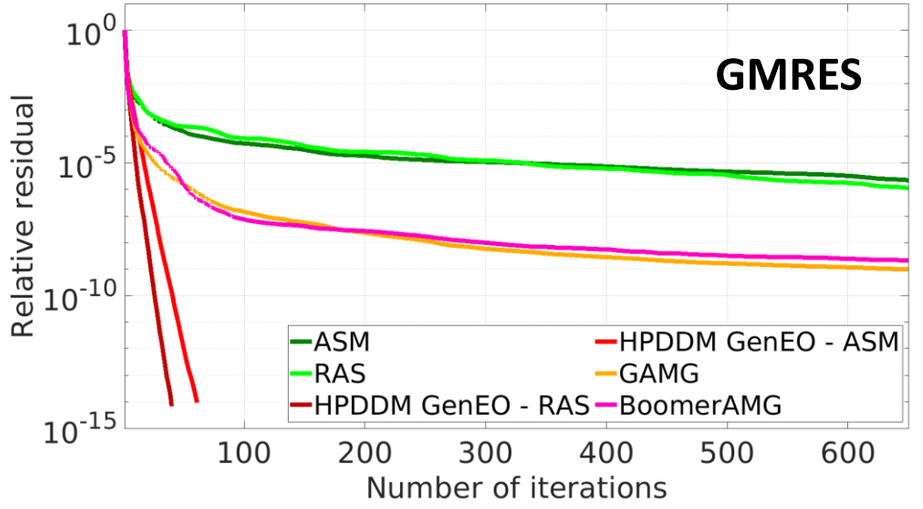

GMRES + HPDDM GenEO – RAS → best performance.
+ strong and weak scaling.

Part 4: DD preconditioner GenEO

Robustness with respect to the number of fractures

GMRES + HPDDM GenEO - RAS. Solver tolerance : 10^{-14}. GMRES restart : 90.

Robustness with respect to the number of fractures

GMRES + HPDDM GenEO - RAS. Solver tolerance : 10^{-14}. GMRES restart : 90.

Robustness with respect to the number of fractures

Test cases with an increasing number of fractures. Decompose so as to keep #dofs / sbdm ~36k.

Test case name	# frac.	# dofs	# sbdm.
[L60geo-FPM-1v100]	40k	19M	522
[L80geo-FPM-1v100]	90k	39M	1,098
[L100geo-FPM-1v100]	174k	72M	2,022
[L130geo-FPM-1v100]	377k	141M	3,985
[L160geo-FPM-1v100]	697k	243M	6,825

GMRES + HPDDM GenEO - RAS. Solver tolerance : 10^{-14}. GMRES restart : 90.

Robustness with respect to the number of fractures

Test cases with an increasing number of fractures. Decompose so as to keep #dofs / sbdm ~36k.

Test case name	# frac.	# dofs	# sbdm.	# it.	PCSetUp mm:ss	KSPSolve mm:ss
[L60geo-FPM-1v100]	40k	19M	522	38	00:33	00:06
[L80geo-FPM-1v100]	90k	39M	1,098	38	00:47	00:08
[L100geo-FPM-1v100]	174k	72M	2,022	40	01:09	00:13
[L130geo-FPM-1v100]	377k	141M	3,985	41	02:11	00:24
[L160geo-FPM-1v100]	697k	243M	6,825	41	02:33	00:37

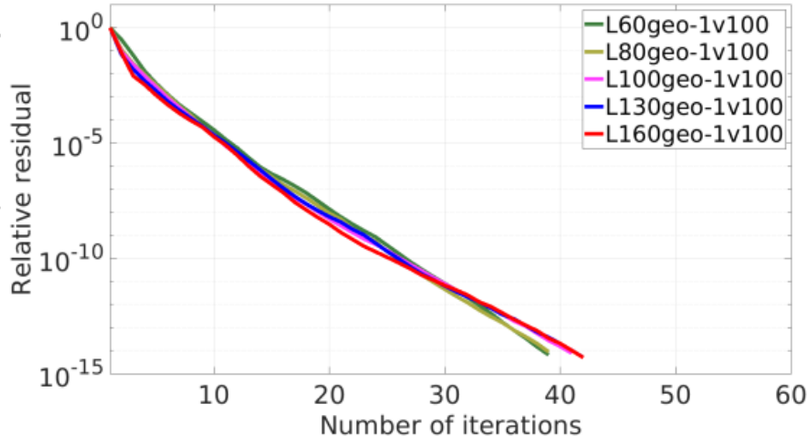

GMRES + HPDDM GenEO - RAS. Solver tolerance : 10^{-14}. GMRES restart : 90.

Robustness with respect to the number of fractures

Test cases with an increasing number of fractures. Decompose so as to keep #dofs / sbdm ~36k.

Test case name	# frac.	# dofs	# sbdm.	# it.	PCSetUp mm:ss	KSPSolve mm:ss
[L60geo-FPM-1v100]	40k	19M	522	38	00:33	00:06
[L80geo-FPM-1v100]	90k	39M	1,098	38	00:47	00:08
[L100geo-FPM-1v100]	174k	72M	2,022	40	01:09	00:13
[L130geo-FPM-1v100]	377k	141M	3,985	41	02:11	00:24
[L160geo-FPM-1v100]	697k	243M	6,825	41	02:33	00:37

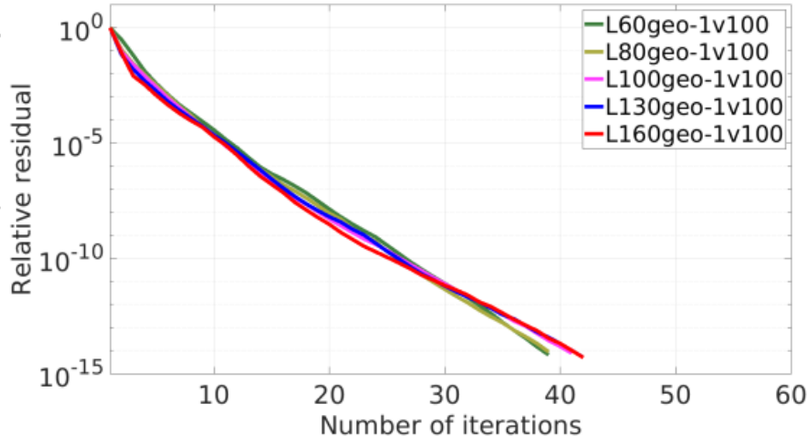

+ Robustness w.r.t. # frac. OK (38-41 it.).

GMRES + HPDDM GenEO - RAS. Solver tolerance : 10^{-14}. GMRES restart : 90.

Robustness with respect to the number of fractures and the heterogeneity of hydraulic conductivity/transmissivity

Test cases with an increasing number of fractures. Decompose so as to keep #dofs / sbdm ~36k.

Test case name	# frac.	# dofs	# sbdm.	# it.	PCSetUp mm:ss	KSPSolve mm:ss
[L60geo-FPM-1v100]	40k	19M	522	38	00:33	00:06
[L80geo-FPM-1v100]	90k	39M	1,098	38	00:47	00:08
[L100geo-FPM-1v100]	174k	72M	2,022	40	01:09	00:13
[L130geo-FPM-1v100]	377k	141M	3,985	41	02:11	00:24
[L160geo-FPM-1v100]	697k	243M	6,825	41	02:33	00:37

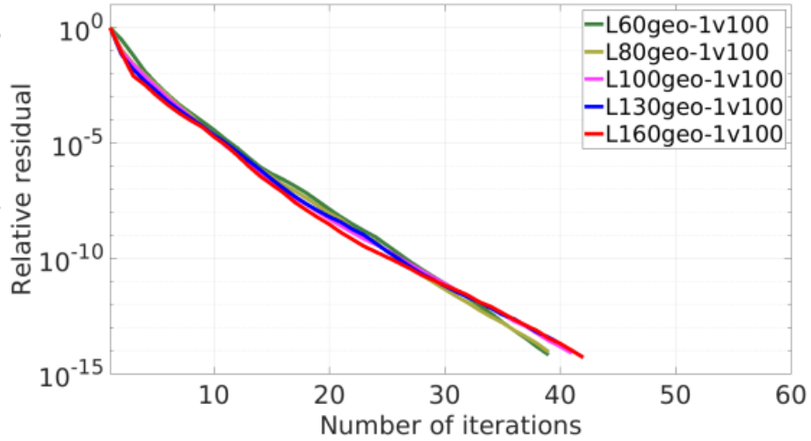

+ Robustness w.r.t. # frac. OK (38-41 it.).

Part 4: DD preconditioner GenEO

GMRES + HPDDM GenEO - RAS. Solver tolerance : 10^{-14}. GMRES restart : 90.

Robustness with respect to the number of fractures and the heterogeneity of hydraulic conductivity/transmissivity

Test cases with an increasing number of fractures. Decompose so as to keep #dofs / sbdm ~36k.

Test case name	# frac.	# dofs	# sbdm.	# it.	PCSetUp mm:ss	KSPSolve mm:ss
[L60geo-FPM-1v100]	40k	19M	522	38	00:33	00:06
[L80geo-FPM-1v100]	90k	39M	1,098	38	00:47	00:08
[L100geo-FPM-1v100]	174k	72M	2,022	40	01:09	00:13
[L130geo-FPM-1v100]	377k	141M	3,985	41	02:11	00:24
[L160geo-FPM-1v100]	697k	243M	6,825	41	02:33	00:37
[L60geo-FPM-heter]	40k	19M	522			
[L80geo-FPM-heter]	90k	39M	1,098			
[L100geo-FPM-heter]	174k	72M	2,022			
[L130geo-FPM-heter]	377k	141M	3,985			
[L160geo-FPM-heter]	697k	243M	6,825			

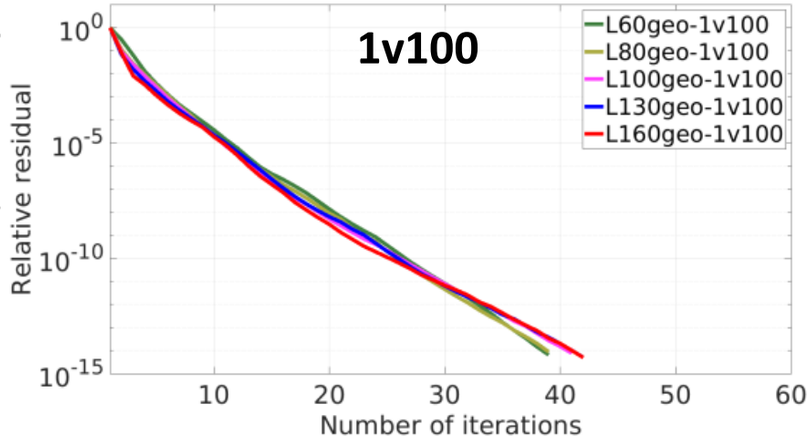

+ Robustness w.r.t. # frac. OK (38-41 it.).

Part 4: DD preconditioner GenEO

GMRES + HPDDM GenEO - RAS. Solver tolerance : 10^{-14}. GMRES restart : 90.

Robustness with respect to the number of fractures and the heterogeneity of hydraulic conductivity/transmissivity

Test cases with an increasing number of fractures. Decompose so as to keep #dofs / sbdm ~36k.

Test case name	# frac.	# dofs	# sbdm.	# it.	PCSetUp mm:ss	KSPSolve mm:ss
[L60geo-FPM-1v100]	40k	19M	522	38	00:33	00:06
[L80geo-FPM-1v100]	90k	39M	1,098	38	00:47	00:08
[L100geo-FPM-1v100]	174k	72M	2,022	40	01:09	00:13
[L130geo-FPM-1v100]	377k	141M	3,985	41	02:11	00:24
[L160geo-FPM-1v100]	697k	243M	6,825	41	02:33	00:37
[L60geo-FPM-heter]	40k	19M	522	39	00:35	00:06
[L80geo-FPM-heter]	90k	39M	1,098	45	00:54	00:10
[L100geo-FPM-heter]	174k	72M	2,022	46	01:23	00:16
[L130geo-FPM-heter]	377k	141M	3,985	50	02:11	00:28
[L160geo-FPM-heter]	697k	243M	6,825	51	03:52	00:49

+ Robustness w.r.t. # frac. OK (38-41 it.).

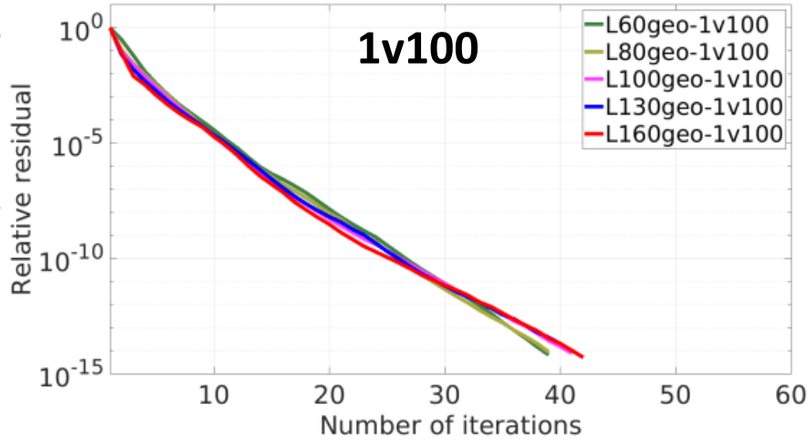

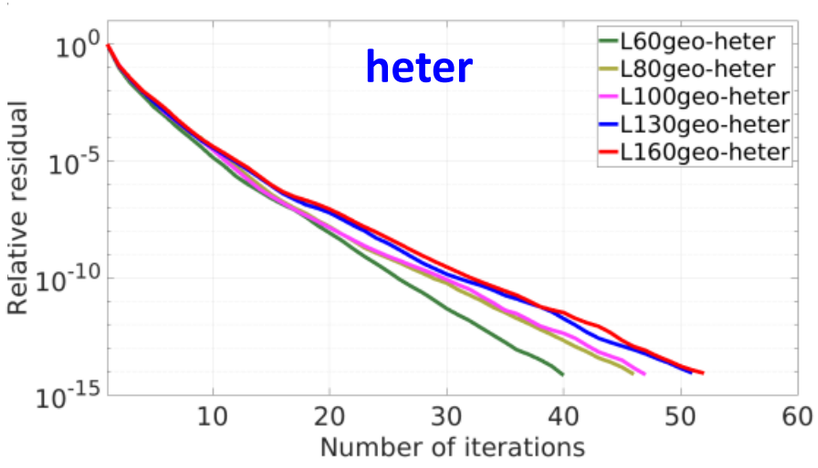

Part 4: DD preconditioner GenEO

GMRES + HPDDM GenEO - RAS. Solver tolerance : 10^{-14}. GMRES restart : 90.

Robustness with respect to the number of fractures and the heterogeneity of hydraulic conductivity/transmissivity

Test cases with an increasing number of fractures. Decompose so as to keep #dofs / sbdm ~36k.

Test case name	# frac.	# dofs	# sbdm.	# it.	PCSetUp mm:ss	KSPSolve mm:ss
[L60geo-FPM-1v100]	40k	19M	522	38	00:33	00:06
[L80geo-FPM-1v100]	90k	39M	1,098	38	00:47	00:08
[L100geo-FPM-1v100]	174k	72M	2,022	40	01:09	00:13
[L130geo-FPM-1v100]	377k	141M	3,985	41	02:11	00:24
[L160geo-FPM-1v100]	697k	243M	6,825	41	02:33	00:37
[L60geo-FPM-heter]	40k	19M	522	39	00:35	00:06
[L80geo-FPM-heter]	90k	39M	1,098	45	00:54	00:10
[L100geo-FPM-heter]	174k	72M	2,022	46	01:23	00:16
[L130geo-FPM-heter]	377k	141M	3,985	50	02:11	00:28
[L160geo-FPM-heter]	697k	243M	6,825	51	03:52	00:49

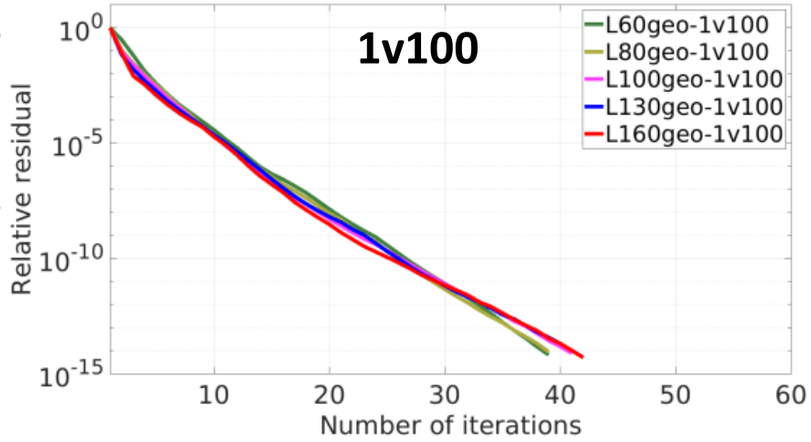

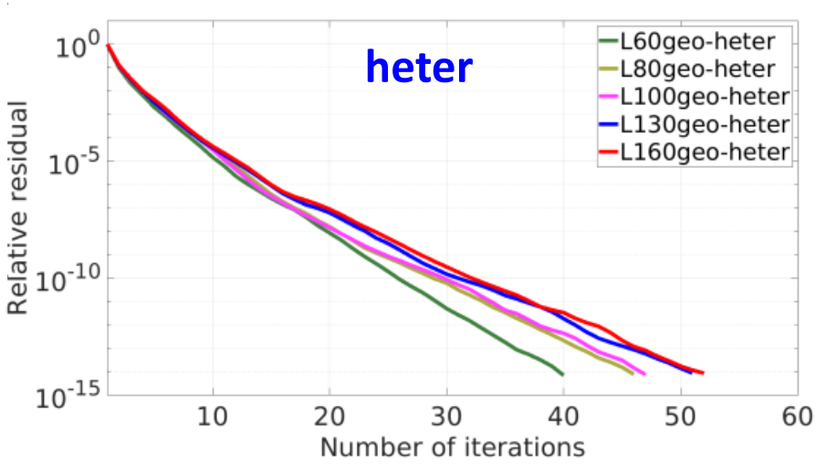

+ Robustness w.r.t. # frac. OK (38-41 it.).

+ Robustness w.r.t. # frac. and heterogeneity OK (39-51 it.).

Part 4: DD preconditioner GenEO

GMRES + HPDDM GenEO - RAS. Solver tolerance : 10^{-14}. GMRES restart : 90.

Robustness with respect to the number of fractures and the heterogeneity of hydraulic conductivity/transmissivity

Test cases with an increasing number of fractures. Decompose so as to keep #dofs / sbdm ~36k.

Test case name	# frac.	# dofs	# sbdm.	# it.	PCSetUp mm:ss	KSPSolve mm:ss	Coarse space size
[L60geo-FPM-1v100]	40k	19M	522	38	00:33	00:06	36k
[L80geo-FPM-1v100]	90k	39M	1,098	38	00:47	00:08	79k
[L100geo-FPM-1v100]	174k	72M	2,022	40	01:09	00:13	153k
[L130geo-FPM-1v100]	377k	141M	3,985	41	02:11	00:24	319k
[L160geo-FPM-1v100]	697k	243M	6,825	41	02:33	00:37	577k
[L60geo-FPM-heter]	40k	19M	522	39	00:35	00:06	37k
[L80geo-FPM-heter]	90k	39M	1,098	45	00:54	00:10	81k
[L100geo-FPM-heter]	174k	72M	2,022	46	01:23	00:16	155k
[L130geo-FPM-heter]	377k	141M	3,985	50	02:11	00:28	325k
[L160geo-FPM-heter]	697k	243M	6,825	51	03:52	00:49	587k

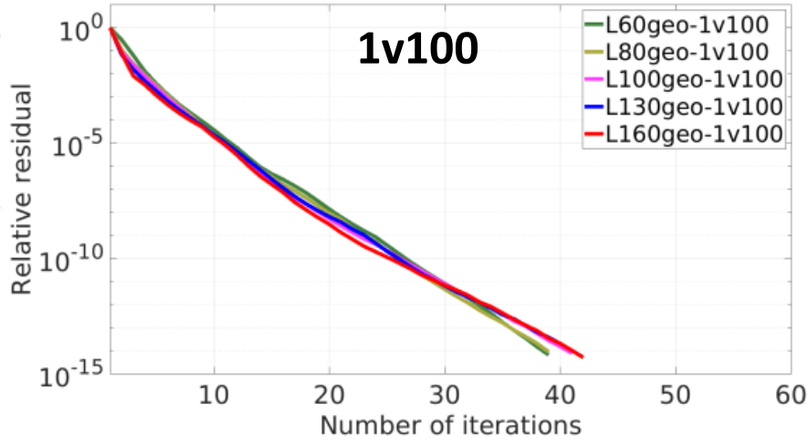

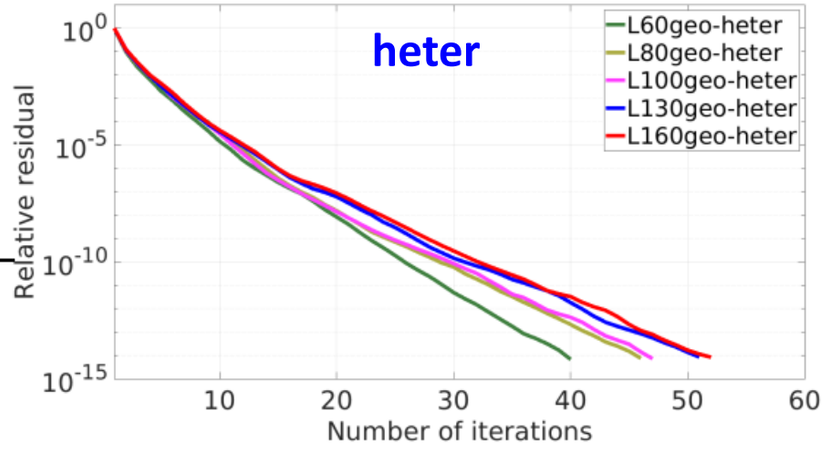

+ Robustness w.r.t. # frac. OK (38-41 it.).

+ Robustness w.r.t. # frac. and heterogeneity OK (39-51 it.).

Part 4: DD preconditioner GenEO

GMRES + HPDDM GenEO - RAS. Solver tolerance : 10^{-14}. GMRES restart : 90.

Robustness with respect to the number of fractures and the heterogeneity of hydraulic conductivity/transmissivity

Test cases with an increasing number of fractures. Decompose so as to keep #dofs / sbdm ~36k.

Test case name	# frac.	# dofs	# sbdm.	# it.	PCSetUp mm:ss	KSPSolve mm:ss	Coarse space size
[L60geo-FPM-1v100]	40k	19M	522	38	00:33	00:06	36k
[L80geo-FPM-1v100]	90k	39M	1,098	38	00:47	00:08	79k
[L100geo-FPM-1v100]	174k	72M	2,022	40	01:09	00:13	153k
[L130geo-FPM-1v100]	377k	141M	3,985	41	02:11	00:24	319k
[L160geo-FPM-1v100]	697k	243M	6,825	41	02:33	00:37	577k
[L60geo-FPM-heter]	40k	19M	522	39	00:35	00:06	37k
[L80geo-FPM-heter]	90k	39M	1,098	45	00:54	00:10	81k
[L100geo-FPM-heter]	174k	72M	2,022	46	01:23	00:16	155k
[L130geo-FPM-heter]	377k	141M	3,985	50	02:11	00:28	325k
[L160geo-FPM-heter]	697k	243M	6,825	51	03:52	00:49	587k

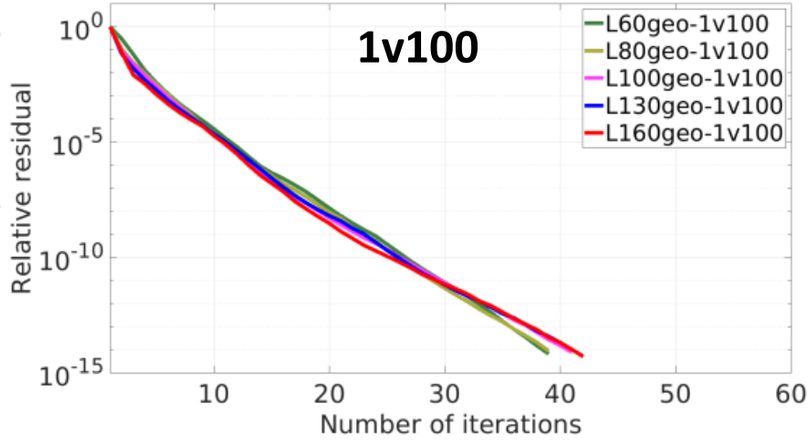

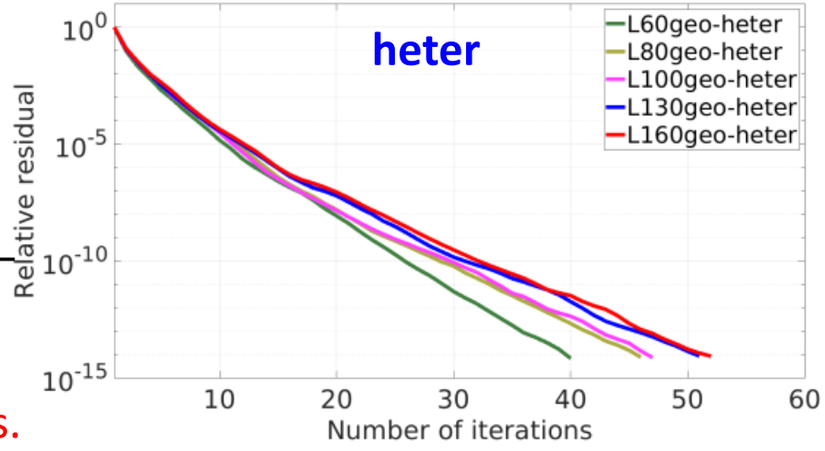

+ Robustness w.r.t. # frac. OK (38-41 it.).
+ Robustness w.r.t. # frac. and heterogeneity OK (39-51 it.).
+ Reasonable wall-clock time for `[L160geo-FPM-heter]`, around 5 minutes.

Conclusion and further work

- Mixed-hybrid finite element (MHFE) formulation for single-phase flow, under the continuous hydraulic head condition.

- Mixed-hybrid finite element (MHFE) formulation for single-phase flow, under the continuous hydraulic head condition.

- Tools for simulation (assemble and/or solve) of single-phase flow with a very large number of fractures, up to hundreds of thousands.

- Mixed-hybrid finite element (MHFE) formulation for single-phase flow, under the continuous hydraulic head condition.

- Tools for simulation (assemble and/or solve) of single-phase flow with a very large number of fractures, up to hundreds of thousands.

- Solver convergence within reasonable wall-clock time thanks to HPDDM-GenEO.

- Mixed-hybrid finite element (MHFE) formulation for single-phase flow, under the continuous hydraulic head condition.

- Tools for simulation (assemble and/or solve) of single-phase flow with a very large number of fractures, up to hundreds of thousands.

- Solver convergence within reasonable wall-clock time thanks to HPDDM-GenEO.

Perspectives:

- Mixed-hybrid finite element (MHFE) formulation for single-phase flow, under the continuous hydraulic head condition.

- Tools for simulation (assemble and/or solve) of single-phase flow with a very large number of fractures, up to hundreds of thousands.

- Solver convergence within reasonable wall-clock time thanks to HPDDM-GenEO.

Perspectives:

- DFM with 1M+ fractures !

- Mixed-hybrid finite element (MHFE) formulation for single-phase flow, under the continuous hydraulic head condition.

- Tools for simulation (assemble and/or solve) of single-phase flow with a very large number of fractures, up to hundreds of thousands.

- Solver convergence within reasonable wall-clock time thanks to HPDDM-GenEO.

Perspectives:

- DFM with 1M+ fractures !

- Extend the parallelism beyond the solver phase: assembly, post-processing, etc.

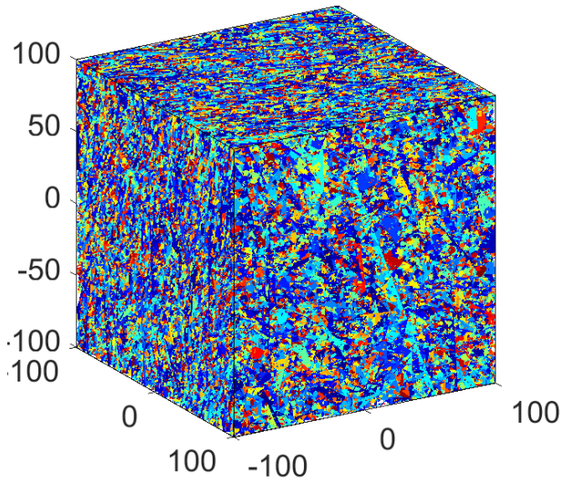

***DFN** with ~1.2M fractures*

A. Ern, F. Hédin, G. Pichot, N. Pignet. *SMAI Journal of Computational Mathematics.* **2022.**

- Mixed-hybrid finite element (MHFE) formulation for single-phase flow, under the continuous hydraulic head condition.

- Tools for simulation (assemble and/or solve) of single-phase flow with a very large number of fractures, up to hundreds of thousands.

- Solver convergence within reasonable wall-clock time thanks to HPDDM-GenEO.

Perspectives:

- DFM with 1M+ fractures !

- Extend the parallelism beyond the solver phase: assembly, post-processing, etc.

- For spectral DD methods: give some information to the partitioner in order to equilibrate the number of computed eigenpairs per subdomain.

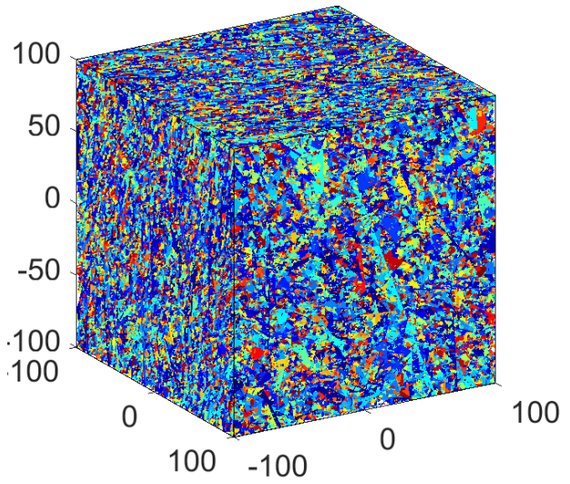

***DFN** with ~1.2M fractures*

A. Ern, F. Hédin, G. Pichot, N. Pignet. *SMAI Journal of Computational Mathematics.* **2022.**

- Mixed-hybrid finite element (MHFE) formulation for single-phase flow, under the continuous hydraulic head condition.

- Tools for simulation (assemble and/or solve) of single-phase flow with a very large number of fractures, up to hundreds of thousands.

- Solver convergence within reasonable wall-clock time thanks to HPDDM-GenEO.

Perspectives:

- DFM with 1M+ fractures !

- Extend the parallelism beyond the solver phase: assembly, post-processing, etc.

- For spectral DD methods: give some information to the partitioner in order to equilibrate the number of computed eigenpairs per subdomain.

- 2D-3D DFM polytopal meshes, HHO.

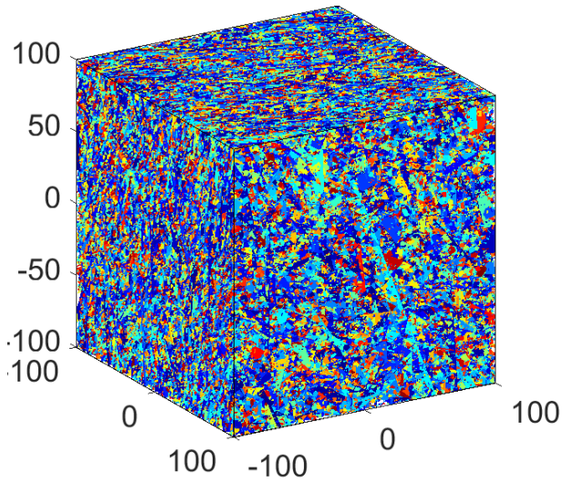

***DFN** with ~1.2M fractures*

A. Ern, F. Hédin, G. Pichot, N. Pignet. *SMAI Journal of Computational Mathematics.* **2022.**

- Mixed-hybrid finite element (MHFE) formulation for single-phase flow, under the continuous hydraulic head condition.

- Tools for simulation (assemble and/or solve) of single-phase flow with a very large number of fractures, up to hundreds of thousands.

- Solver convergence within reasonable wall-clock time thanks to HPDDM-GenEO.

Perspectives:

- DFM with 1M+ fractures !

- Extend the parallelism beyond the solver phase: assembly, post-processing, etc.

- For spectral DD methods: give some information to the partitioner in order to equilibrate the number of computed eigenpairs per subdomain.

- 2D-3D DFM polytopal meshes, HHO.

- Hydrogeological studies, Monte-Carlo simulations.

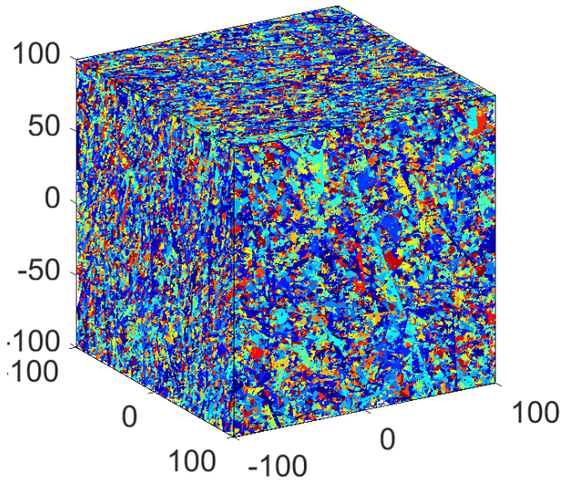

***DFN** with ~1.2M fractures*

A. Ern, F. Hédin, G. Pichot, N. Pignet. *SMAI Journal of Computational Mathematics.* **2022.**

Thank you !

Bonus

From hydrogeological point properties to infinitesimal calculus

Main characteristics of porous media :

- permeability k (m^2), hydraulic conductivity ($m \cdot s^{-1}$), $\mathcal{K} = \frac{k\rho g}{\mu}$
- porosity.

Macroscopic Darcy's Law : $Q = -\frac{kA}{\mu}\frac{\Delta P}{L}$

Porosity and permeability can neither be defined nor measured at a single point: below a certain volume scale, loss of their physical meaning.

→ ***Representative Elementary Volume (REV)***: definition and measurement of the "average" property of the considered volume.

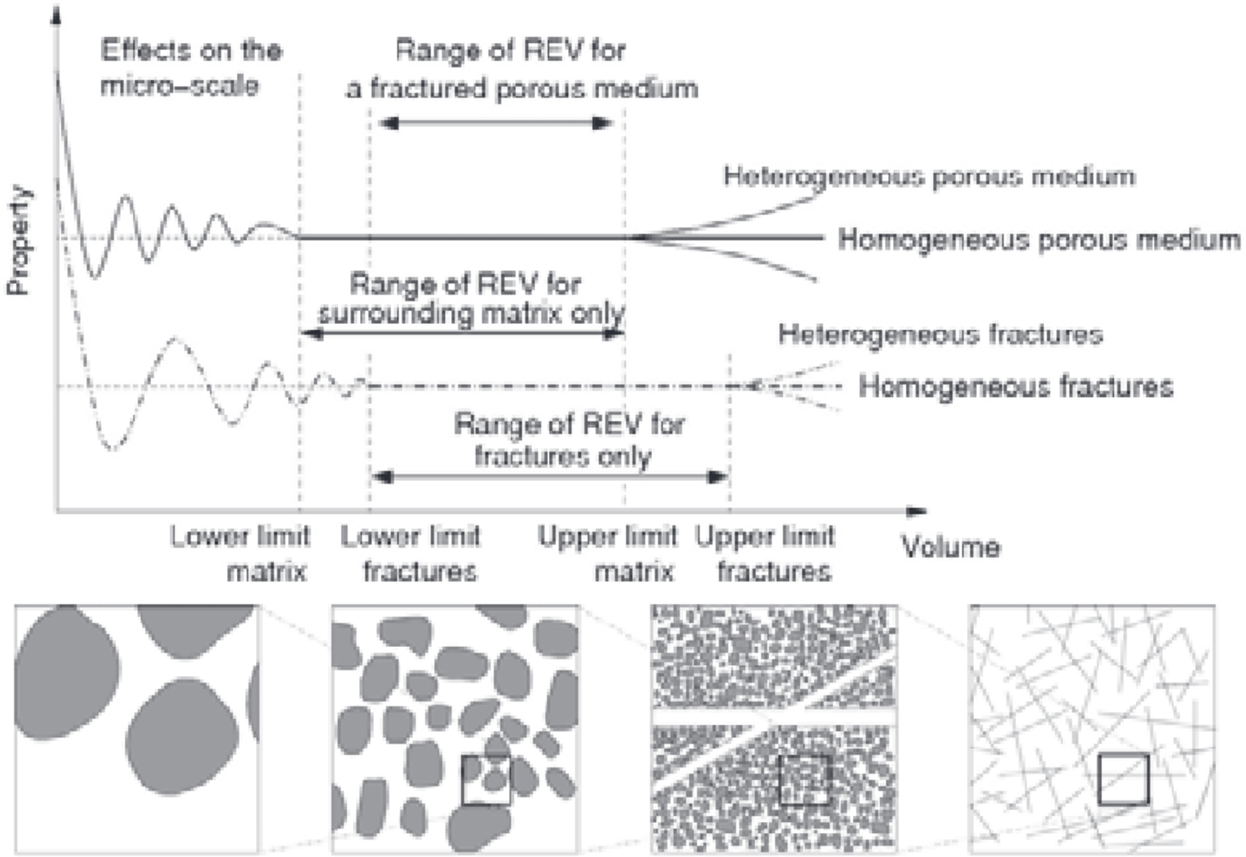

Representative Elementary Volume (REV). *Adapted in thesis by Alexandru Tatomir (Stuttgart Univ., 2012) from Bear et al., 1983.*

Reduced model for flow in DFM

V. Martin, J. Jaffré, and J. E. Roberts. *Modeling fractures and barriers as interfaces for flow in porous media.* SIAM Journal on Scientific Computing. **2005.**

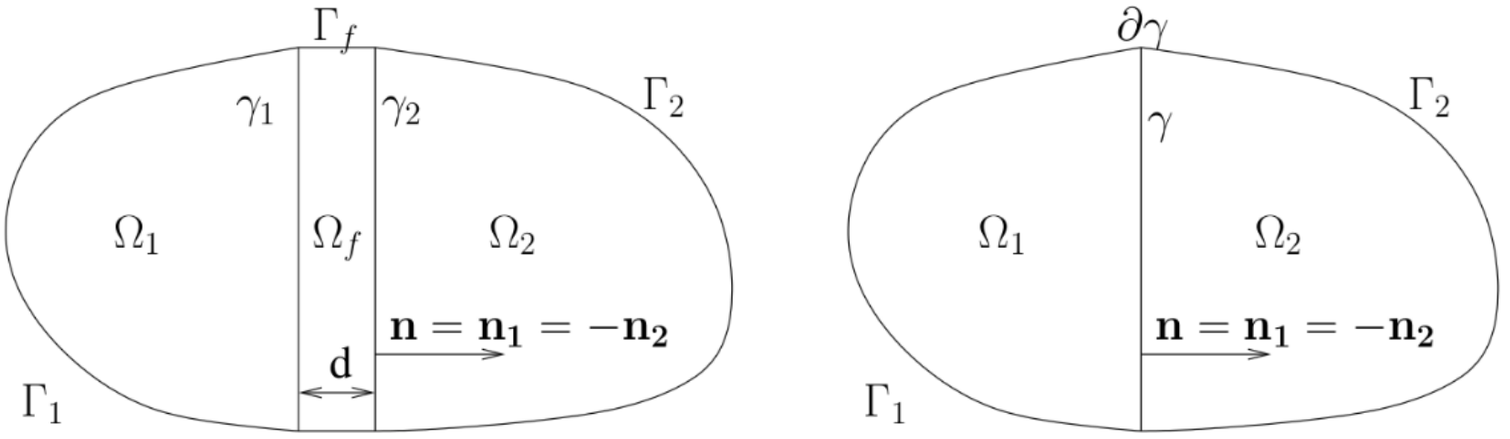

Scheme of the reduced model. The given example is in two dimensions.

Left: global domain Ω, fracture domain Ω_f with a thickness d, separating the global domain into two rock-matrix subdomains Ω_1 and Ω_2 .

Right: fracture modeled as an interface γ, a hyperplane (codimension 1) with normal unit vectors $n = n_1 = -n_2$.

$$\Omega_f = \left\{ x \in \Omega \;\middle|\; \exists s \in \gamma : \exists r \in \left] \frac{-d(s)}{2}, \frac{d(s)}{2} \right[: x = s + rn \right\}$$

Permeameter boundary conditions (BC)

Gradient of the hydraulic heads (rock matrix and fracture network) on two opposite sides of the cube.

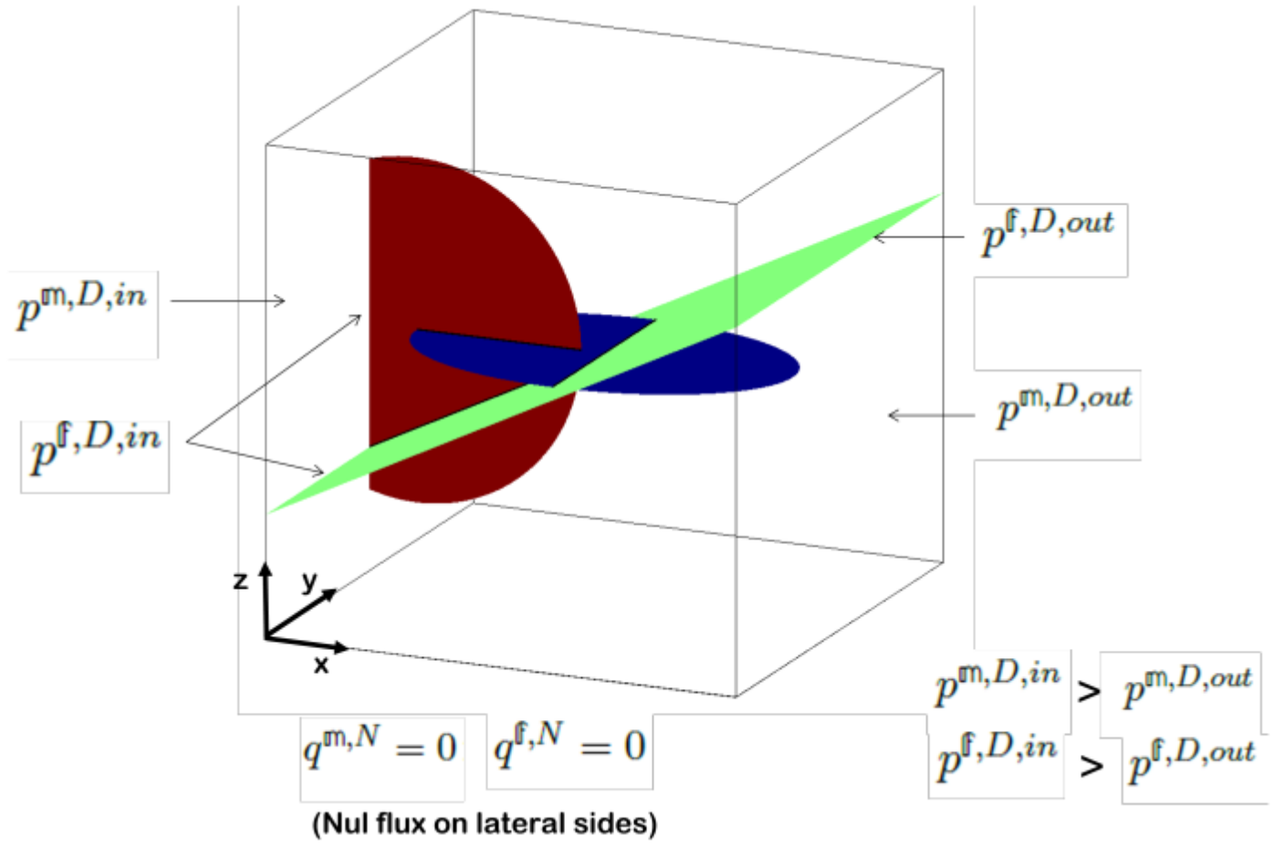

Direct methods are too expensive in terms of RAM.

Cholesky and LU factorizations (parallel simulations with 48 MPI processes).

Test case	Solver	Solver time hh:mm:ss	RAM (GB)
[L20geo-FPM-1v100]	CHOL	00:00:57	27.3
[L60geo-FPM-1v100]	CHOL	00:06:26	107
[L20geo-FPM-1v100]	LU	00:01:21	41.3
[L60geo-FPM-1v100]	LU	00:08:50	159

Bonus

D. Demidov. *An Efficient, Flexible, and Extensible Algebraic Multigrid Implementation.* Lobachevskii J. Math. **2019.**

Classic preconditioners suffer from breakdowns

Conjugate Gradient (PCG) preconditioned with
- Incomplete Cholesky factorization (MATLAB implementation)
- AMGCL (C++ / MEX external library)

Sequential simulations with `[L20geo-FPM-1v100]` test case.

Solver tolerance : 10^{-14}

Precond.	# it.	Solver time hh:mm:ss
iCHOL	9,972 <!>	02:55:36 <!>
AMGCL	2,869	00:28:01

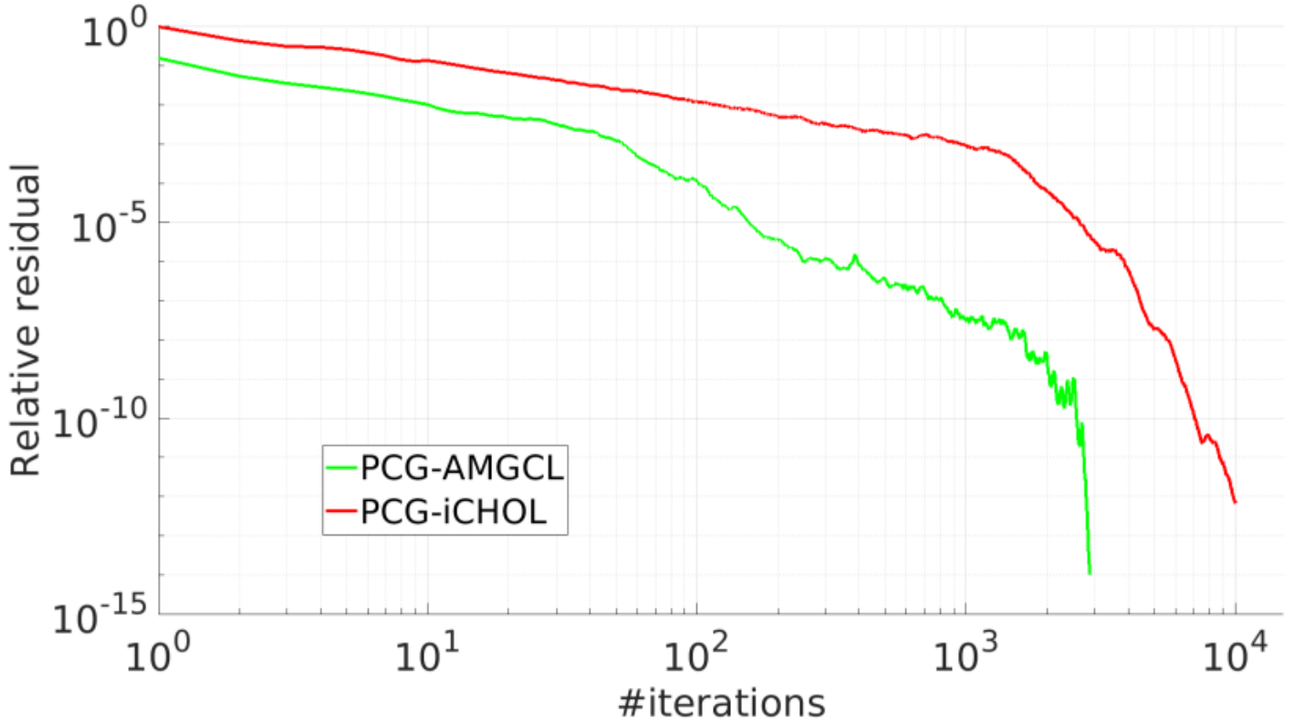

Bonus

Choosing iterative solver tolerance

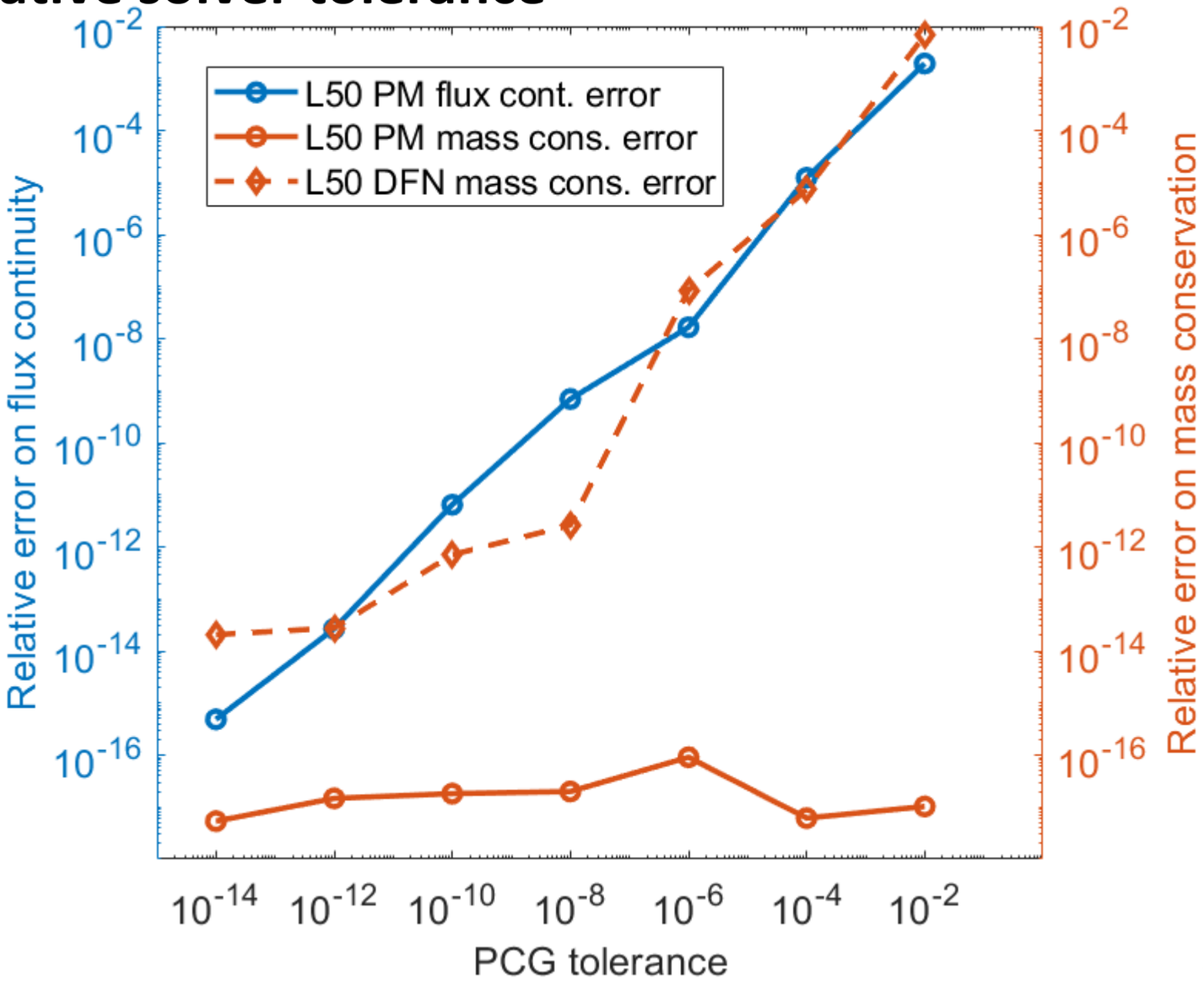

Continuous weak mixed solution

L^2 spaces for p (hydraulic head): $S = L^2(\Omega^{\mathrm{m}}) \times L^2(\Omega^{\mathrm{f}})$.

$H(\mathrm{div})$ spaces for u (velocity): $V = \tilde{V} + \texttt{conditions on intersections}$, with:

$$\tilde{V} = \{v = (v^{\mathrm{m}}, v^{\mathrm{f}}) \text{ s.t.: } v^{\mathrm{f}} \in L^2(\Omega^{\mathrm{f}}) \text{ and } \forall \alpha \in \mathcal{C},\ v_\alpha^{\mathrm{m}} \in H(\mathrm{div}, \omega_\alpha), \gamma_n^{\mathrm{m}} v_\alpha^{\mathrm{m}} = 0 \text{ on } \Gamma_\alpha^N,$$
$$\forall \ell \in \mathcal{I},\ (\nabla_\tau \cdot v_\ell^{\mathrm{f}} - [[v^{\mathrm{m}}]]_{|\gamma_\ell}) \in L^2(\gamma_\ell)\}.$$

Problem statement. Find $u = (u^{\mathrm{m}}, u^{\mathrm{f}}) \in V$ and $p = (p^{\mathrm{m}}, p^{\mathrm{f}}) \in S$ such that:

$$\begin{aligned} a(u,v) - b(v,p) &= L_a(v), \quad \forall v \in V, \\ b(u,s) &= L_b(s), \quad \forall s \in S, \end{aligned}$$

where:

$$a(u,v) = \int_{\Omega^{\mathrm{m}}} (\mathcal{K}^{\mathrm{m}})^{-1} u^{\mathrm{m}} \cdot v^{\mathrm{m}} + \int_{\Omega^{\mathrm{f}}} (\mathcal{K}^{\mathrm{f}})^{-1} u^{\mathrm{f}} \cdot v^{\mathrm{f}},$$

$$b(v,p) = \sum_{\alpha \in \mathcal{C}} \int_{\omega_\alpha} p_\alpha^{\mathrm{m}}\, \nabla \cdot v_\alpha^{\mathrm{m}} + \sum_{\ell \in \mathcal{I}} \int_{\gamma_\ell} p_\ell^{\mathrm{f}} \left(\nabla_\tau \cdot v_\ell^{\mathrm{f}} - [[v^{\mathrm{m}}]]_{|\gamma_\ell}\right).$$

a is continuous and coercive. b satisfies the inf-sup condition.

$\Longrightarrow$ Weak mixed formulation has a **unique solution** $(u,p) \in V \times S$.

Discrete mixed approximation

Simplicial conforming meshes: the rock matrix mesh (tetrahedra) is supported by the fracture network mesh (triangles).

Piecewise constant functions for the hydraulic head p_h.
Lowest order Raviart-Thomas(-Nédélec) for the velocity u_h.

Problem statement.
Find $u_h = (u_h^{\mathrm{m}}, u_h^{\mathrm{f}}) \in V_h \subset V$ and $p_h = (p_h^{\mathrm{m}}, p_h^{\mathrm{f}}) \in S_h \subset S$ such that:

$$\begin{aligned} a(u_h, v_h) - b(v_h, s_h) &= L_a(v_h), \quad \forall v \in V_h, \\ b(v_h, s_h) &= L_b(s_h), \quad \forall s_h \in S_h. \end{aligned}$$

b satisfies the discrete inf-sup condition.
$\Longrightarrow$ Mixed approximation has a **unique discrete solution** $(u_h, p_h) \in V_h \times S_h$.

A priori error estimates. `+ Regularity conditions.`

$$\|u - u_h\|_V \leq h\|u\|_1, \qquad \|p - p_h\|_S \leq h\left(\|u\|_1 + \|p\|_{H^1(\Omega)}\right),$$

where:

$$\|u\|_1^2 = \sum_{\alpha \in \mathcal{C}} \left(|u_\alpha^{\mathrm{m}}|_{H^1(\omega_\alpha)}^2 + |u_\alpha^{\mathrm{m}}|_{H^1(\omega_\alpha)}^2\right) + \sum_{\ell \in \mathcal{I}} \left(|u_\ell^{\mathrm{f}}|_{H^1(\gamma_\ell)}^2 + |u_\ell^{\mathrm{f}}|_{H^1(\gamma_\ell)}^2\right).$$

Bonus

Mixed-Hybrid Finite Element (MHFE) method

Key idea: relax the continuity of the normal trace of the velocity *across the interior faces*.

→ $M_{h,0,D}$ = Lagrange Multiplier space of piecewise constant functions on the interior faces and all the edges.

→ $V_h^{\mathrm{hyb}} = V_h + \texttt{relaxed continuity constraints}$.

→ Introduce $b_{\mathcal{T}}$, a mesh-dependent version of b over $V_h^{\mathrm{hyb}} \times S_h$.

→ c bilinear form over $V_h^{\mathrm{hyb}} \times M_{h,0,D}$.

Problem statement. Find $u_h = (u_h^{\mathrm{m}}, u_h^{\mathrm{f}}) \in V_h^{\mathrm{hyb}}$, $p_h = (p_h^{\mathrm{m}}, p_h^{\mathrm{f}}) \in S_h$ and $\lambda_h = (\lambda_h^{\mathrm{m}}, \lambda_h^{\mathrm{f}}) \in M_{h,0,D}$ such that:

$$
\begin{aligned}
a(u_h, v_h) - b_{\mathcal{T}}(v_h, p_h) + c(\lambda_h, v_h) &= L_a(v_h), && \forall v_h \in V_h^{\mathrm{hyb}},\\
b_{\mathcal{T}}(u_h, s_h) &= L_b(s_h), && \forall s_h \in S_h,\\
c(u_h, \mu_h) &= 0, && \forall \mu_h \in M_{h,0,D}.
\end{aligned}
$$

The MHFE formulation is **equivalent** to the mixed approximation → unique solution (u_h, p_h, λ_h) .

Bonus

`nef-flow-fpm`: an MHFE MATLAB code - validation

Analytical solution: numerical convergence

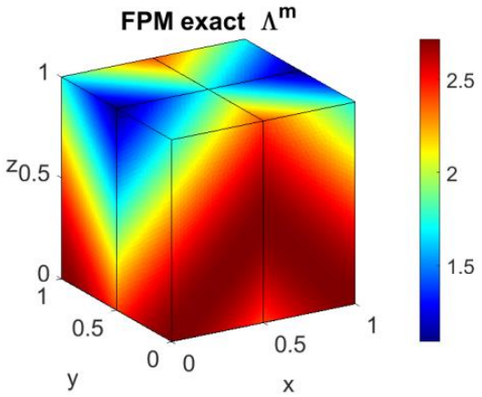

(a) Trace of hydraulic heads $\Lambda_{\mathbb{m}}$.

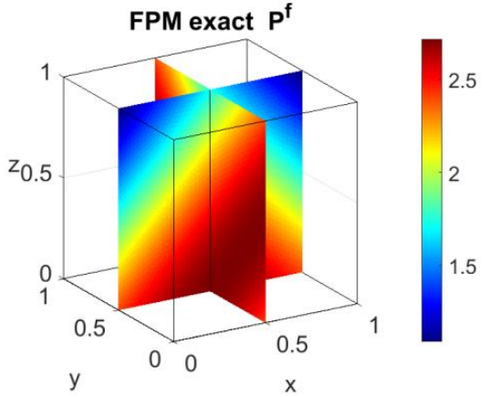

(b) Mean hydraulic heads $P_{\mathbb{f}}$.

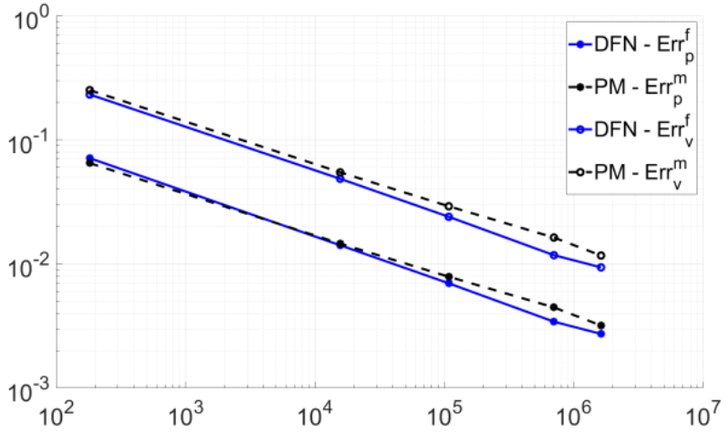

K. Brenner, M. Groza, C. Guichard, G. Lebeau, and R. Masson. *Numerische Mathematik.* **2016.**

Benchmark test case, flow and transport simulations

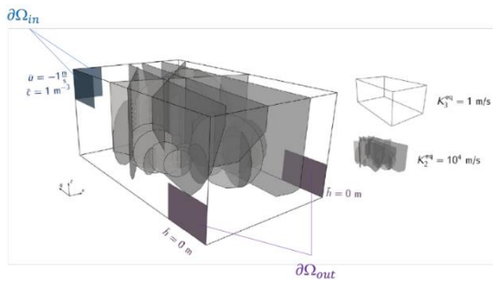

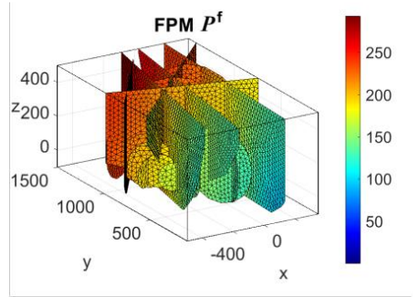

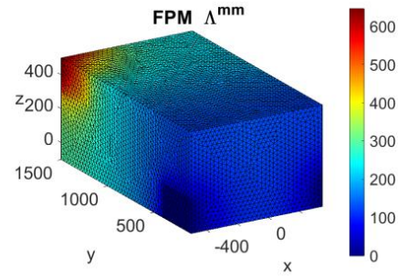

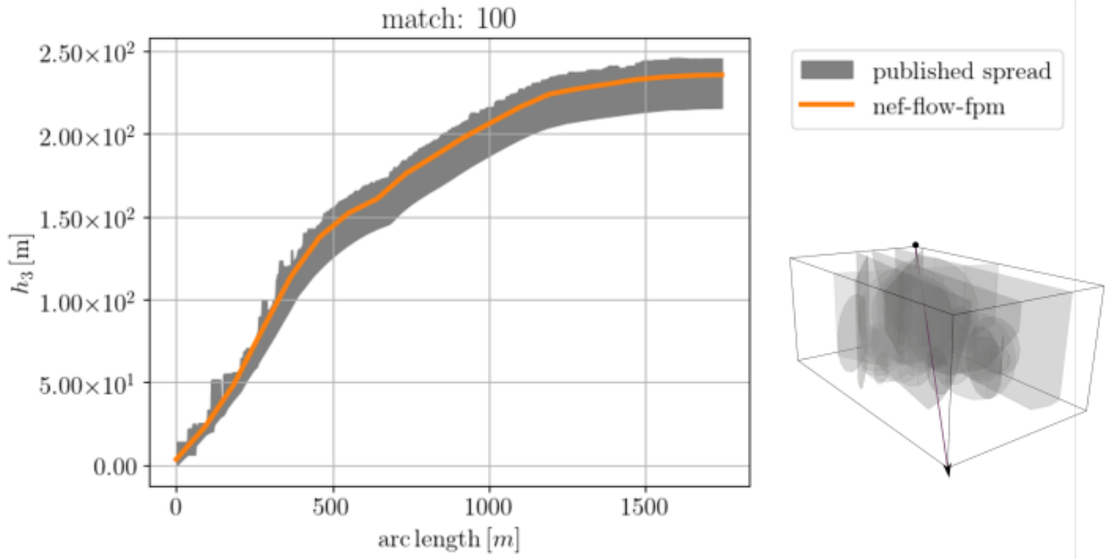

I. Berre, W. M. Boon, B. Flemisch, A. Fumagalli, D. Gläser, E. Keilegavlen, A. Scotti, I. Stefansson, A. Tatomir, K. Brenner, S. Burbullah, P. Devloo, O. Duran, M. Favino, J. Hennicker, I. Lee, K. Lipnikov, R. Masson, K. Mosthaf, M. G. C. Nestola, C. Ni, K. Nikitin, P. Schälde, D. Svyatskiy, R. Yanbarisov, P. Zulian. *Advances in Water Resources.* **2021.**

Bonus

Physical phenomena and applications

Key role in industrial applications:

- oil and gas extraction,
- CO_2 sequestration in the subsurface,
- geothermal energy production,
- underground nuclear waste storage,
- water extraction (for drinking, irrigation, industrial processes, …),
- etc.

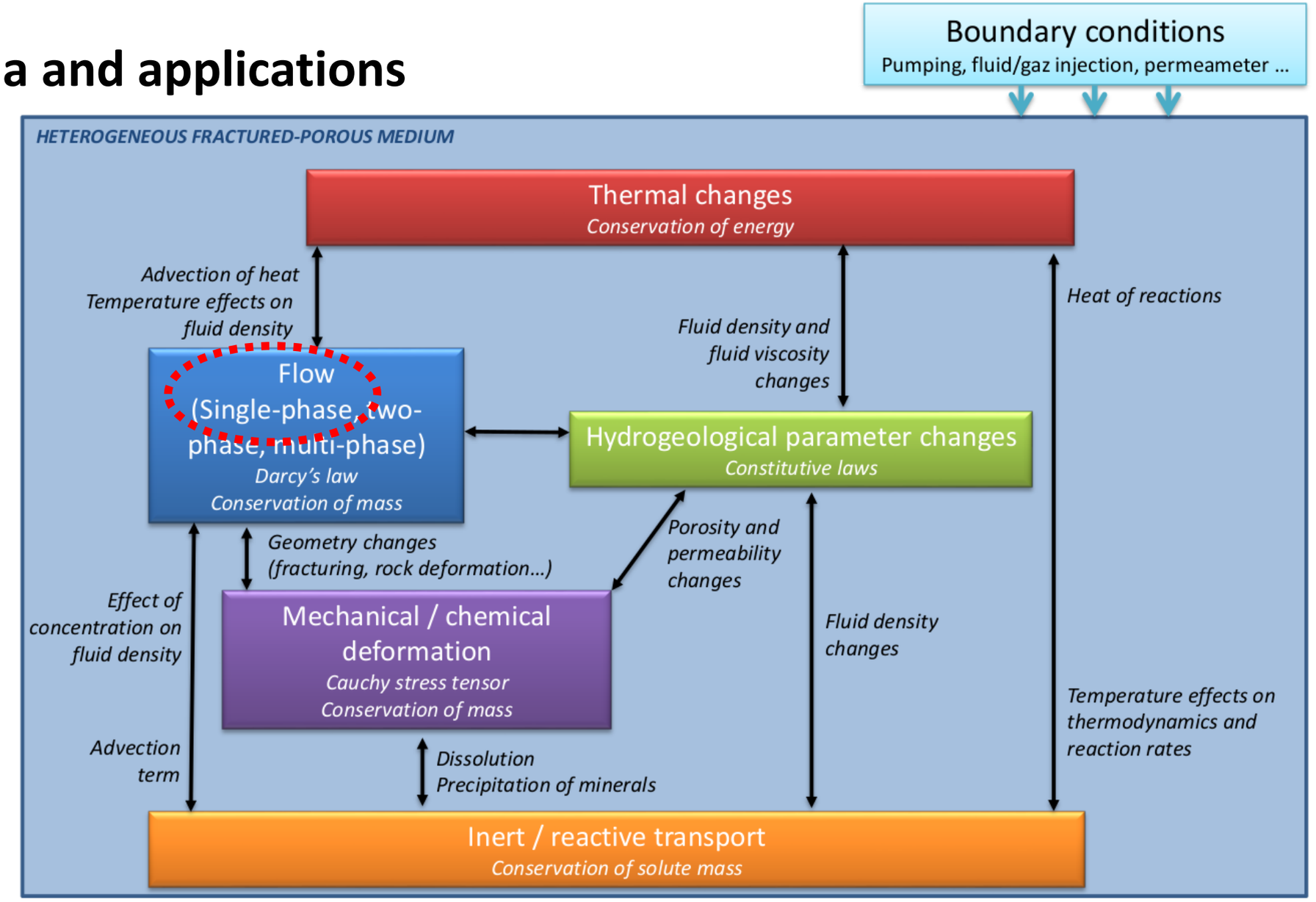

Bonus

Mesh generation

2D main challenge. Small angles, up to millions of fractures.

Dedicated software **MODFRAC (Inria Gamma, Serena & UTT)**, an **efficient parallel** unstructured surface mesh generator with a **user input minimum quality.**

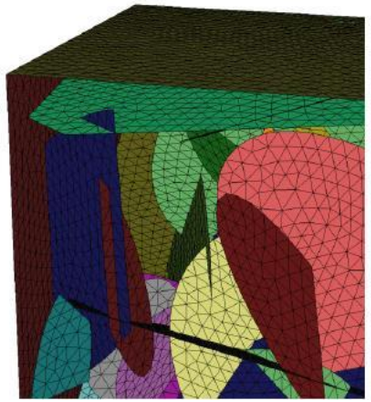

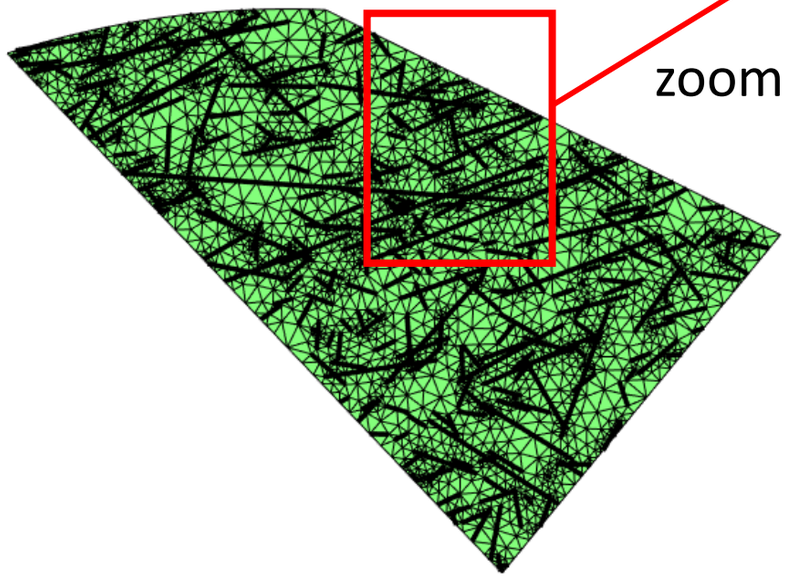

zoom

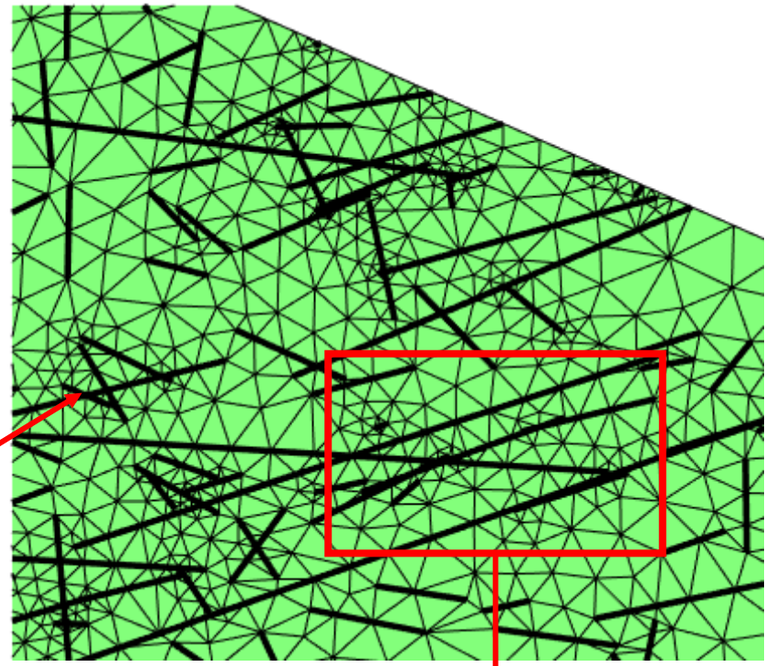

zoom

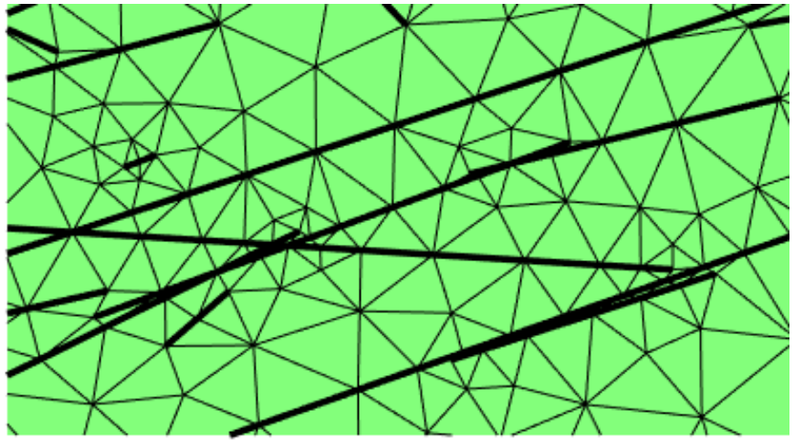

P. Laug, G. Pichot. *MASCOT IMACS Series in Computational and Applied Mathematics, Vol. 22.* **2018.**

H. Borouchaki, P. Laug, P.L. George. *International Journal for Numerical Methods in Engineering.* **2000.**

Bonus

Mesh generation

3D main challenge. Use the triangular mesh generated by MODFRAC as an input to generate the tetrahedral mesh.

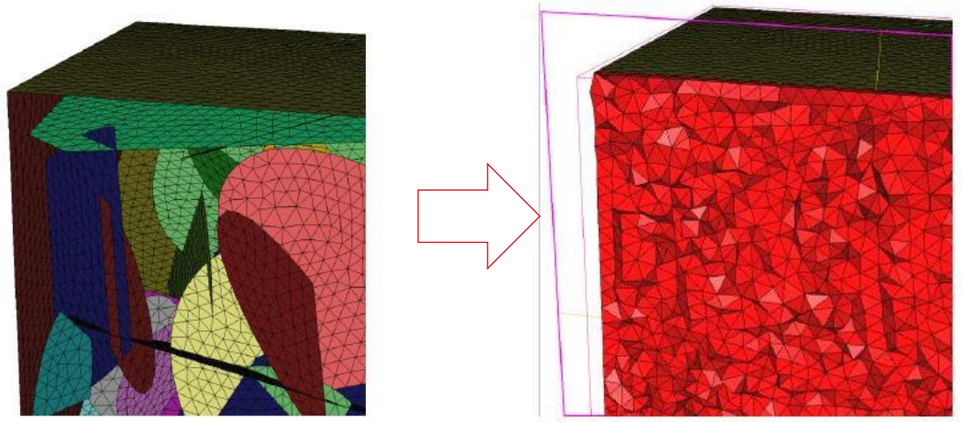

MODFRAC GHS3D

H. Borouchaki, P. Laug, P.-L. George. *International Journal for Numerical Methods in Engineering.* **2000.**

P.-L. George, H. Borouchaki, F. Alauzet, A. Loseille, P. Laug, L. Maréchal. *ISTE Group.* **2018.**

→ Dedicated software **GHS3D (Inria Gamma)**, an **efficient** unstructured volume mesh generator**.**

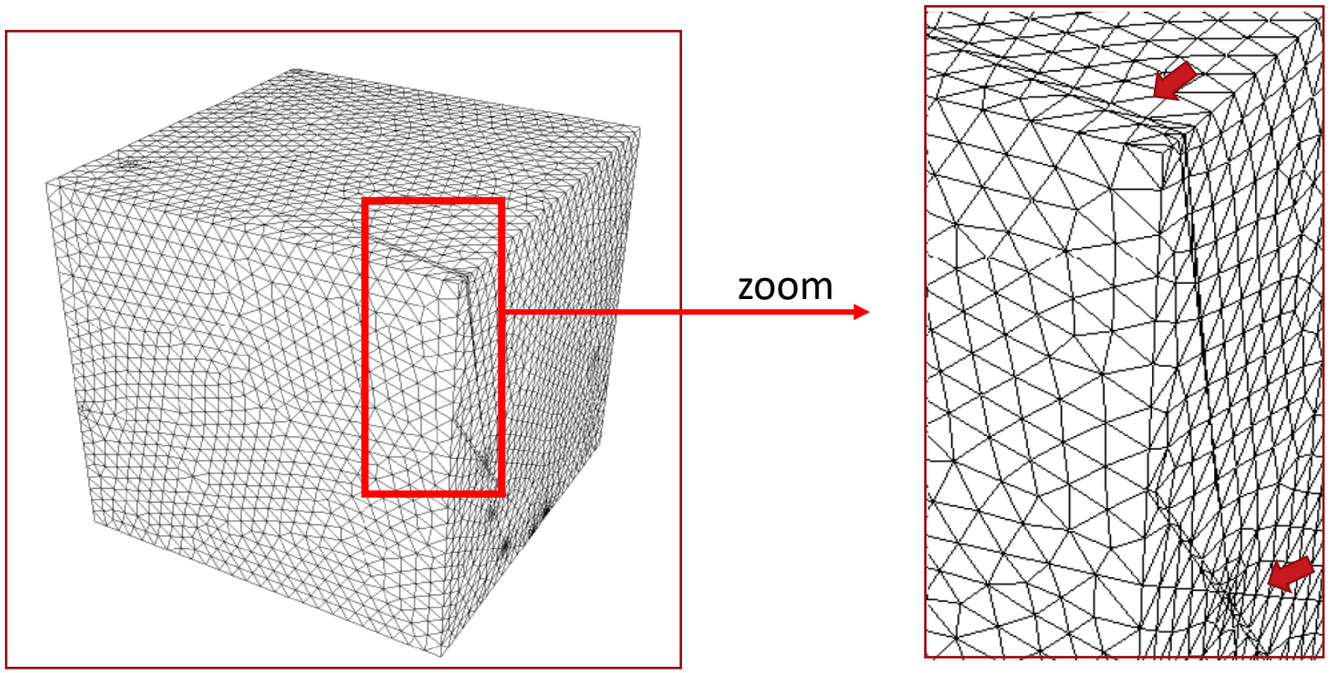

Bonus

Mesh generation

2D main challenge. Small angles, up to millions of fractures.

3D main challenge. Use the triangular mesh generated by MODFRAC as an input to generate the tetrahedral mesh.

P. Laug, G. Pichot. *MASCOT IMACS Series in Computational and Applied Mathematics, Vol. 22.* **2018.**

H. Borouchaki, P. Laug, P.L. George. *International Journal for Numerical Methods in Engineering.* **2000.**

On a Laptop
4 cores
Intel(R) Core(TM) i7-7820HQ CPU @ 2.90GHz
32GiB RAM
4 POSIX-threads

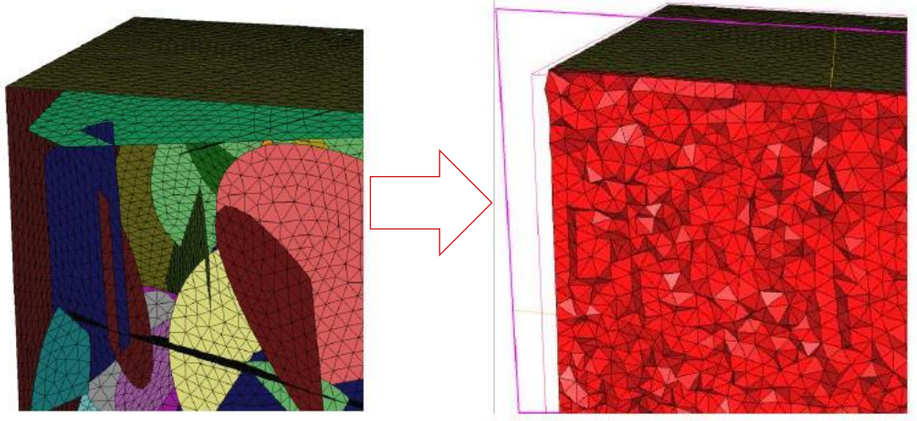

On a Mac Cluster
16 cores
Intel(R) Xeon(R) W-3245 CPU @ 3.20GHz
64GiB RAM
Sequential run

H. Borouchaki, P. Laug, P.-L. George. *International Journal for Numerical Methods in Engineering.* **2000.**

P.-L. George, H. Borouchaki, F. Alauzet, A. Loseille, P. Laug, L. Maréchal. *ISTE Group.* **2018.**

MODFRAC
Inria Gamma, Serena & UTT.
Parallel unstructured surface mesh generator with a user input minimum quality.

GHS3D
Inria Gamma.
Unstructured volume mesh generator.

Mesh name	# tetra.	# faces	# triang. frac.	# edges	MODFRAC time mm:ss	GHS3D time mm:ss
[L60geo-FPM]	8M	16M	2M	3M	00:55	03:02
[L80geo-FPM]	17M	33M	4M	6M	02:02	08:25

Bonus

Networks with a large number of fractures

LabCom *fractory*:
- Itasca Consultants (France)
- Géosciences Rennes
- CNRS

Fractures = disks.

e.g.: L20 is a cube of side 20 m.

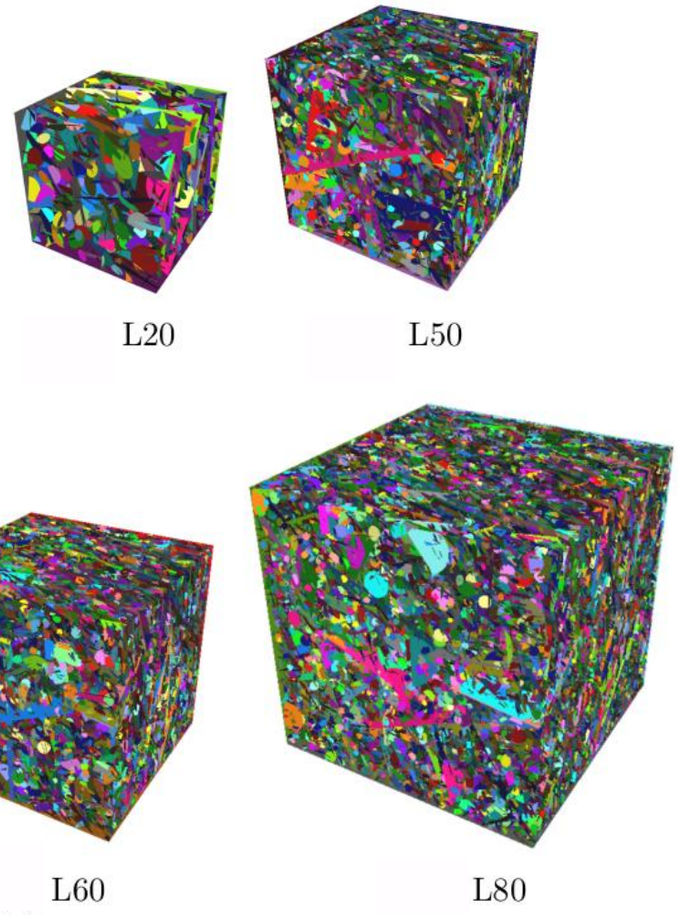

P. Davy, R. Le Goc, C. Darcel, O. Bour, J.-R. de Dreuzy, R. Munier. *Journal of Geophysical Research: Solid Earth.* **2010.**

P. Davy, R. Le Goc, and C. Darcel. *Journal of Geophysical Research: Solid Earth.* **2013.**

Geometry name	# frac.	# frac-frac intersections
[L20-FPM]	2k	3k
[L50-FPM]	23k	39k
[L60-FPM]	40k	66k
[L80-FPM]	90k	155k
[L100-FPM]	174k	305k
[L130-FPM]	377k	675k
[L160-FPM]	697k	1.3M

Bonus

Rock matrix hydraulic conductivity and fracture network tangential transmissivity

- **"1v100".** Rock matrix: K^m = 1 m/s. Fracture network: K^f = 100 m^2/s (the same for all fractures)

- **"heter".** Rock matrix: $K^m = 10^{-8}$ m/s. Fracture network: K^f takes one value per fracture in the range $[10^{-6}, 20]$ m^2/s (data from **LabCom *fractory***)

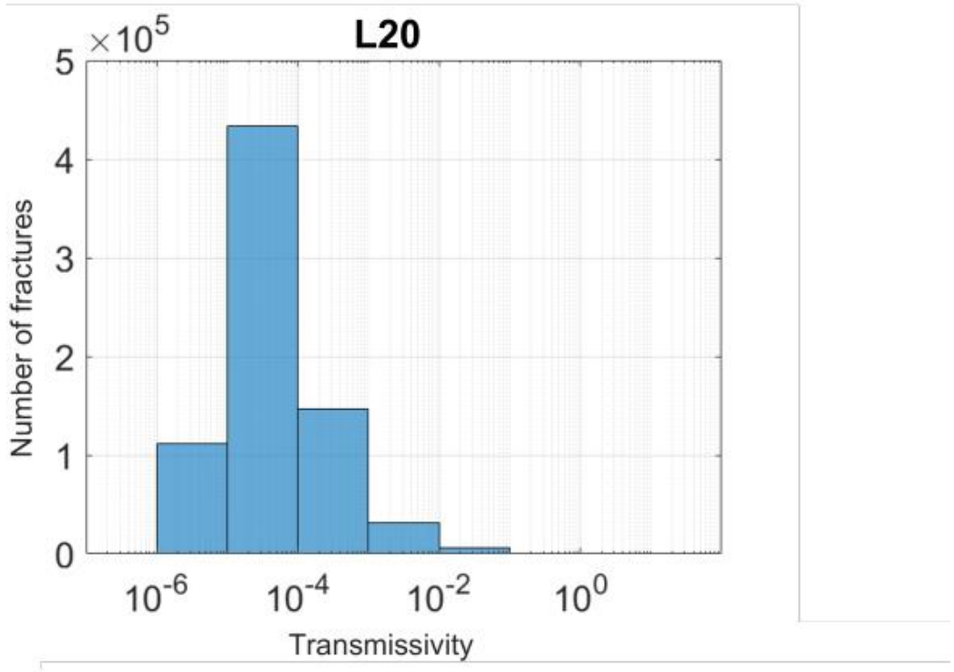

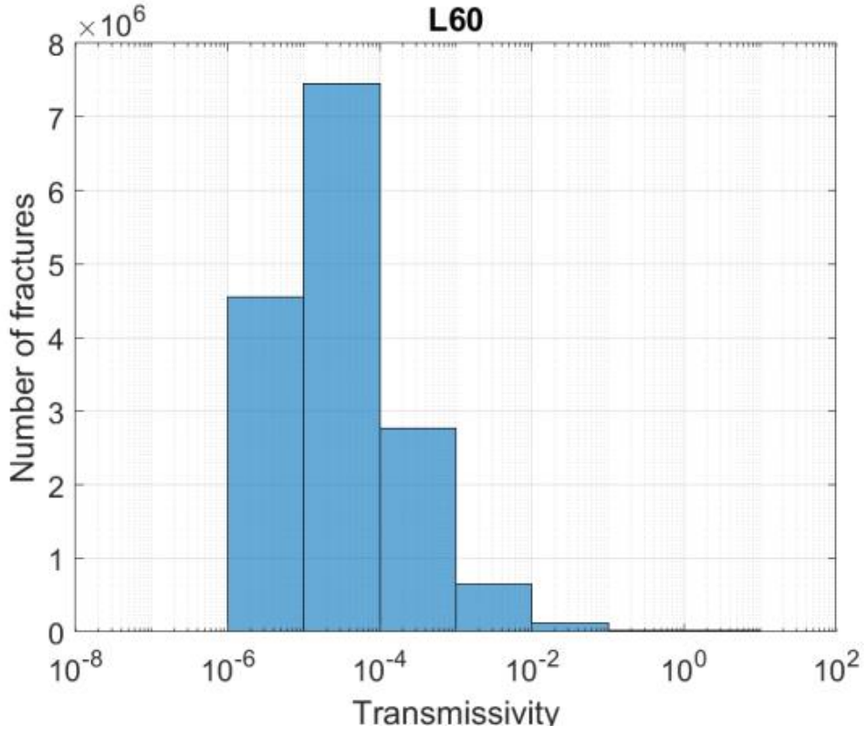

Sequential PCG-AMGCL. Solver tol.: 10^{-14}.

Geometry complexity impact on solver convergence

1. Choose a test case: `[L80-FPM-1v100]`.
2. Choose other geometries with a lower number of fractures: `[L50-FPM]`, `[L20-FPM]`. + 1v100.
3. **Refine so as to obtain the same number of tetra. → ~Same number of dofs:** `[L50fine-FPM-1v100]`, `[L20fine-FPM-1v100]`.

Test case	# frac.	# tetra.	# dofs
[L80geo-FPM-1v100]	90k	17M	39M
[L50fine-FPM-1v100]	23k	17M	37M
[L20fine-FPM-1v100]	2k	17M	34M

Test case	# it.	Solver time dd-hh:mm:ss	RAM (GB)
[L80geo-FPM-1v100]	40k	02-18:36:54	16
[L50fine-FPM-1v100]	5k	00-08:09:28	14
[L20fine-FPM-1v100]	2k	00-03:09:38	13

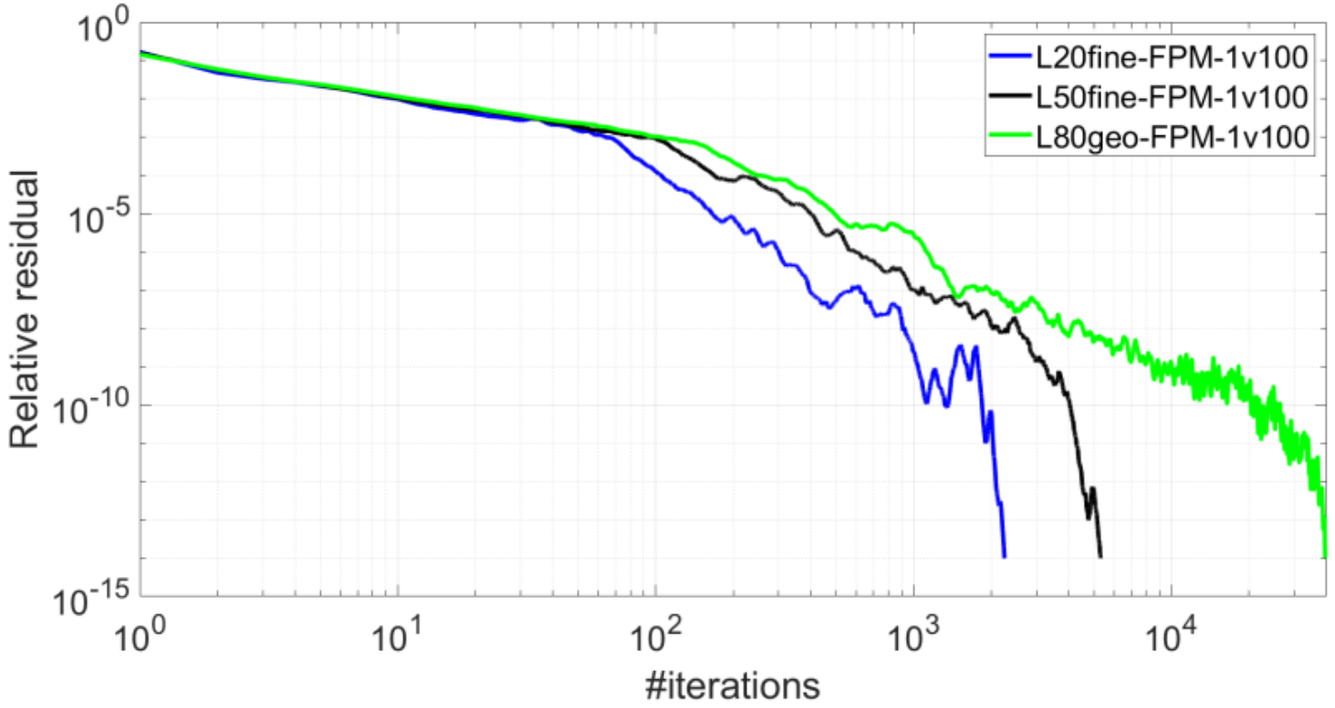

+ Simulations with 90k fractures now possible.

- Convergence of the iterative method slows down (time and iterations) as the complexity of the fracture network increases.

GMRES + HPDDM GenEO - RAS. Solver tolerance : 10^{-14}. GMRES restart : 90.

Strong scaling

Solve the same linear system with an increasing number of MPI processes.
Test case: `[L60geo-FPM-1v100]`: 40k fractures, 19M dofs.

	# MPI procs.	# dofs / sbdm.	# it.	PCSetUp mm:ss		KSPSolve mm:ss		Coarse space size
	64	289k	35	18:47	÷4.1	00:40	÷2.4	15k
x2	128	145k	36	04:37	÷3.3	00:17	÷2.1	21k
x2	256	72k	36	01:25	÷2.7	00:08	÷1.6	27k
x2	512	36k	38	00:32	÷2.0	00:05	÷1.0	36k
x2	1,024	18k	40	00:16	÷1.2	00:05	÷1.0	47k
x2	2,048	9k	39	00:13		00:05		61k

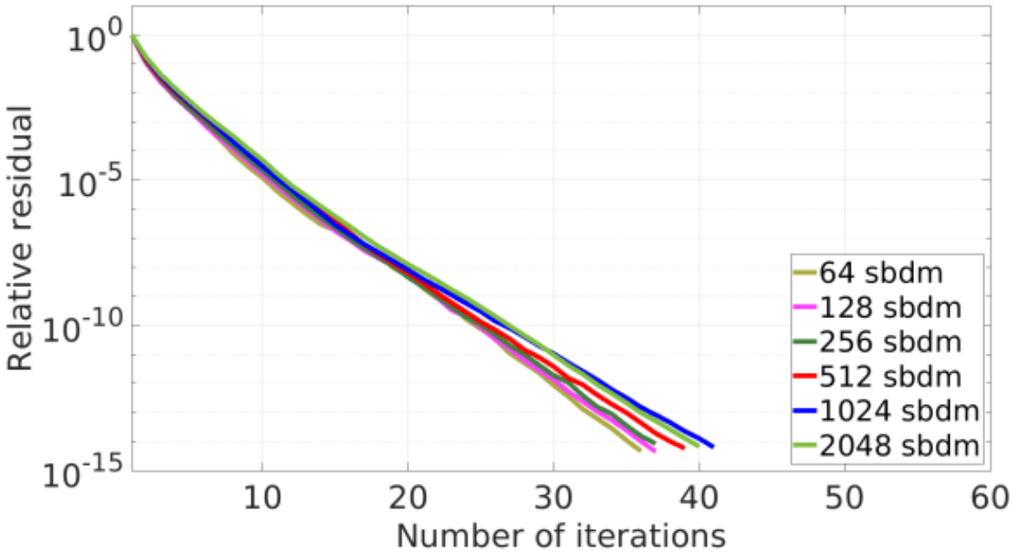

+ **Strong scaling OK w.r.t. iterations** (35-40).
- Wall-clock time saturation beyond 512 MPI procs.
“Sweet spot” : ~36k dofs / sbdm.

GMRES + HPDDM GenEO - RAS. Solver tolerance : 10^{-14}. GMRES restart : 90.

Weak scaling

1. **Choose a test case:** `[L60geo-FPM-1v100], 40k fractures`
2. **Refine and generate linear systems:** `[L60fineA-FPM-1v100], [L60fineB-FPM-1v100], [L60fineC-FPM-1v100].`
3. **Decompose so as to keep the number of dofs constant per sbdm.: ~36k dofs/sbdm.**

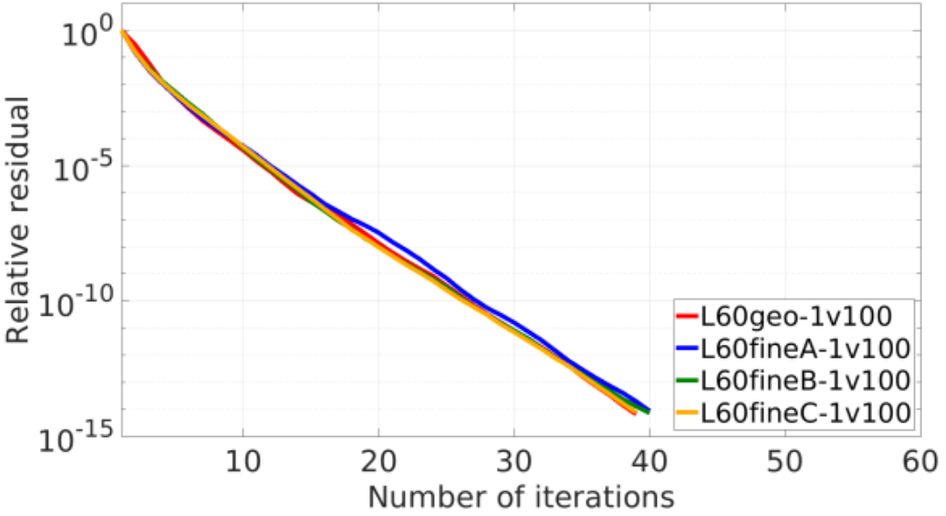

Test case name	# tetra	# dofs	# sbdm.	# it.	PCSetUp mm:ss	KSPSolve mm:ss	Coarse space size
[L60geo-FPM-1v100]	8M	19M	522	38	00:33	00:06	36k
[L60fineA-FPM-1v100]	16M (x2.0)	37M	1,033	39	00:42 (x1.9)	00:08 (x2.3)	70k
[L60fineB-FPM-1v100]	30M (x1.9)	66M	1,857	39	00:40	00:10	116k
[L60fineC-FPM-1v100]	60M (x2.0)	129M	3,631	39	01:03	00:14	207k

+ **Weak scaling OK w.r.t. iterations** (38-39).

- **Wall-clock time saturation** after the first refinement.

Bonus

Ill-conditioned and large and linear systems

Test case	# frac.	# dofs	nnz	`condest`
[L20geo-FPM-1v100]	2k	4M	30M	1.71e+11
[L20geo-FPM-heter]				6.86e+16
[L160geo-FPM-1v100]	697k	243M	1.8B	—
[L160geo-FPM-heter]				—

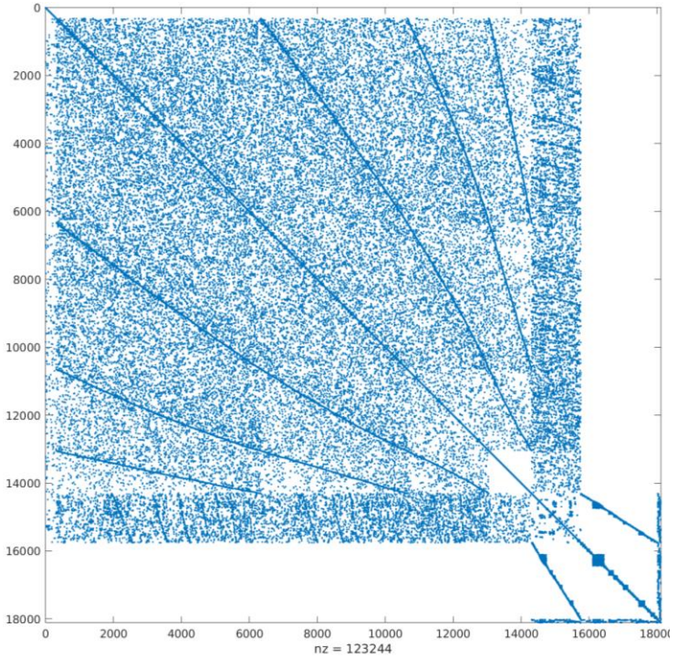

Shape of the linear system matrix from a very coarse test case (not presented here)